**UNIVERSITY OF CUKUROVA**
**INSTITUTE OF NATURAL AND APPLIED SCIENCES**

**PhD THESIS**

**Nisa NACAR ÇIKAN**

# MODELLING AND ANALYSIS OF COLORLESS SOURCES BASED ON WAVELENGTH DIVISION MULTIPLEXED PASSIVE OPTICAL NETWORKS

**DEPARTMENT OF ELECTRICAL AND ELECTRONICS ENGINEERING**

**ADANA-2020**

**ABSTRACT**

**PhD THESIS**

**MODELLING AND ANALYSIS OF COLORLESS SOURCES BASED ON WAVELENGTH DIVISION MULTIPLEXED PASSIVE OPTICAL NETWORKS**

**Nisa NACAR ÇIKAN**

**UNIVERSITY OF ÇUKUROVA**
**INSTUTE OF NATURAL AND APPLIED SCIENCES**
**DEPATMENT OF ELECTRIC-ELECTRONICS ENGINEERING**

Supervisor : Assoc. Prof. Dr. Murat AKSOY
Year: 2020, Pages: 156
Jury : Assoc. Prof. Dr. Murat AKSOY
: Prof. Dr. Mustafa GÖK
: Assoc. Prof. Dr. Sami ARICA
: Asst. Prof. Dr. Şule ÇOLAK
: Asst. Prof. Dr. Emine AVŞAR AYDIN

Having the scalable channel capacity for each customer in access networks is crucial for fulfilling the extreme demand on fast internet. Wavelength division multiplexed passive optical network (WDM PON) distributes separate wavelengths to guarantee high bandwidth to every subscriber. Although WDM PON technology has many advantages, the implementation of this technology into the access part is created difficulties due to mainly two reasons as high infrastructure costs and complexity. In this thesis, efficient and applicable solutions have been presented to solve these problems. Employment of colorless sources at optical network units (ONUs) is considered as a key solution to reduce the system cost. To further reduce the system cost and to simplify the system, the remodulation technique is applied, which eliminates the additional optical source usage at the central office. However, in this technique, the residual downstream data should be erased at ONU before the upstream transmission process occurs to prevent the crosstalk. The main contribution of this thesis is to investigate the data erasing efficiency of the colorless sources in a bidirectional WDM PON network by employing the remodulation method.

**Keywords:** Colorless Sources, Data Erasing Technique, WDM PON, Remodulation.

# ÖZ

## DOKTORA TEZİ

**MODELLING AND ANALYSIS OF COLORLESS SOURCES BASED ON WAVELENGTH DIVISION MULTIPLEXED PASSIVE OPTICAL NETWORKS**

**Nisa NACAR ÇIKAN**

**ÇUKUROVA ÜNİVERSİTESİ**
**FEN BİLİMLERİ ENSTİTÜSÜ**
**ELEKTRİK-ELEKTRONİK ANA BİLİM DALI BAŞKANI**

Danışman : Doç. Dr. Murat AKSOY
Yıl: 2020, Sayfa: 156
JÜRİ : Doç. Dr. Murat AKSOY
: Prof. Dr. Mustafa GÖK
: Doç. Dr. Sami ARICA
: Dr. Öğr.Üyesi Şule ÇOLAK
: Dr. Öğr.Üyesi Emine AVŞAR AYDIN

Erişim ağlarındaki her müşterinin farklı kanal kapasitesine sahip olması, hızlı internet erişimindeki yoğun talebi karşılamak için çok önemlidir. Dalgaboyu bölmeli çoğullamalı pasif optik ağ (WDM PON), her aboneye yüksek bant genişliği sağlamak için ayrı dalga boyları kullanır. WDM PON teknolojisinin birçok avantajı olmasına rağmen, bu teknolojinin erişim ağları kısmına uygulanması, yüksek altyapı maliyetleri ve karmaşıklık olmak üzere başlıca iki nedenden dolayı zorluklar yaratmaktadır. Bu tezde, bu problemleri çözmek için verimli ve uygulanabilir çözümler sunulmuştur. Optik ağ birimlerinde (ONU) renksiz kaynakların kullanılması, sistem maliyetini düşürmek için önemli bir çözümdür. Maliyeti daha fazla düşürebilmek ve sistemi basitleştirebilmek için yeniden modülasyon tekniği uygulanmıştır. Bu metod, merkez ofiste extra optik kaynak kullanımını ortadan kaldırarak maliyetin düşmesini sağlar. Fakat bu teknikte, indirme yönünden gelen verilerin; yükleme yönündeki veriler ile karışmasını engelleyebilmek adına silinmesi gerekmektedir. Bu tezin literatüre ana katkısı, çift yönlü WDM PON' a dayalı yeniden modülasyon sisteminde renksiz kaynakların veri silme verimliliğinin analiz edilmesidir.

**Anahtar Kelimeler:** Renksiz kaynaklar, Veri Silme Tekniği, WDM PON, Yeniden Modülasyon.

## EXTENDED SUMMARY

Presenting broad bandwidth, and cost-efficient access networks to the internet and mobile users are crucial to deal with growing data traffic. Although streaming high definition (HD) video services such as YouTube and Netflix can handle present data traffic, the improving new high bandwidth technologies like virtual reality, internet-of-things (IoT), augmented reality, and even yet unexplored technologies are expected to increase data traffic rates exponentially. This growth is even further build-up with other technologies. The device connection will grow as a 10% Compound Annual Growth Rate (CAGR) from 2018 to 2023. It is estimated that the two-thirds of the world population will have internet connection by 2023 and the IP traffic will be triple times of the world population [1]. The machine-to-machine(M2M) connection will hold a large part (about 50%) of internet usage. The smartphone usage will place in the second row. This will be followed by TVs with 11%, non-smartphones with 5%, PCs with 4%, other devices with 3.9%, and tablets with 3%.

Optical fiber technology makes high data rate transmission possible among core, metro, and access networks. The link between these three networks can be explained as follows. Core networks put to use advanced and long-lasting dense wavelength division multiplexed (DWDM) technology. The core network first sends massive data traffic to the metro network and the metro ring transmits the data to the service providers. Subsequently, the data is transferred to the users by the access network. In addition, access networks require to provide higher data rates with increasing data traffic over time. Thus, fiber optic-based access networks are started to be extensively deployed.

The integration of optical fiber technology into access networks began in the 1980s. 10 years later around the 1990s, the standardization process was completed. However, the higher costs were the problem due to expensive components such as amplifiers at the beginning. Therefore, service providers

started to seek solutions to decrease the cost. Thus, the passive optical network (PON) came into prominence as the assertive solution. Additionally, time-division-multiplexing (TDM) technology, which allows the users to share the network, has been started to widely deploy to lower the cost of the access networks. On the other hand, TDM PON has some matters like security and limited capacity that burdens access networks. WDM PON has been considered as a good option to be applied in access networks as well because of its favorable outcomes in metro and core networks. WDM PONs allow every user to have a single wavelength that enables the users to carry out a point-to-point (PtP) connection. Single wavelength usage lets the subscribers have a secure connection, attain higher data rates, and longer reach transmission.

Although WDM PON technology has many advantages, the implementation of this technology into the access part is created difficulties due to mainly two reasons as high infrastructure and transmitter costs. The development of transmitters with variable wavelengths has been offered as a solution. These access network components are named as colorless transmitters and can perform in an extensive wavelength range. In this way, identical transmitters, which lowers the system cost and simplifies the system, can be churned out.

The subject of this thesis is to figure out the way of designing an economical WDM PON system by exploring cheap and simple colorless transmitters. Although the application of colorless sources at the user ends partially solved the cost problem, there were still some problems that degrade the transmitter performance. Injection-locking (IL) has also been proposed to enhance the transmission performance of the transmitters. IL is an innovative method that provides high-speed transmission and overcomes the degrades in transmission performance. To set up an injection-locked system, a laser is needed (usually called as master) to inject photons into the slave laser. There are two major effecting factors of injection locking. The first one is to enhance the slave laser characteristics. The second is to provide the synchronization of slave and master

lasers. The application of injected-locked lasers instead of the tunable lasers at the user ends also decreases the cost of the system. To further reduce the system cost, the remodulation technique is applied, which eliminates the additional optical source usage at the central office. However, in this technique, the residual downstream data should be erased at ONU before the upstream transmission process occurs to prevent the crosstalk.

The main contribution of this thesis is to analyze the data deletion performance of the IL-FPLD and wavelength seeded RSOA colorless sources in a bidirectional WDM PON network using the remodulation technique. The technical features of these two colorless sources will reduce the cost of the system and enable internet subscribers to have reliable, low cost, and fast internet access. The prominent chapter handles a particular study of the data deletion performance of FPLD. The IL-FPLD is also another main part of the thesis.

The impacts of many factors, such as the confinement factor (CF), biasing current, injection power, and extinction ratio (ER), on data deletion abilities of FPLD and RSOA have been discussed. Primarily, the mathematical model of FPLD, IL-FPLD and RSOA are presented to explain the laser's working principle. The system speed is set as 5 Gb/s. The power has been injected into the system was started from - 25 dBm and was increased up to 0 dBm. The biasing current of the system was applied as between 20 mA and 100 mA.

First, FPLD was implemented at the optical network unit (ONU) as a colorless source. Successful upstream communication has been achieved when biasing current higher than 30 mA was applied and power was injected less than 0 dBm. Increasing the bias current applied to FPLD created the extinction ratio to decrease below 0.5 dB, which was the desired result. CF is another important parameter that has an impact on the deletion of the rest downstream data at ONU. Increasing the CF also helps to obtain error-free upstream communication.

The second major subject studied in the thesis is that the mirror values of IL-FPLD should remain between reasonable values. The laser's front and rear

mirror values are highly effective in deleting data that comes from the central office on the carrier wavelength and affects upstream communication. In order to clearly see the effects of mirror values on the laser's ability to delete data, firstly, upstream data was not applied on the ONU side. As the second process, 2.5 Gb /s data was applied to the user side and the results obtained were compared with the first applied process. The results showed that a quality upstream delivery was achieved with an increase in the rear mirror facet value of 90% and above and the front mirror facet value from 0.2% to 7%, also depending on the injected power range.

In the thesis, the ability of RSOA, another colorless source, to delete unnecessary data has also been studied. When the RSOA laser is applied to the ONU side, it has been determined that it prevents crosstalk between ONU and CO by increasing the bias current over 50 mA, the confinement factor over 0.4, and the injection power over -15 dBm.

As a result, with the developing technology, it has become inevitable to use WDM PON in access networks. In this thesis, a model is presented to implement low-cost WDM PON technology into access networks, and to meet the high bandwidth requirement arises from gradually increasing new technologies. The data deletion skills of the colorless sources used on the ONU side of the system were studied and appropriate parameter values were determined.

## GENİŞLETİLMİŞ ÖZET

İnternet ve mobil kullanıcılara hızlı ve uygun maliyetli bant genişliği sunmak, giderek artan veri trafiğine olan ihtiyacı karşılamak açısından çok önemlidir. YouTube ve Netflix gibi yüksek çözünürlük (HD) gerektiren video hizmetleri mevcut veri trafiğini karşılamada yeterli olsa da sanal gerçeklik, nesnelerin interneti (IoT), artırılmış gerçeklik ve hatta henüz keşfedilmemiş gelişime açık yüksek bant genişliği gerektiren yeni teknolojilerin veri trafiğini yüksek oranda artırması öngörülmektedir. Veri trafiğindeki büyüme, diğer teknolojilerle birlikte daha da artmaktadır. Cihazlar arasındaki bağlantı, 2018'den 2023 yılları arasında %10 Bileşik Yıllık Büyüme Oranı (CAGR) kadar gelişim gösterecektir. 2023 yılına kadar dünya nüfusunun üçte ikisinin internet bağlantısının olacağı ve IP trafiğinin dünyanın üç katı olacağı tahmin ediliyor [1]. Makineler arası(M2M) bağlantılar, internet kullanımının büyük bir bölümünü (yaklaşık olarak %50) kapsayacaktır. Akıllı telefon kullanımı ikinci sırada yerini alacaktır. Bunu %11 ile TV'lerin, %5 ile akıllı olmayan telefonların, %4 ile PC'lerin, %3,9 ile diğer cihazlar ve %3 ile tabletlerin takip etmesi ön görülmektedir.

Optik fiber teknolojisi ile, çekirdek, metro ve erişim ağları arasında yüksek veri hızı iletimi sağlanmaktadır. Bu üç ağ arasındaki bağlantı şu şekilde açıklanabilir. Çekirdek ağlar, gelişmiş ve dayanıklı olan yoğun dalga boyu bölmeli çoğullama (DWDM) teknolojisini kullanır. Çekirdek ağ öncelikle yoğun olan veri trafiğini metro ağına gönderir ve metro hattı da hizmet sağlayıcılarına iletir. Daha sonra veriler, erişim ağı tarafından kullanıcılara aktarılır. Ayrıca erişim ağları, zamanla artan veri trafiğine daha yüksek hızlı verilerde sağlamalıdır. Böylelikle, erişim ağlarında fiber optik kablo kullanımı yaygınlaşmaya başlamıştır.

Optik fiber teknolojisinin erişim ağlarına entegrasyonu 1980'lerde başlamıştır. Bundan 10 yıl sonra 1990 yıllarında standardizasyon süreci tamamlanmıştır. Fakat ilk yıllarda yükselteç gibi pahalı cihazların kullanımı

maliyeti yükseltmiştir. Bu nedenle servis sağlayıcılar maliyeti düşürmek için çözümler aramaya başladı. Böylece iddialı çözüm olarak pasif optik ağ (PON) ön plana çıktı. Ayrıca, kullanıcıların ağı paylaşmasına olanak tanıyan zaman bölmeli çoğullama (TDM) teknolojisi, erişim ağlarının maliyetini düşürmek için yaygın olarak kullanılmaya başlanmıştır. Öte yandan, TDM PON teknolojisinin erişim ağlarını zorlayan güvenlik ve sınırlı kapasite gibi bazı sorunları vardır. WDM PON, metro ve çekirdek ağlardaki olumlu sonuçlarından dolayı erişim ağlarında da uygulanabilecek iyi bir seçenek olarak görülmüştür. WDM PON'lar, her kullanıcının noktadan noktaya (PtP) bağlantı gerçekleştirebilmesi için ayrı dalga boylarında ver iletimi yapmasını sağlar. Her müşterinin ayrı dalga boyu kullanımı, abonelerin güvenli bir bağlantıya sahip olmasını, daha yüksek veri hızlarına ulaşmasını ve daha uzak mesafelere ulaşabilmelerini sağlar.

WDM PON teknolojisinin birçok avantajı olmasına rağmen, bu teknolojinin erişim ağları bölümüne uygulanması ile yüksek maliyetli altyapı ve verici cihazları nedeniyle zorluklar oluşturmaktadır. Çözüm olarak değişen dalga boylarına sahip vericilerin geliştirilmesi önerilmiştir. Erişim ağlarında maliyetin düşmesini sağlayan bu cihazlar renksiz vericiler olarak adlandırılır ve bu vericiler geniş bir dalga boyu aralığında çalışabilirler.

Bu tezin konusu, uygun maliyetli ve basit renksiz vericileri kullanarak ekonomik bir WDM PON sistemi tasarlamaktır. Sistemde renksiz kaynakların uygulanması maliyet sorununu kısmen çözmüş olsa da verici performansını düşüren bazı sorunlar hala mevcuttur. Vericilerin iletim performansını artırmak için enjeksiyon kilitleme (IL) yöntemi önerilmiştir. IL, yüksek hızlı iletim sağlayan ve iletim performansındaki düşüşlerinin üstesinden gelen yenilikçi bir yöntemdir. Enjeksiyon kilitli bir sistem kurmak için, fotonları bir lazere enjekte edebilmek için başka bir lazere (genellikle ana olarak adlandırılır) ihtiyaç vardır. Enjeksiyon kilitlemesini etkileyen iki ana faktör vardır. Birincisi, enjekte edilen lazerin özelliklerini geliştirmektir. İkincisi, enjekte edilen ve enjekte eden lazerlerin arasındaki senkronizasyonu sağlamaktır. Kullanıcı uçlarında ayarlanabilir lazerler

yerine enjekte-kilitli lazerlerin kullanılması sistemin maliyetini de düşürmektedir. Sistem maliyetini daha da azaltmak için, merkez ofiste ek optik kaynak kullanımını ortadan kaldıran yeniden modülasyon(remodulation) tekniği uygulanır. Yeniden modülasyon tekniğinde indirme ve yüklenme yönündeki verilen taşınması için aynı dalga boyu kullanılır. Aynı taşıyıcının iki yönde iletim içinde kullanılmasından dolayı indirme ve yükleme yönündeki verilerde karışım oluşabilir ve buda iletim kalitesini bozar. Bu sebeple, yükleme yönünde iletim gerçekleşmeden önce indirme yönünden gelen verilerin silinmesi gerekmektedir.

Bu tezin ana katkısı, yeniden modülasyon tekniği kullanılarak çift yönlü WDM PON ağında IL - FPLD ve dalga boyu tohumlamalı RSOA renksiz kaynaklarının veri silebilme performanslarını analiz etmektir . Bu iki renksiz kaynağın teknik özellikleri, sistemin maliyetini düşürecek ve internet abonelerinin güvenilir, düşük maliyetli ve hızlı internet erişimine sahip olmalarını sağlayacaktır. Tezin büyük bir bölümünde, geniş kapsamlı olarak FPLD'nin veri silebilme performansına ilişkin çalışmalar yapılmıştır.

FPLD ve RSOA'nın veri silebilmesini etkileyen hapsetme faktörü (CF), ön besleme akımı, enjeksiyon gücü ve sönüm oranı (ER) gibi birçok faktörün etkileri tartışılmıştır. Öncelikle, FPLD ve IL-FPLD'nin matematiksel modeli, lazerin çalışma prensibi açıklamak için sunulmaktadır. Sistem hızı 5 Gb/s' dır. Sisteme enjekte edilen güç -25 dBm'den başlayarak ve 0 dBm'e kadar çıkarılmıştır. Sistemin ön besleme akımı 20 mA ile 100 mA arasında uygulanmıştır.

İlk olarak renksiz bir kaynak olan FPLD yükleme yönünde iletimi sağlayabilmek için optik ağ biriminde (ONU) uygulanmıştır. 30 mA'dan yüksek ön besleme akımı uygulandığında ve güç 0 dBm'den daha az enjekte edildiğinde başarılı bir yükleme yönünde iletim sağlanmıştır. FPLD'ye uygulanan ön gerilim akımının artırılması, sönme oranının 0,5 dB'nin altına düşmesini sağlamıştır ki bu da iyi veri iletimi sağlanabilmesi için istenen sonuçtur. CF, ONU'da indirme yönünden kalan verilerin silinmesine etkisi olan bir başka önemli parametredir. CF'yi artırmak yükleme yönünde hatasız olarak iletimin gerçekleşmesini sağlar.

Tezde incelenen ikinci ana konu, IL-FPLD'nin ayna değerlerinin makul değerler arasında kalması gerektiğidir. Lazerin ön ve arka ayna değerleri, merkez ofisten taşıyıcı dalga boyunda gelen gereksiz verilerin silinmesinde oldukça etkilidir. Ayna değerlerinin lazerin verileri silme yeteneği üzerindeki etkilerini net bir şekilde görebilmek için öncelikle ONU tarafında (yükleme yönünde) veri uygulanmamıştır. İkinci işlem olarak kullanıcı tarafına 2,5 Gb/sn hızında veri uygulanmış ve elde edilen sonuçlar ilk uygulanan işlem ile karşılaştırılmıştır. Sonuçlar, aynı zamanda enjekte edilen güç aralığına bağlı olarak, lazerin arka ayna değerinin %90 ve üzerinde ve ön ayna yüz değerinin de %0,2'den başlayarak %7'ye kadar olan bir artışla kaliteli bir yükleme yönünde iletim sağlandığı gösterilmiştir.

Tezde ayrıca diğer bir renksiz kaynak olan RSOA'nın gereksiz verileri silebilme özelliği incelenmiştir. RSOA ONU tarafına uygulandığında, ön besleme akımını 50 mA'nın üzerine, hapsetme faktörünü 0.4'ün üzerine ve enjeksiyon gücünü -15 dBm'nin üzerine çıkararak ONU ile merkez ofis arasındaki veri karışımını önlediği belirlenmiştir.

Sonuç olarak gelişen teknoloji ile birlikte erişim ağlarında WDM PON kullanılması kaçınılmaz hale gelmiştir. Bu tezde, WDM PON teknolojinin erişim hatlarına düşük maliyet ile uygulanabilmesi ve giderek artan yeni teknolojilerin ihtiyaç duyduğu yüksek bant genişliğinin karşılanabilmesi için bir model sunulmuştur. Sistemin ONU tarafında kullanılan renksiz kaynakların veri silme becerileri üzerinde çalışmalar yapılarak uygun parametre değerleri belirlenmiştir.

**ACKNOWLEDGMENTS**

I would like to express my sincerest gratitude to Assoc. Prof. Dr. Murat AKSOY for his mentoring, patience, confidence in me, and guidance through the preparation of this thesis. It has been a great honor to have Assoc. Prof. Dr. Murat AKSOY as supervisor.

I would like to thank my thesis committee Prof. Dr. Mustafa GÖK, Assist. Prof. Dr. Şule ÇOLAK, Assoc. Prof. Dr. Sami ARICA and Assist. Prof. Dr. Emine AVŞAR AYDIN for their insightful comments.

I would like to thank and acknowledge the Scientific Research Project Unit of Cukurova University (Project Number: FDK-2016-7683) for financially supporting this thesis.

My deepest appreciation goes to my parents, A. Faruk NACAR and Raziye NACAR, for their unconditional love, a constant source of encouragement, support, limitless patience, empathy, and understanding. I am grateful to my brother, Mehmet Can NACAR, and sister F. Burcu NACAR YÜCE, who stand behind and support me in any condition and under any circumstances. Last but not least, my special thanks go to my beloved husband, Murat ÇIKAN, for his boundless love and unquestioning support, all through my life.

**CONTENTS** **PAGE**

ABSTRACT ..... I
ÖZ ..... II
EXTENDED SUMMARY ..... III
GENİŞLETİLMİŞ ÖZET ..... VII
ACKNOWLEDGMENTS ..... XI
CONTENTS ..... XII
LIST OF TABLES ..... XVI
LIST OF FIGURES ..... XVIII
LIST OF ABBREVITIONS ..... XXII
1. INTRODUCTION ..... 1
1.1. Access Technologies ..... 1
1.2. Passive Optical Networks ..... 5
1.2.1. Classification of Passive Optical Network Architectures ..... 6
1.2.1.1. Time Division Multiplexed Passive Optical Network ..... 7
1.2.1.2. Wavelength Division Multiplexed Passive Optical Network 10
1.3. Motivation of the Thesis and Contributions ..... 13
1.4. Thesis Outline ..... 14
2. COLORLESS SOURCES BASED ON WDM PON ..... 17
2.1. Self- Emitting Technique ..... 18
2.1.1. Spectrum-slicing Technique ..... 18
2.1.2. Tunable Laser Sources ..... 20
2.1.3. Research on Self-Emitting Technique ..... 21
2.2. Self-Seeded WDM PON Technology ..... 22
2.2.1. Transmission Limitations of RSOA ..... 25
2.2.1.1. Faraday Rotator Mirror ..... 26
2.2.1.2. Array Waveguide Gratings ..... 27
2.2.1.3. Rayleigh Backscattering ..... 28

2.2.1.4. Chromatic Dispersion ..... 29
2.2.1.5. Cavity Losses ..... 31
2.2.1.6. Reflective Crosstalk ..... 31
2.2.1.7. Extinction Ratio ..... 34
2.2.1.8. Length of The Cavity ..... 34
2.2.1.9. Coupling Ratio ..... 34
2.2.1.10. Longitudinal Modes ..... 35
2.2.1.11. Narrow Band ASE ..... 35
2.2.1.12. Gain Compression ..... 35
2.2.1.13. Filter Type ..... 35
2.2.1.14. Polarization Sensitivity ..... 36
2.2.2. Research on Self-Seeded RSOA ..... 36
2.3. Seeding Light from Central Office (Loop Back) ..... 39
2.3.1. Remodulation Technique ..... 41
2.3.1.1. Injection-Locking ..... 42
2.3.2. Research on Loop Back Technique ..... 43
2.4. Comparison of Colorless Methods ..... 43
3. CHARACTERISTICS AND DATA ERASURE ANALYSIS OF REFLECTIVE SEMICONDUCTOR OPTICAL AMPLIFIER ..... 45
3.1. Historical Background of RSOA ..... 45
3.2. The Theory of RSOA ..... 47
3.3. Data Erasure Analysis of RSOA in Bidirectional WDM PON System ..... 53
3.3.1. System Setup ..... 54
3.3.2. Results and Discussion ..... 57
4. FABRY PEROT LASER DIODE CHARACTERISTICS ..... 63
4.1. The Characteristics of the FPLDs ..... 63
4.2. Injection-Locked Technique ..... 68
4.2.1. Injection Locking on FPLD ..... 69
4.2.2. Weak Resonant Cavity FPLD ..... 70

4.2.3. Theoretical Model of IL-FPLD ..... 70
5. DATA ERASURE ANALYSIS OF FPLD BASED ON REMODULATION BIDIRECTIONAL PON SYSTEM ..... 75
5.1. Overview ..... 75
5.2. System Setup ..... 77
5.3. Results and Discussion ..... 79
6. DATA ERASURE IN FABRY-PEROT DIODE LASERS: EFFECTS OF FACET REFLECTIVITY ..... 91
6.1. Overview ..... 91
6.2. System Setup ..... 93
6.3. Results and Discussion ..... 95
7. CONLUSION ..... 107
REFERENCES ..... 111
BIOGRAPHY ..... 139
APPENDIX ..... 140

**LIST OF TABLES** **PAGE**

Table 1.1. Comparison of popular access technologies ..... 9
Tablo 2.1. Comparison of colorless methods and sources. ..... 44
Table 3.1. RSAO Specifications ..... 56
Table 4.1. FPLD Spesifications ..... 73

**LIST OF FIGURES** **PAGE**


Figure 1.1. The architecture of communication network; CO: central office ..... 2
Figure 1.2. Global consumer internet traffic ..... 3
Figure 1.3. The internet usage in a minute, a: In the year of 2019, b: In the year of 2020 ..... 4
Figure 1.4. Passive optical network general system structure ..... 6
Figure 1.5. TDM PON architecture design ..... 7
Figure 1.6. The progress of PON technology ..... 10
Figure 1.7. WDM PON system architecture ..... 11
Figure 2.1. Classification of colorless methods for WDM PON technology ..... 18
Figure 2.2. BLS optical sources embedded in ONUs in a PON system ..... 19
Figure 2.3. Operation of spectrum slicing method ..... 19
Figure 2.4. Schematic diagram of self-seeded RSOA based on WDM PON ..... 23
Figure 2.5. Schematic of Faraday Rotator Mirror ..... 27
Figure 2.6. Schematic of AWG architecture ..... 28
Figure 2.7. Chromatic Dispersion cause the pulse to broaden. The input pulse to the fiber is given on the left and the output pulse from the fiber is given on the right ..... 30
Figure 2.8. Block diagram for a. delay method; b. differentiation method (feedforward) ..... 32
Figure 2.9. Block diagram for adaptive feedback approach ..... 33
Figure 2.10. Remotely seedings: a. separate wavelength for upstream&downstream; b. reusing of downstream carrier ..... 40
Figure 2.11. Remodulation method utilizing RSOA as a transmitter ..... 41
Figure 3.1. Schematic of RSOA device. One of the facets is HR and the other is AR coated ..... 45

Figure 3.2. The transitions between bands in a semiconductor: (a) absorption, (b) spontaneous emission and (c) stimulated emission ..... 48
Figure 3.3. Lorentz g (ω) gain profile and corresponding gain spectrum amplifier G (ω) ..... 50
Figure 3.4. RSOA Saturation Curve ..... 51
Figure 3.5. RSOA as a transmitter in bidirectional WDM PON ..... 55
Figure 3.6. Gain plot of RSOA with regard to: a. bias current, b. injected power ..... 58
Figure 3.7. Extinction ratio versus bias current plot at different values ..... 59
Figure 3.8. BER versus bias current plot ..... 60
Figure 3.9. BER versus received power plot ..... 61
Figure 3.10. $ER_d$ versus biased current plot at different CF and $P_{inj}$ values ..... 62
Figure 4.1. The design of the FPLD ..... 64
Figure 4.2. The basic schematic of FPLD: optic medium with end mirrors ..... 65
Figure 4.3. a. The gain spectrum, b. produced lasing modes ..... 66
Figure 4.4. Simulation result of ASE spectrum sliced, free running and injection locked FPLD ..... 74
Figure 5.1. Carrier remodulation system based on bidirectional WDM PON using FPLD at ONU ..... 78
Figure 5.2. FPLD gain characteristics; a: reflective facet %93; b: reflective facet %0.2 ..... 80
Figure 5.3. Power versus current response of FPLD; a: reflective facet %93; b: reflective facet %0.2 ..... 82
Figure 5.4. Eye diagrams and downstream residual ER&FPLD bias current plot at different injection power levels; a: reflective facet %93; b: reflective facet %0.2 ..... 84

Figure 5.5. Eye diagrams and downstream residual extinction ratio result for different ER and Pinj levels ..... 85
Figure 5. 6. BER result at OLT for several injection power levels ..... 86
Figure 5.7. Upstream BER results vs. received power at OLT for 50 mA FPLD biased current ..... 88
Figure 5 8. Downstream ER vs. Bias current for different values of CF and Pinj ..... 89
Figure 6.1. Remodulation technique based WDM PON system employing FPLD at ONU ..... 94
Figure 6.2. Output power& biased current plot of free running FPLD: a. Front facet reflectivity between 0.2%-7%; b. Front facet reflectivity between 25%-90%. ..... 96
Figure 6.3. Output power& biased current plot of free running FPLD at front facet reflectivity between 0.8%-15%; a. Biased current smaller than 20 mA; b. Biased current bigger than 20 mA ..... 97
Figure 6.4. Output power& biased current plot of injection locked FPLD: a. Front facet reflectivity between 0.2%-7%; b. Front facet reflectivity between 8%-12%; c. Front facet reflectivity between 15%-90%. ..... 99
Figure 6.5. Output power& biased current plot of injection locked FPLD with <-10 dB: a. Front facet reflectivity between 0.2%-7%; b. Front facet reflectivity between 15%-90%. ..... 100
Figure 6.6. WRC FPLD without data: a. Front facet reflectivity & Downstream residual ER; b. Front facet reflectivity & Q factor; c. Eye diagrams ..... 102
Figure 6.7. WRC FPLD with 2.5 Gb/s NRZ data: a. Front facet reflectivity & Downstream residual ER; b. Front facet reflectivity & Q factor; c. Eye diagrams ..... 104

**LIST OF ABBREVITIONS**

| | |
|---|---|
| ADSL | : Asymmetric Digital Subscriber Line |
| CO | : Central Office |
| CAGR | : Compound Annual Growth Rate |
| M2M | : Machine-to-Machine |
| DSL | : Digital Subscriber Line |
| PON | : Passive Optical Network |
| VDSL | : Very High Bit Rate Digital Subscriber Line |
| FTTx | : Fiber to the x |
| PtMP | : Point to Multipoint |
| PtP | : Point to Point |
| OLT | : Optical Line Terminal |
| RN | : Remote Node |
| ONU | : Optical Network Unit |
| TDM | : Time Division Multiplexed |
| WDM | : Wavelength Division Multiplexed |
| DWDM | : Dense Wavelength Division Multiplexed |
| FDM | : Frequency Division Multiplexed |
| OFDM | : Orthogonal Frequency Division Multiplexed |
| EPON | : Ethernet Passive Optical Network |
| BPON | : Broadband Passive Optical Network |
| GPON | : Gigabit Passive Optical Network |
| ITU | : International Telecommunication Union |
| IL | : Injection Locking |
| CF | : Confinement Factor |
| ER | : Extinction Ratio |
| FPLD | : Fabry Perot Laser Diode |
| RSOA | : Reflective Semiconductor Optical Amplifier |

| | |
|---|---|
| IoT | : Internet of Things |
| DFB | : Distributed Feedback |
| TLS | : Tunable Laser Source |
| ASE | : Amplified Spontaneous Emission |
| LED | : Light Emitting Diode |
| DBR | : Distributed Bragg Reflector |
| SS-RSOA | : Self Seeded Reflective Semiconductor Optical Amplifier |
| AWG | : Array Waveguide Grating |
| FRM | : Faraday Rotator Mirror |
| HPDG | : High Polarization Dependent Gain |
| FBG | : Fiber Bragg Gratings |
| TFM | : Thin Film Filters |
| RBS | : Rayleigh Backscattering |
| CD | : Chromatic Dispersion |
| EVM | : Error Vector Magnitude |
| PSSL | : Pre-Spectrum Slicing Source |
| BER | : Bit Error Rate |
| FEC | : Forward Error Correction |
| REAM | : Reflective Electro Absorption Modulator |
| ASK | : Amplitude Shift Keying |
| SOA | : Semiconductor Optical Amplifier |
| BPSK | : Binary Phase Shift Keying |
| FSK | : Frequency Shift Keying |
| SCM | : Subcarrier Multiplexing |
| HR | : Highly Reflective |
| AR | : Anti Reflective |
| TE | : Transverse Electric |
| TM | : Transverse Magnetic |
| CB | : Conduction Band |

VB : Valence Band

FWHM : Full Width at Half Maximum

NF : Noise Figure

SNR : Signal to Noise Ratio

ONU : Optical Network Terminal

OpEX : Operational Expenditure

CapEX : Capital Expenditure

WRC : Weak Resonant Cavity

OOK : On-Off-Keying

MZ : Mach-Zehnder

NRZ : Non-Return-to-Zero

**NOTATIONS**

$\beta$ : Mode propagation constant

$\lambda$ : Wavelength

$v_g$ : Group velocity

$n_g$ : Group index

$g_0$ : Peak gain

$\omega_0$ : Frequency of transition between energy bands

n : Refractive index

L : Cavity length

$\Delta N$ : Carrier number above threshold

G : Linear gain coefficient

$\alpha$ : Linewidth enhancement factor

$\gamma$ : Loss factor

$k_c$ : Coupling efficiency

$\Gamma$ : Confinement factor

$\chi$ : Material susceptibility

$\mu_0$ : Vacuum permeability

$\varepsilon_0$ : Vacuum permittivity

$\sigma$ : Conductivity

# 1. INTRODUCTION

The necessity of communication networks has increased over the years. The vital impact of communication networks on global society and the economy has shown escalation in the world. Society and companies have started to use social media actively. There has been a huge increase in data transmission and reception in a minute with the start of business and education activities mostly over the Internet. Especially, the new technologies such as the internet of things applications will increase the data traffic exponentially. The researchers, business services, and communication providers are continuously working on new solutions to deal with huge data traffic.

In this chapter, the summary of the communication structure is explained in a logical way. The communication system structure is divided into three sections. These are named as core, metro and access networks. At the beginning, the history of the access networks, the consisting parts of the communication structure, and in the subsection, solutions to the growing internet demand are presented.

## 1.1. Access Technologies

The access networks link communication providers with the user ends. Increasing multimedia applications leads to customers to need wider bandwidth and lower-cost access(Kazovsky et al., 2011). A range of access technologies has emerged to fulfill these growing demands. The communication network structure consists of three categories as demonstrated in figure 1.1(Kazovsky et al., 2011). The first segment is the core network that links continents, nations, and, big cities. The second segment links the central offices (CO) in metro networks using a ring topology. The third segment links the end-users in the access network to the service providers' COs.

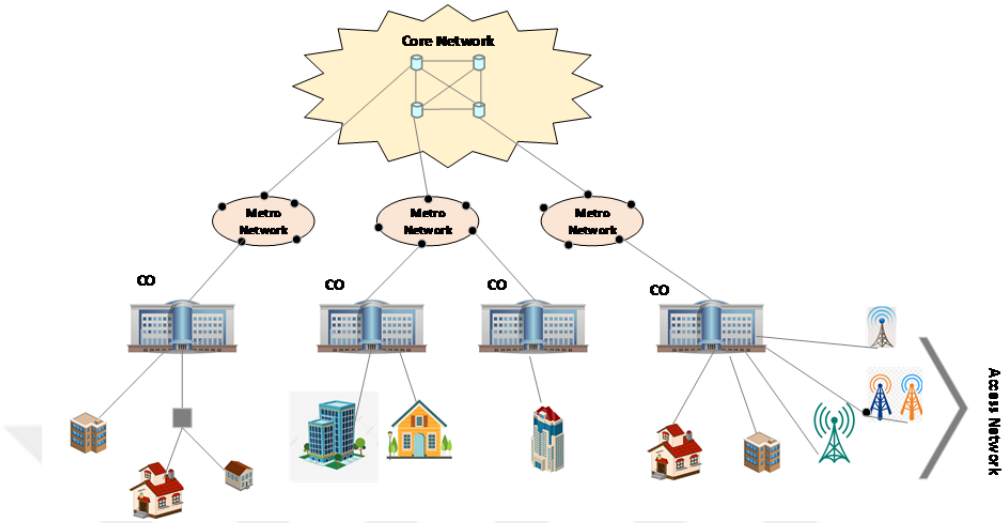



Figure 1.1. The architecture of communication network; CO: central office

The core network transfers massive quantities of data over the continents. It leans on optical fiber technologies and reaches very long distances. The second segment delivers a large amount of data through the core network to metro networks as demonstrated in Fig. 1.1. It also accumulates and carries data from the access network to the core network. The last segment carries the data from end-users to the COs or vice versa. All these investments to convey the data cause a great cost. End-users have to pay the access connection price, and that prevents service providers to make expensive investments. This has prompted service providers and researchers to focus on systems, which have relatively high data rates, and can reach longer distances at low budgets. Various service companies apply different economical solutions to deliver the demanded bandwidth. These solutions differ depending on the type of subscriber such as home, company, workplace, building, etc.

The increasing demand for high bandwidth has urged the improvement of new technologies to appease the exponential rise in demand. The access network segment is often considered as a multi-technology zone, due to the broad range of technologies(Gumaste and Antony, 2004). Fig. 1.2 demonstrates the global

connection growth from 2018 to 2023(Cisco, 2020, March 9). The device connection will increase as a 10% Compound Annual Growth Rate (CAGR) from 2018 to 2023. It is estimated that two out of three of the worldwide people will have internet connectivity until 2023 and the IP traffic will be triple times of the world population(Cisco, 2020, March 9). The machine-to-machine(M2M) connection will hold a large part (about 50%) of internet usage. The smartphone usage will take place in the second row. This will be followed by TVs with 11%, non-smartphone with 5%, PCs with 4%, other devices with 3.9%, and tablets with 3%.

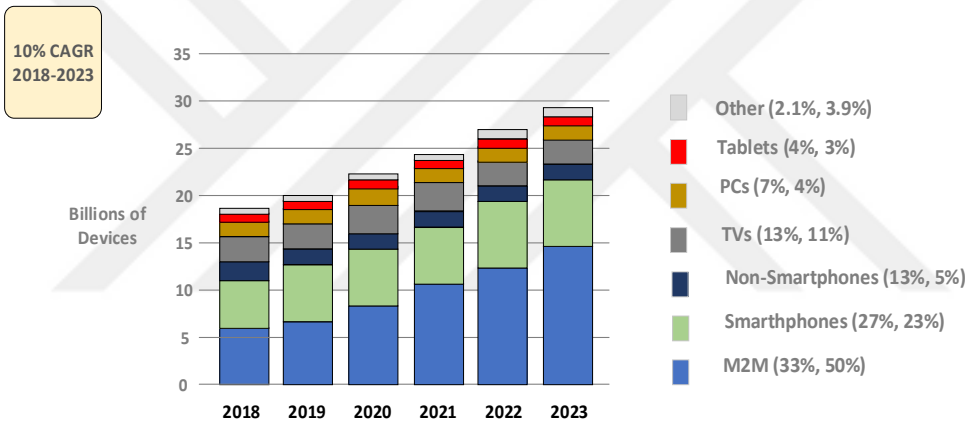



Figure 1.2. Global consumer internet traffic (2018-2023)

Internet usage in a minute in the year 2019 and 2020 is demonstrated in figure 1.3(Lorilewismedia, 2020). The increase in various applications usage is pretty amazing. For instance, application usage in a minute shows increment as follows: google usage increased from 3.8 million to 4.1 million, YouTube usage increased from 4.5 million to 4.7 million, message usage increased from 41.6 million to 59 million and Facebook usage increased from 1 million to 1.3 million(Lorilewismedia, 2020). All these applications require a very large bandwidth. In addition, each year different applications are presented to the users

depend on meeting the needs of the era. Overall, internet usage and devices that need the internet connection will largely increase over the period of time.

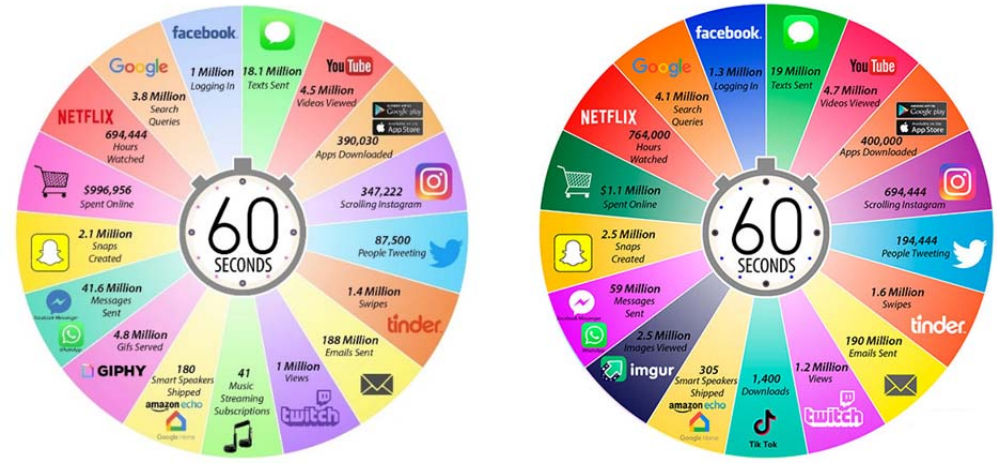



Figure 1.3. The internet usage in a minute, a: In the year of 2019, b: In the year of 2020(Lorilewismedia, 2020)

Cheap and fast internet access is an important issue to enjoy having all these applications. Copper-based access solutions such as digital subscriber line (DSL) are still in use in some parts of the world. The communication service providers apply different technologies to distribute the necessary bandwidth. The applied technology can differ depending on the customer type as a business, apartment, home, and office. The communication networks need to develop with time due to the various applications and increased number of internet users. Especially, the access network part of the communication system must be easily upgradable and open to new implementations. The copper-based networks are not able to deal with the increasing demand any longer. Therefore, the fiber access technology has emerged to present solutions to the demands.

### 1.2. Passive Optical Networks

The most common forms of DSL are very high bit-rate digital subscriber line (VDSL) and asymmetric digital subscriber line (ADSL). ADSL provides asymmetric data transmission and can deliver data and telephone service over the same line. VDSL provides the fastest data transmission among the DSL services. However, copper-based infrastructure cannot reach high-speed data rates. Therefore, optical fiber technology is proposed to overcome the copper-based problems.

The optical fibers have particular properties such as low weight, small size, low loss, secure and broad bandwidth that make them excellent candidates to solve the capacity problems for present and future. The single-mode fiber has been deployed to metro and core networks and there are also attempts to deploy it in the access part of the system. The widely used name is fiber to the x (FTTx), where x refers to distance of the fiber to the customers such as home, curb, premises, building, and so on(Lin, 2006; Europe, 2014). The fiber cable distribution could be in point to multipoint (PtMP) or point to point (PtP). PtP distribution causes high costs due to the usage of the dedicated device per user. Active optic network also requires a powered device that causes cost as well. The most economical and uncomplicated way to distribute fibers is provided by the passive optical network (PON). The PON employs the passive star structure that benefits from PtMP architecture.

Access networks based on PON is an effective technology that can fulfill the high bandwidth demands and introduced in 1988 for the first time (Stern et al., 1988). The fundamental characteristic of the PON is existence of particular passive items in the territory, which work without using electric power. PON systems provide low noise, low loss, passive components and, larger bandwidth. Thus, the PON infrastructure is deployed widely in recent years.

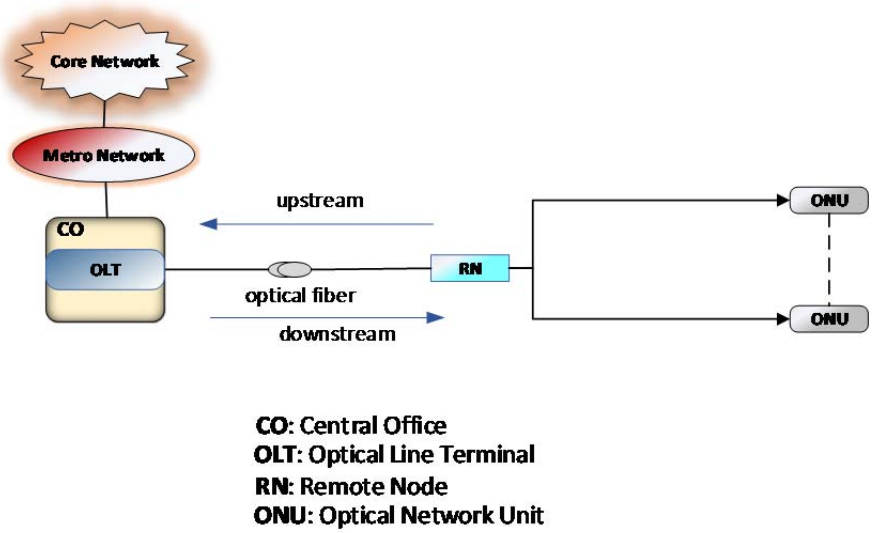



Figure 1.4. Passive optical network general system structure

The general design of the PON topology is given in figure 1.4. The core network delivers the data among the continents, the metro network delivers among cities and the access network part delivers the data to the end-users. OLT is settled at the CO and transmits data towards the optical ONU. Passive components are implanted at the RN. The information flow from CO to ONU can be explained as downstream and the data traffic from ONU to OLT can be explained as upstream traffic. The data transmission and reception can be transmitted using multiplexing techniques.

### 1.2.1. Classification of Passive Optical Network Architectures

The PON technology can be divided into three classes as time division multiplexed (TDM), wavelength division multiplexed (WDM), and frequency division multiplexed (FDM). The orthogonal subcarriers are employed to transmit data in orthogonal frequency division multiplexed (OFDM) systems. The two main types of PON multiplexing techniques are TDM and WDM. In the following section, the details of these two dominant techniques are discussed.

#### 1.2.1.1. Time Division Multiplexed Passive Optical Network

TDM PON has been the most prevalent architecture due to its advantages such as simplicity. Each user has its own time slot on the common medium, shown in figure 1.5. The OLT broadcasts the data to the users at ONUs. The end-users detect and receive the time frames allocated for them. The user recognizes the data with address labels and processes these labels. In the upstream transmission, the signals from the ONUs must be adjusted and synchronized to abstain from any interference. The sizes of the time slots may vary depending on the users' requirements. This procedure is defined as dynamic bandwidth allocation controlled by the central office.

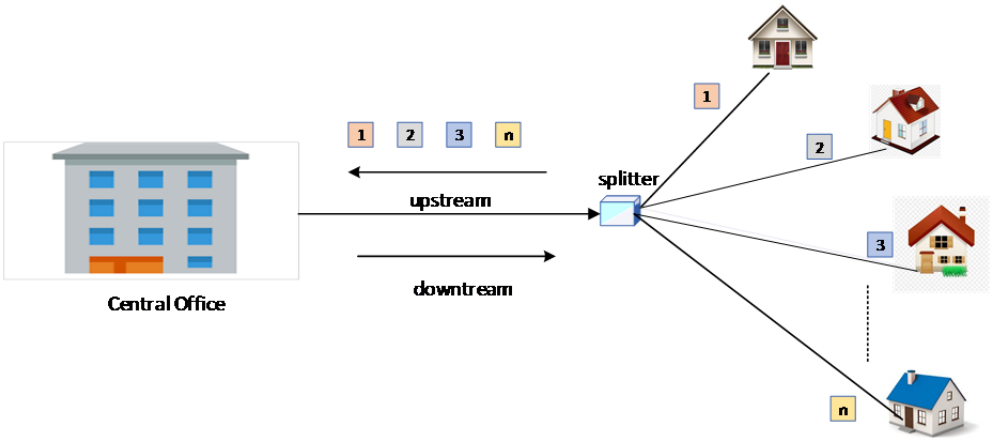



Figure 1.5. TDM PON architecture design

The main TDM PON types are Ethernet PON(EPON), broadband PON(BPON), and gigabit PON(GPON)(Trojer et al.; Koonen, 2006; Iwatsuki and Kani, 2009; Elbers, 2010). BPON used as the first architecture in commercial deployment and standardized by international telecommunication union (ITU). EPON based on 802.3 standards and uses Ethernet packets with 1.25 Gb/s bidirectional transmission. GPON is based on ITU standards. It provides higher

bandwidth when compared with other services. The comparison of the TDM PON standards is as follows.

- BPON
  - Standardized by ITU-T G.983 (ITU-T, 2019, April 11)
  - Based on ATM protocol
  - The data rates are upstream at 155 Mb/s and downstream at155-622 Mb/s
  - It has between 1490 nm and 1550 nm downstream wavelengths
  - It has 1310 nm upstream wavelength
- EPON
  - Standardized by IEEE 802.3 ah (IEEE SA, 2004)
  - Based on Ethernet protocol
  - The symmetric data rates are 1.25 Gb/s for downstream and upstream
  - It has 1550 nm downstream wavelength
  - It has 1310 nm upstream wavelength
- GPON
  - Standardized by ITU-T G.984 (ITU-T, 2020,February 10)
  - The data rates are at 1.25 Gb/s upstream and 2.5 Gb/s downstream
  - Employ ATM, Ethernet and GEM protocols
  - It has between 1490 nm and 1550 nm downstream wavelengths
  - It has 1310 nm upstream wavelength

TDM PON technique has deployed widely in the world. However, TDM PONs have some disadvantages that impede them to be applied in the future (Soo-Jin et al., 2004; Lee et al., 2006; Lam, 2011). The disadvantages of TDM PON can be listed as follows.

- The usage of the same wavelength among the users decreases the security and data rates.
- The power losses due to the optical splitter also restrain the maximum reach of the signals.
- Bandwidth sharing protocol increases the complexity.
- The requirement of prompt synchronization between users.
- Sharing the same wavelength increases the complexity of the bandwidth allocation.

The comparison of TDM PON and DSL technologies are given in Table 1 (Consortium, 2007; Mr. G. Pesavento, 2007; Management Association, 2010; ITU-T, 2019, April 11).

Table 1.1. Comparison of popular access technologies

| Service | | Downstream (Mbps) | Upstream (Mbps) | Max.Reach (km) |
|---|---|---|---|---|
| **ADSL** | Twisted pair | 8 | 0.896 | 5.5 |
| **ADSL2** | Twisted pair | 25 | 3.8 | 5.5 |
| **VDSL1** | Twisted pair | 50 | 30 | 1.5 |
| **VDSL2** | Twisted pair | 100 | 30 | 0.5 |
| **HFC** | Coaxial cable | 40 | 9 | 25 |
| **Wi-Fi** | Free space | 54 | 54 | 0.1 |
| **WiMAX** | Free space | 134 | 134 | 5 |
| **BPON** | Fiber | 1244 | 622 | 20 |
| **GPON** | Fiber | 2488 | 1244 | 20 |
| **EPON** | Fiber | 1250 | 1250 | 20 |

The GPON technology's data speed is upgraded to 10 Gb/s which is called as XG-PON. The XGPON is divided into two sections as XGPON1 and XGPON2. However, only the XGPON1 is standardized. Hence, XGPON took place in the subclass of next generation PON1(NGPON1). The NGPON1 increased the splitting ratio of the system and data rates for each user. However, the previously deployed TDM receivers limit the XG-PON.

To summarize, the progress of TDM-PON technology over time is shown in figure 1.6.

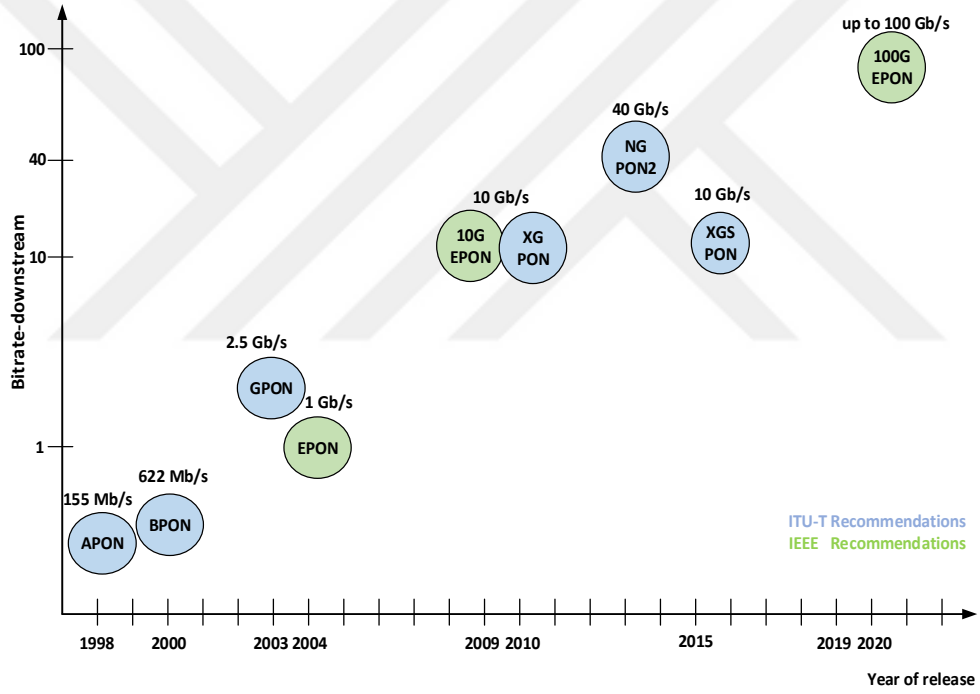



Figure 1.6. The progress of PON technology

### 1.2.1.2. Wavelength Division Multiplexed Passive Optical Network

Nowadays, telecommunication companies are searching for ways to deliver cheap, continuous, and larger bandwidths to their customers. WDM PON has emerged because of having many advantages such as providing point-to-point

communication and separate wavelengths for each user, which ensures higher bandwidth for costumers.

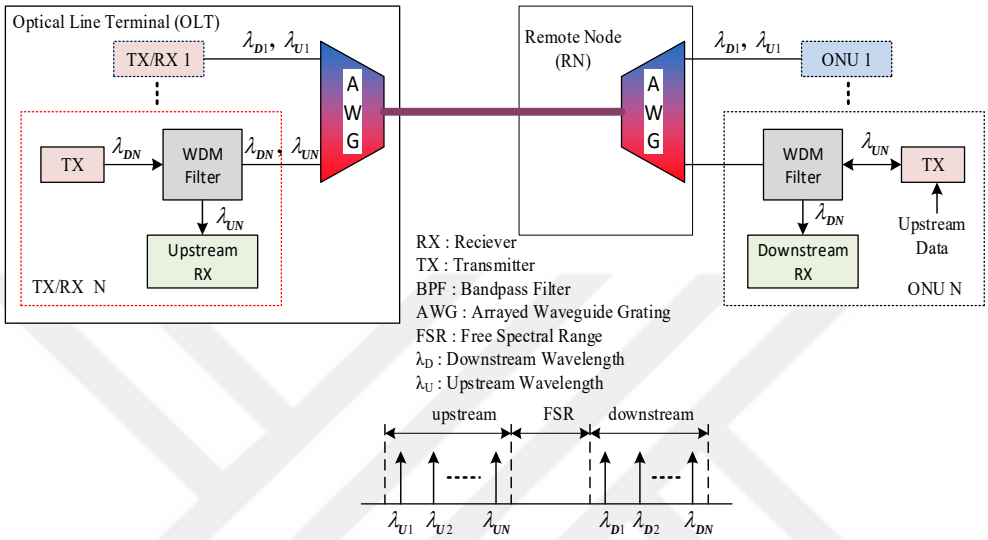



Figure 1. 7. WDM PON system architecture

WDM technology proposed in (Frigo et al., 1994) for the first time. As demonstrated in the figure 1.7, each ONU communicates with OLT that has a dedicated separate wavelength. Essentially, a virtual PtP link is established between ONU and OLT in a PtP structure. Each ONU can enjoy having the highest data rate, and prop various services like coaxial and wireless.

The transmission from OLT to ONU is ensured with an array of tunable laser sources (TLS) placed at CO. The array waveguide grating (AWG) or filters at the RN separate the wavelengths and assign them to the ONUs. The AWGs have a cyclic feature which provides the transmission of downstream and upstream in different wavelengths. Each ONU has its own transmitter and receiver parts. The upstream data is modulated onto separate wavelength at ONU and send the modulated signal back to the receiver part of the OLT. WDM method provides

each user with high bandwidths such as 1 Gb/s. The system works as P2MP at TDM method.

Unlike TDM PON, WDM PON applies a PtP connection, which builds up security in lines. The capacity of the network can easily be upgraded as well.

The advantages of WDM PON can be listed as follows:

- Provides dedicated bandwidth and privacy
- Transparency on protocols
- Upgradability of the system
- Longer transmission distance
- Higher bandwidth
- Less complexity
- AWG provides high fault tolerance
- Easy management of the system
- Secure communication

All of these advantages make WDM PON the perfect option for future wideband access networks. However, a lot of daunting problems still need to be tackled before it can be implemented widely around the world. The WDM-PON might not be profitable compared to the TDM-PON, due to the comparatively higher costs for the dedicated wavelength usage and permanent light sources needed at the ONUs. Cost is the main problem when implementing and deploying WDM PONs. Therefore, the colorless operation has been proposed to solve the cost problem at user sides. In addition, a significant amount of data needed to be transmitted over the internet network with the improvement of various applications such as video conferencing. But broad bandwidth and efficient transmission are required to enhance network capacity. WDM PON allows only the PtP transmission between ONU and OLT. Hence, WDM PON experience single-mode

data transmission. The transmission limits network capability when multiple modes are required.

### 1.3. Motivation of the Thesis and Contributions

The access networks based on optical fibers are crucial to meet the increasing bandwidth demand by users. Currently deployed access networks are low-priced but limited in capacity and not easily upgradable. Therefore, WDM PON technology which provides security and upgradability is offered as a solution to be deployed in access networks. Although WDM PON technology has many advantages, the implementation of this technology into the access part is created difficulties due to mainly two reasons as high infrastructure and transmitter costs.

The main focus of this thesis is to figure out the way of designing an economical WDM PON system by exploring cheap, feasible and simple colorless transmitters. The achievements of this dissertation are shortly presented as follows:

- The development of transmitters with variable wavelengths has been offered as a solution. These access network components are named as colorless transmitters and can perform in an extensive wavelength range. In this way, identical transmitters, which lowers the system cost and simplifies the system, are used.
- By using the remodulation model, the system cost has been reduced by avoiding the use of separate carriers in the download and upload directions.
- Although the application of colorless sources in a remodulation model as an upstream transmitter partially solved the cost problem, there were still some problems that degrade the transmitter performance. Injection-locking (IL) has also been proposed to enhance the transmission performance of the transmitters. IL is an innovative method that provides high-speed transmission and overcomes the degrades in transmission performance.

- Using the identical carrier in the remodulation model causes crosstalk. For this reason, the downstream data remaining on the carrier must first be erased in the ONU and then used again to modulate the upstream data. While performing this process, the data deletion skills of colorless sources have been studied instead of using an external data eraser device, which increases the system cost at ONU.
- The impacts of many factors, such as the confinement factor (CF), biasing current, injection power, and extinction ratio (ER), on data deletion abilities of FPLD and RSOA have been discussed.

### 1.4. Thesis Outline

Chapter 1 introduce an overall presentation to communication networks and summarizes the passive optical network structure. The PON technology is investigated by dividing mainly into two types as TDM PON and WDM PON.

Chapter 2 presents the motivation behind colorless technology based on WDM PON. Colorless sources can be considered as devices covering a wide spectrum of wavelengths. WDM PON systems are required to use colorless sources to be widely applied since they can provide low-cost operation and installation. Especially these colorless sources are applied to ONUs to provide low-cost communication to customers. In this chapter, a general classification of colorless sources and a comparison of them are studied in detail.

Chapter 3 deals with reflective semiconductor optical amplifiers (RSOAs). It shortly presents how these devices work and affect the optical communication networks as a colorless source. Firstly, the working principle and the theory of RSOA are presented. The usage of identical wavelength for both downstream wavelength and upstream wavelength degrades the performance due to the interference between DS and US carrier wavelength in a remodulation system. This is due to the modulated downstream data that may not be erased fully in remodulation scheme. It is difficult to examine the downstream data deletion skill

of RSOA in experimental work. Hence, in this study, the data deletion analysis of RSOA in a remodulation model is investigated. RSOA performance and behavior are affected by several factors. In this chapter of the thesis, these parameters that affect the erasure of the residual downstream data inside the RSOA is investigated.

Chapter 4 discusses the characteristics of FPLD and IL-FPLD. FPLD has advantages such as low power consumption, simplicity, high data rates, and low cost. Thus, it provides an efficient and powerful solution to the user ends in a WDM PON network. However, the application of the FPLD is limited due to its multimode operation. This operation can increase the intensity noise and decrease the bandwidth and power budget. To overcome these problems, the injection of the laser diode to one mode is proposed. Locking laser to a specific wavelength decreases the chirping, noise, and increase the modulation bandwidth. Thus, the data rate improves with reduced device and maintenance cost. In this section of the thesis, the FPLD is studied in detail. Firstly, the theory of the FPLD is explained. Secondly, the injection-locked FPLD is investigated.

Chapter 5 presents the data deletion skills of FPLD. It has been investigated in a WDM PON network which is using the remodulation technique. The data-deletion technique is a feasible cost-effective choice for prospective broadband networks. Many parameters affecting the data deletion efficiency of FPLD were examined and the obtained results were discussed. One of the important contributions of the thesis to the literature is to show the results of the FPLD which has a highly increased front mirror facet. The system speed is set as 5 Gb/s. The power has been injected into the system was started from - 25 dBm and was increased up to 0 dBm. The biasing current of the system was applied as between 20 mA and 100 mA. Successful upstream communication has been achieved when biasing current higher than 30 mA was applied and power was injected less than 0 dBm. Increasing the bias current applied to FPLD created the extinction ratio to decrease below 0.5 dB, which was the desired result.

Chapter 6 presents the impacts of facet reflectivity on FPLD 's data deletion ability. First, no upstream data was applied to the laser to see exactly how much the FPLD deleted the remaining data. Next, 2.5 Gb / s of data was applied and the results were compared. It was determined that FPLD had the best performance when the front mirror face values were kept between 0.2% and 7%.

Chapter 7 summarizes the thesis. It also introduces a perspective for prospective works.

## 2. COLORLESS SOURCES BASED ON WDM PON

WDM PON technology has been considered a promising solution for access networks. Researchers and communication companies have put a lot of work into creating feasible WDM PON technologies in different ways. These technologies include spectrum sliced, injection locked, externally seeded, self-seeded and wavelength reused ONU sources. A review of these subjects is studied with detail in this chapter.

The PtP communication in WDM-PON systems requires that each ONU performs on a particular wavelength, which is determined by the specific port of the AWG. Using optical source with a certain wavelength at ONU, such as a distributed feedback (DFB) laser, is offered as a solution. However, the laser mostly needs a thermoelectric cooler for stable transmission. Furthermore, the wavelength-locker is required to operate the laser at a specified wavelength(Amitabha Banerjee, 2005). Despite the fact that DFB lasers provide higher speeds in modulation, they cost a lot because many DFBs need to be used in the system and each laser must be operated separately. Using a laser with different wavelengths for each channel of WDM PON is expensive, complex and difficult to maintain. Although customers demand limitless bandwidth, they do not want to pay more than their previous service. For these reasons, researchers and companies have sought ways to provide low-cost communication.

Colorless ONU has been presented as a solution to decrease the cost of the WDM PON systems because identical optical sources can be applied to user ends and the designated wavelengths can be managed by the central office. Colorless sources can be considered as devices covering a wide spectrum of wavelengths. WDM PON systems are required to use colorless sources to be widely applied since they can provide low-cost operation and installation. Especially these colorless sources are applied to ONUs to provide low-cost communication to customers. In the subsection, a general classification of colorless sources and a

comparison of them are given in detail. The main categories of the colorless methods based on WDM PON technology can be classified as in figure 2.1.

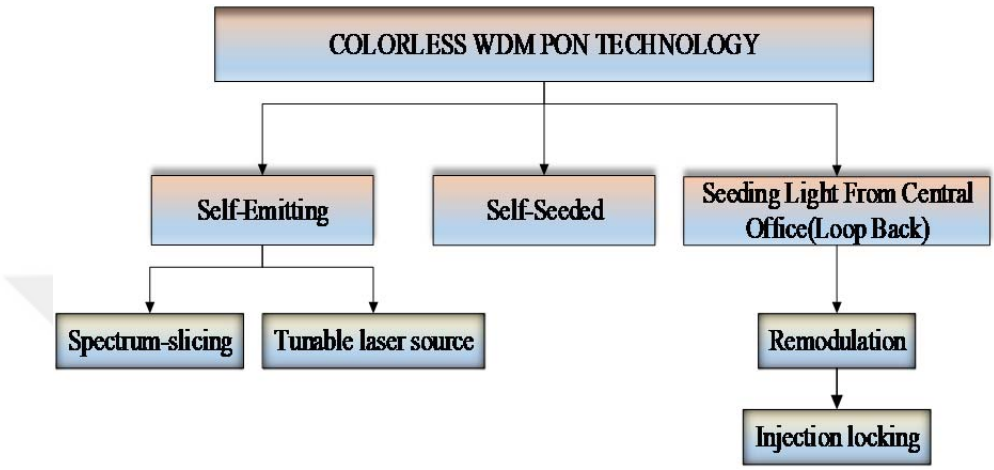



Figure 2.1. Classification of colorless methods for WDM PON technology

### 2.1. Self- Emitting Technique

The self-emitting of colorless method can be classified in two categories as spectrum slicing technique and TLS.

#### 2.1.1. Spectrum-slicing Technique

The spectrum-slicing technique has been introduced to fulfill the cost criteria of the PON systems. In this structure, comparatively cheap broadband light sources (BLS) are generally located at each user ends. The types of BLSs can be listed as superluminescent diodes (SLDs), amplified spontaneous emission sources (ASE) such as semiconductor optical amplifiers (SOAs), light-emitting diodes (LEDs), and Fabry-Perot Laser Diodes (FPLDs)(Reeve et al., 1988; Wagner and Chapuran, 1990; Zirngibl et al., 1995; Feldman et al., 1998; Jung et al., 1998; Woodward et al., 1998; Jung et al., 2000; Han et al., 2004; Park et al., 2007). The upstream data can be modulated on these optical sources. For instance, a portion of

the light emitted from a LED match with a channel of the AWG as demonstrated in figure 2.2.

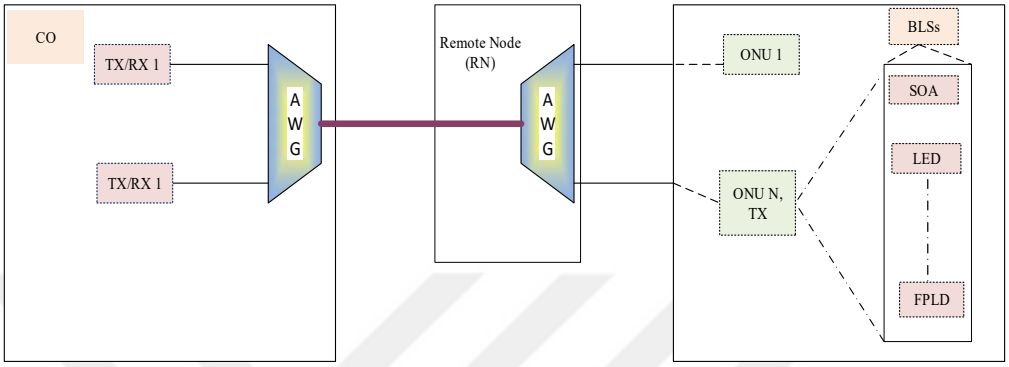



Figure 2.2. BLS optical sources embedded in ONUs in a PON system

The operation of the BLS, which is located at the ONU or OLT in a PON system, is shown in Figure 2.3(Bobrovs et al., 2013).

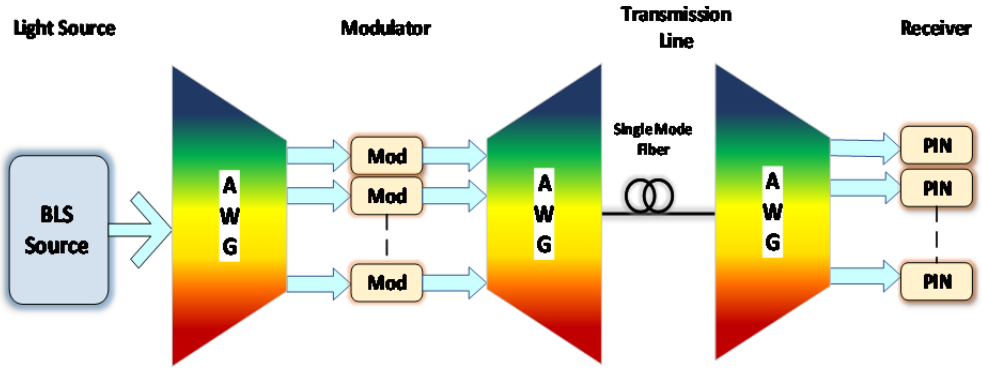



Figure 2.3. Operation of spectrum slicing method

The specific wavelength emitted from LED depends on the AWG channel where LED is connected. Identical optical sources can be used at ONUs and thus colorless activity is performed. Spectrum slicing technique is an efficient way to reduce the problems of managing several lasers that have different wavelengths. The sources used in the spectrum slicing technique are cheap and simple devices.

However, these transmitters cannot reach high speeds and long distances. The power budget is considerably reduced due to the attenuation that occurs during filtering. In addition, since these ASE sources have a wide bandwidth, RIN noise, and chromatic dispersion occurs during the spectrum slicing process. Moreover, ASE causes additional amplitude noise in the receiver. Therefore, bit rates cannot reach higher data rates and have not been further interested in by researchers.

### 2.1.2. Tunable Laser Sources

Tunable lasers are presented as colorless sources for WDM PON systems. The identical TLSs can be applied to all end users. The wavelength of the end-user is determined in the mounting process of TLSs.

TLSs have capabilities to tune wavelength very fast and dynamically reconfigure the wavelength assignment (Venghaus and Grote, 2012). However, TLSs are expensive devices and the cost should be decreased to be used in the access networks. They also need to be controlled during the tuning. The nominees of the TLSs can be listed as DFB, external cavity laser (ECL), vertical-cavity surface-emitting laser (VCSEL), and distributed Bragg reflector (DBR) laser. Choosing one of these sources depends on the complexity of the tuning technique and range. The tuning techniques can be thermally controlled like DFB, electrically controlled like DBR, and mechanical controlled like ECL and VCSEL.

The mechanically controlled lasers have a broad tuning spectrum and precise wavelength efficiency. However, they need external modulators to reach fast modulation speeds and cannot provide constant stability in long periods (Banerjee et al., 2005).

DFB laser has the frequency-shift feature and uses this characteristic since the laser highly sensitive to temperature variations. The tuning time of this laser is very long and this property of the laser limits it in where fast switching needed in the system. On the other hand, this laser can be beneficial where a specific wavelength applied in the PON systems.

Although the tuning times of the DBR and DFB lasers have caused problems, it can be efficiently adjusted by applying current into more segments of the laser cavity. The injected current changes the refractive index of the cavity which cause a change in wavelength. The disadvantage of the laser is that it is vulnerable to mode competition and hopping due to a lot of electrodes on the cavity need injected current (Zirngibl et al., 1994; Hong et al., 1998; Agrawal, 2012). Therefore, the performance of the system degrades.

### 2.1.3. Research on Self-Emitting Technique

A typical ECL is costly and bulky. It cannot protect its stability for a long time and also needs an external modulator to increase modulation speed. An integrated ECL was manufactured on polymer waveguide to solve the problem(Jie Hyun et al., 2005; Jeong et al., 2006; Noh et al., 2008; Yoon et al., 2010; Kaminow et al., 2013). It was showed that these lasers can increase the modulation rate of up to 10 Gb/s by curtailing the length of the cavity and by improving the grating design based on polymers [46]. In (Jie Hyun et al., 2005; Jeong et al., 2006; Noh et al., 2008; Yoon et al., 2010; Kaminow et al., 2013), it has been discussed whether these lasers would be cost-effective for use in WDM PONs. Moreover, studies have been made on the fact that TLSs can be integrated monolithically(Akulova et al., 2002; Ward et al., 2005; Buus and Murphy, 2006; Kaminow et al., 2013). Since TLSs require a wavelength cabinet and thermoelectric cooler to achieve a stable laser output, WDM does not meet the cost requirement to be implemented in PONs. In (Park et al., 2000; Roppelt et al., 2011; Roppelt et al., 2012), a single wavelength-locker, that can be shared by all TLS, was used in OLT to reduce the cost.

In (Reeve et al., 1988; Wagner et al., 1988; Wagner and Chapuran, 1990; Lee et al., 1993; Chung et al., 1994; Pendock and Sampson, 1996; Liou et al., 1997; Jung et al., 1998; Oksanen et al., 2002; Han et al., 2004; Kaminow et al., 2013) many studies have been carried out to develop the spectrum slicing

technique. In (Lee et al., 1993), the working principle of the spectrum slicing technique is explained. It is reported in (Jung et al., 1998; Han et al., 2004) that spectrum slicing can be performed automatically by using AWGs in WDM PON. Thus, the use of optical filters has been eliminated. It has been shown in (Lee et al., 1993; Chung et al., 1994; Pendock and Sampson, 1996) that this technique can be used for the WDM PON system running faster than 1 Gb / s per wavelength. However, the performance of this technique is low due to the high-intensity noise caused by the ASE elements (Lee et al., 1993). In (Keating et al., 1995; Arya and Jacobs, 1997; Koyama et al., 2000; McCoy et al., 2004), preamplifier receivers, saturated SOA, and feed-forward techniques have been used to reduce the dispersion penalty arising from broadband use. It has been shown in (Kawanishi et al., 1999; Boivin et al., 2000) that this problem can be reduced by using coherent lights with a wide optical spectrum such as supercontinuum generators and femtosecond laser. However, these light sources are not convenient to be applied in ONUs. In order to reduce the losses caused by slicing, it was tried to increase the output power of BLSs in (Sampson and Holloway, 1994; Liou et al., 1996; Koyama, 1997) and to use forward error correction (FEC) codes in (Han et al., 2004; Kaneko et al., 2006; Briand et al., 2007). It has been shown in (Fattal et al., 2008) that it is possible to develop an LED with a modulation bandwidth at 10 GHz.

### 2.2. Self-Seeded WDM PON Technology

The self-seeded reflective semiconductor optical amplifier (SS-RSOA) technique was first presented in 2006 by Wong, Lee and Anderson (Wong et al., 2006; Wong et al., 2007). The self-seeded cavity was offered as a low-cost and colorless solution for WDM access networks (Maho et al., 2016). The usage of self-seeded RSOA at the ONU part of a WDM PON system supports access networks such as mobile fronthaul/backhaul and makes it an attractive solution because of its large capacity, low latency and compatibility with Gb/s data rates

(Brunero et al., 2016; Cheng et al., 2016). The self-seeded architecture aims to automatically and passively assign the desired wavelength (Brunero et al., 2016).

The first proposed WDM setup with a colorless RSOA transmitter schematic is shown in figure 2.4 (Wong et al., 2006; Wong et al., 2007).

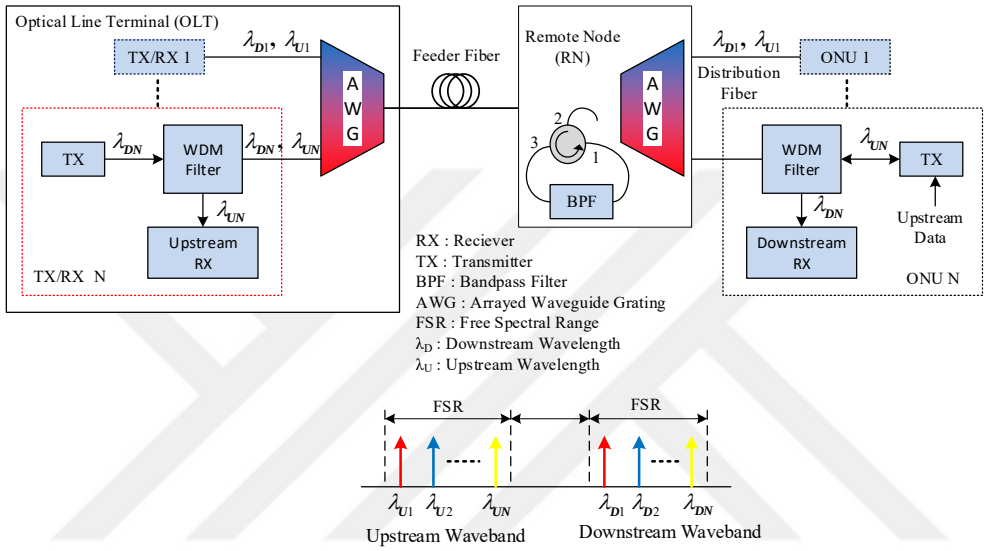



Figure 2. 4. Schematic diagram of self-seeded RSOA based on WDM PON(Wong et al., 2007)

In this architecture (Wong et al., 2006; Wong et al., 2007), each ONU consists of a WDM filter to separate the upstream and downstream wavelengths for each channel, and an RSOA is a directly modulated colorless transmitter. The WDM filter is also used at each optical line terminal (OLT) to separate the upstream and downstream wavelengths for each channel as in ONU. AWGs occur at both remote network (RN) and OLT because the upstream and downstream wavelengths must be separated and combined. In this schematic (Wong et al., 2007), a band-pass filter (BPF) and a circulator occur at the RN which are used to reflect only one wavelength to seed the RSOA at ONU. RSOA acts like a partial mirror.

The self-seeding occurs as follows: RSOA emits amplified ASE light, which is first filtered by the WDM filter at ONU and generates the upstream wavelength in this method. Then, this filtered upstream wavelength is spectrally sliced by AWG at RN, and part of the light is fed back to the seed RSOA at ONU. The RSOA amplifies the light, and this process proceeds many times until it becomes stable and a small peak signal appears. When the loss of the self-seeding cavity is equal to the gain of the RSOA, stable self-seeding is established (Xiong et al., 2013).

To sum up, the RSOA mainly plays three roles in the self-seeding cavity:

- It provides and maintains the cavity gain to lase (Marazzi et al., 2012; Gebrewold et al., 2015).
- It functions as a direct modulator, modulates the signal with its bias current and recirculates inside the cavity (Marazzi et al., 2012; Gebrewold et al., 2015).
- It nonlinearly suppresses any modulation from the input signals (Marazzi et al., 2012; Gebrewold et al., 2015).

The advantages of SS-RSOA are:

- The use of SS-RSOA decreases the cost.
- The wavelength is only determined by the passive components in the distribution network; in general, these components are: AWG, WDM filter, and BPF.
- A robust and stable transmission wavelength can be gained because the wavelength is determined by passive components.
- Temperature control is not required because of the fixed lasing modes (Kang et al., 2007).

- Identical RSOAs are used at each ONU, which provides the colorless transmission.
- It removes the requirement of using external sources; hence, backscattering is prevented (Pachnicke et al., 2014; Parolari et al., 2014).
- The external cavity causes a promising performance in both power budget and bit rate (Wong et al., 2007; Wong, 2012).
- The assigned wavelength of each channel is automatically matched with the emitting wavelength of the transmitter, and the transmitted wavelength at each ONU is not affected by temperature changes (Kang et al., 2007), which eliminates the wavelength tuning.
- If the RSOA gain and response have less temperature dependence, even an uncooled operation can be obtained.
- An external seeding source or external mechanisms are not required here to control the wavelength stability compared with other colorless technologies (Saliou et al., 2015).

Disadvantages of the self-seeded RSOA are:

- Currently available RSOA devices have a small electro-optical bandwidth, which limits the bit rate for transmitters (Brunero et al., 2016).
- The self-seeded RSOA application should have saturated output power and signal gain and a low polarization-dependent gain(Park et al., 2007; Xiong et al., 2013).

### 2.2.1. Transmission Limitations of RSOA

WDM PON has many advantages for next-generation access networks (NGAN). In particular, the use of one ONU for all users provides colorless transmission as explained in the previous sections. The colorless self-seeded

transmission can be achieved using FP lasers (Kashima, 2006) or RSOAs (Park et al., 2007). Many criteria affect the performance of the SS RSOA cavity and these affecting components are presented following in detail.

#### 2.2.1.1. Faraday Rotator Mirror

The Faraday rotator mirror (FRM) has two Faraday rotators: one next to the partial reflective mirror and the other in front of the RSOA to stabilize and manage the polarization state of the reflected signal because of the high polarization-dependent gain (HPDG) RSOA (Martinelli et al., 2012). Hence, the combination of the Faraday rotator after RSOA and the partially reflective mirror at RN indicate the FRM. Birefringence variations in the self-seeding cavity, which are associated with the distribution fiber, cause a nonstable operation of the system. Some research works (Marazzi et al., 2013; Presi et al., 2013) have shown that the FRM plays a crucial role in managing the polarization in the cavity (Maho et al., 2016). It helps to provide stable operation in the cavity (Saliou et al., 2015) and enables the use of high polarization dependent-gain RSOAs (Martinelli et al., 2012; Saliou et al., 2015). The schematic of the FRM is demonstrated in figure 2.5. The rotation occurs by the light passing through the Faraday rotator (FR). The Polarization of light changes by $45^0$ by passing through the rotator. The mirror placed after the rotator also returns the light back with the same angle. The FR polarizes the light second time and the light is polarized $90^0$ in total (Bobrovs et al., 2013).

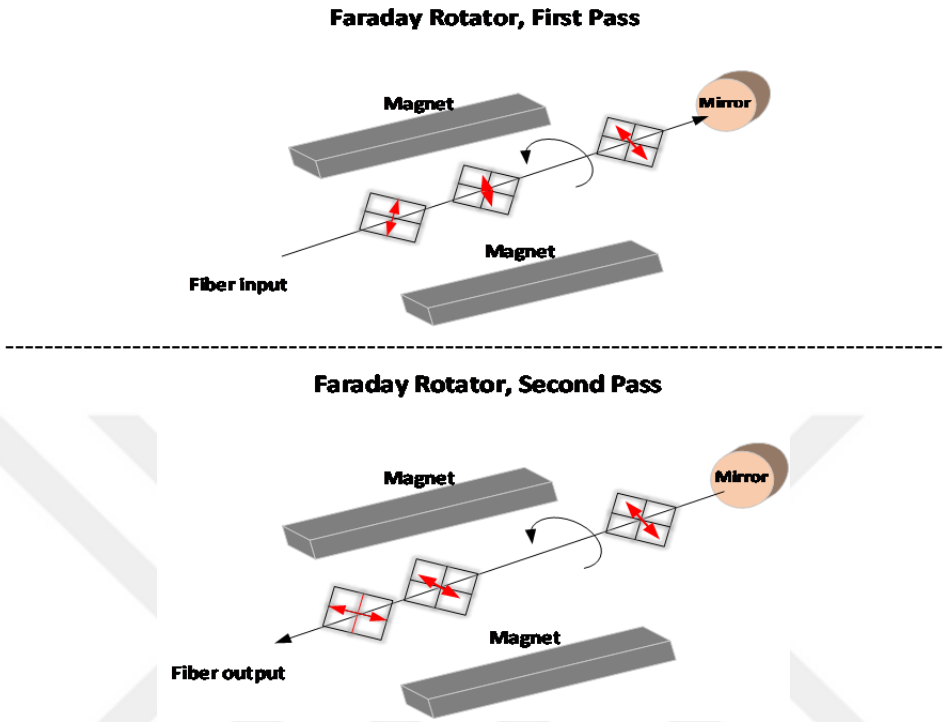



Figure 2.5. Schematic of Faraday Rotator Mirror(Bobrovs et al., 2013)

### 2.2.1.2. Array Waveguide Gratings

Multiplexers/Demultiplexers (Mux/Demux) are devices that multiplex different wavelengths of an optical signal and demultiplex the multiplexed signal. The types of Mux/Demux designs are AWG, fiber Bragg gratings (FBG), and thin-film filters (TFM). The AWG provides a flexible design regarding the wavelength spacing and number of channels. AWG schematic is shown in Figure 2.6.

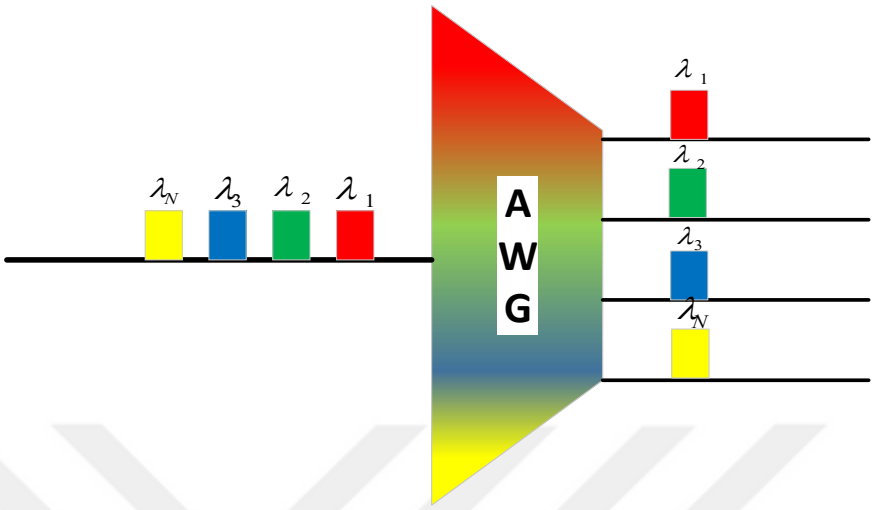



Figure 2. 6. Schematic of AWG architecture (Lee et al., 2006; Zhou et al., 2010)

With more channels, the costs per channel are decreased because more channels can be placed in smaller areas. The wavelength dispersion is notably low in AWGs, which makes AWGs suitable for high bit rates and provides an important role for WDM systems.

The source emission wavelength is automatically determined by the optical channel design of the AWG, which provides robust self-tuning capabilities and eliminates the need for precise wavelength locking between the AWG and the transmitters (Zhan et al., 2015; Maho et al., 2016). The quality of the transmitted signal also depends on AWG (Maho et al., 2016). The bandwidth of the signal depends on the full width at half maximum (FWHM) and shape of the AWG (Maho et al., 2016). The relative intensity noise (RIN) increases with a narrow FWHM; on the contrary, the chromatic dispersion increases with a larger output spectrum of a wider filter (Parolari et al., 2012; Parolari et al., 2015).

#### 2.2.1.3. Rayleigh Backscattering

A tuning source at the OLT may cause Rayleigh backscattering (RBS) and Brillouin backscattering (Talli et al., 2006) because of the crosstalk of different

bands such as L and C bands for downstream and upstream signals, respectively. RBS occurs because of the incoherent crosstalk in the transmission of the upstream signal (Wong et al., 2007). The self-seeded RSOA is proposed as a solution to remove tuning external optical seeding sources and decrease the crosstalk penalty caused by Rayleigh backscattering (Wong et al., 2007; Wong, 2013). The standard single-mode fiber and variable optical attenuator positions are switched in (Saliou et al., 2015) to evaluate the RBS. The RBS impact is reduced when SSMF and variable optical attenuator (VOA) are switched. In (Saliou et al., 2015), when the length of the fiber immediately after the RSOA and multiplexer increases, the RBS impact increases. In (Saliou et al., 2015), some solutions are offered to minimize this problem:

- Decreasing the power at the input: RBS is not observed when the attenuation is higher than 7 dB (Saliou et al., 2015).
- When RSOA is modulated, the backscattering decreases because of the modulation gain dependent of RSOA (Saliou et al., 2015).
- RBS does not affect lasing in the cavity at notably long fibers; thus, long cavity laser can be used for metropolitan and access applications (Saliou et al., 2015).

#### 2.2.1.4. Chromatic Dispersion

Chromatic dispersion (CD) is one of the main limitations in fiber transmission. CD arises from the interaction between electrons of the medium and electromagnetic waves. Each pulse in the fiber has several wavelength components. These components have different refractive indexes and thus moves at various speeds. Therefore, the pulse expands and lowers its amplitude as it moves through the fiber as shown in figure 2.7. It is difficult to obtain a high data bit rate and a long reach transmission distance in the presence of chromatic dispersion.

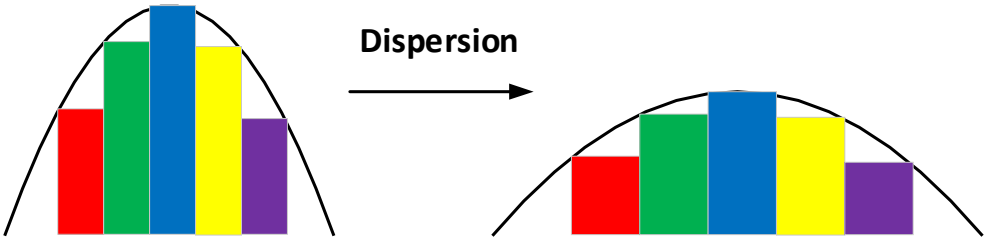



Figure 2. 7. Chromatic Dispersion cause the pulse to broaden. The input pulse to the fiber is given on the left and the output pulse from the fiber is given on the right.

The dispersion can be expressed mathematically as in equation (2.1)

$$D = \frac{\partial B_1}{\partial \lambda} = \frac{-2\pi c}{\lambda^2}\beta_2 \tag{2.1}$$

Where $\beta$ is the mode propagation constant and $\lambda$ is the wavelength. The derivatives of the $\beta$ can be calculated as in equation (2.2a) and (2.2b)

$$\beta_1 = \frac{\partial \beta}{\partial \omega} = \frac{1}{\upsilon_g} = \frac{n_g}{c} = \frac{1}{c}\left(n + \omega\frac{\partial n}{\partial \omega}\right) \tag{2.2a}$$

$$\beta_2 = \frac{\partial^2 \beta}{\partial \omega^2} = \frac{1}{c}\left(2\frac{\partial n}{\partial \omega} + \omega\frac{\partial^2 n}{\partial \omega^2}\right) \tag{2.2b}$$

Where, $v_g$ is the group velocity and $n_g$ is the group index. Group velocity dispersion is expressed with $\beta_2$. As demonstrated in equations (2.2a) and (2.2b), the pulse dispersion mainly depends on wavelength, mode propagation, and refractive index of the material. The wavelength of the pulse should be chosen carefully, taking into account where the dispersion is close to zero. Experimental

works show that the chromatic dispersion decreases with the operation in the O band (Parolari et al., 2014).

#### 2.2.1.5. Cavity Losses

The relative intensity noise and cavity losses limit the transmission in the absence of chromatic dispersion (Maho et al., 2016). The increasing distance negatively affects the cavity and increases cavity losses. This reduces the power at the output and so, the cost for transmission (Maho et al., 2016).

#### 2.2.1.6. Reflective Crosstalk

Reflective crosstalk occurs because of multiple reflections in the self-seeding cavity and degrades the transmission performance (Cheng et al., 2016). The approaches to mitigate the reflective crosstalk are listed as follows.

- Extinction Ratio Reduction (Xiong et al., 2013): The extinction ratio reduction with gain saturation in RSOA alleviates the reflective crosstalk but compromises the receiver sensitivity.
- Modulation Averaging (Komljenovic et al., 2012): The modulation average requires additional components (e.g., multiple reflective mirrors) at the remote site.
- Dual RSOA (Deng et al., 2014): One RSOA is biased with the fixed current, and the other is under direct modulation, which increases the cost and complexity.
- Feedforward Crosstalk Cancellation (Cheng and Effenberger, 2015; Cheng et al., 2016): As demonstrated in (Cheng and Effenberger, 2015; Cheng et al., 2016), reflective crosstalk increases with lower cavity loss or higher reflectivity from the partial reflection mirror. Because the remodulation crosstalk is generated from the transmitted signal that is reflected from the partial reflection mirror and subsequently re-amplified by the RSOA, a feedforward approach is proposed to cancel the remodulation crosstalk as shown in figure 2.8 (a).

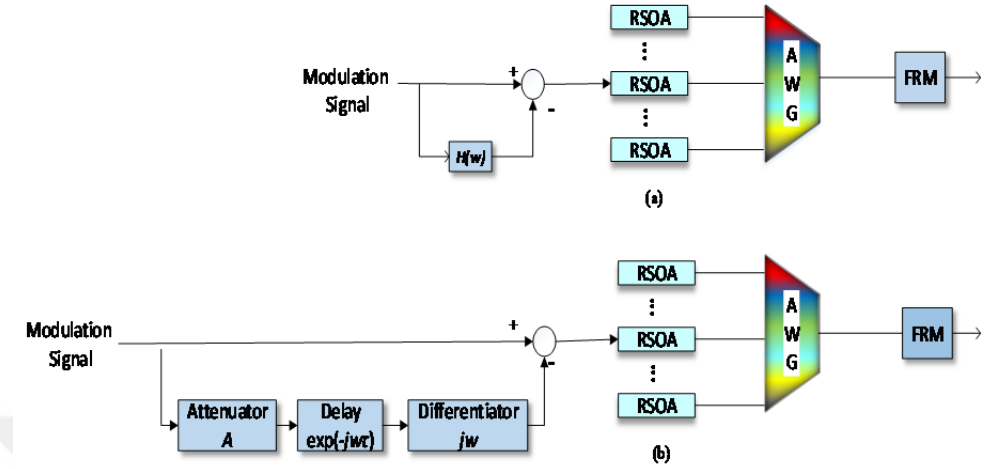



Figure 2.8. Block diagram for a. delay method; b. differentiation method (feedforward) (Cheng and Effenberger, 2015; Cheng et al., 2016)

The frequency response of the feedforward filter is $H_0(\omega)$; and the signal passes through the filter, the output signal is ablated from the initial modulating signal. If the system is assumed as linear, the first and consecutive reflected and re-amplified pulses are eliminated. The reflected crosstalk signals may not be deleted in such a feedforward system because the RSOA is nonlinear. As shown in figure 2.8 (b), the feedforward differentiation method (FDM) is used instead of $H_0(\omega)$ to cancel the remodulation crosstalk $H_0(\omega)$ is approximated as $H_0(\omega)=j\omega Ae^{-j\omega\tau}$ (Cheng and Effenberger, 2015; Cheng et al., 2016). The initial pulse of the electrical signal is for direct modulation, and the other pulse, which is generated from the delay and differentiation of the first pulse, is for remodulation crosstalk mitigation. The first optical pulse is partially transmitted and reflected back to the RSOA. Simultaneously, the crosstalk cancellation signal, which consists of a pulse to suppress this reflected signal, is applied to the RSOA. The transmission performance of the SS-RSOA is tested at 2.5Gb/s using the FDM technique in channel 16 with a

center frequency of 1545.32 nm in a 32- channel WDM PON system. The results of the sensitivity at BER was -34.8 dBm after 20 km feeder fiber, whereas it was -33.1 dBm without FDM. Hence, the feedforward crosstalk cancellation improved the transmission performance by 1.7 (Cheng and Effenberger, 2015; Cheng et al., 2016).

- Adaptive Crosstalk Cancellation (Cheng and Zhou, 2015; Cheng et al., 2016): Compared to the feedforward crosstalk cancellation method (Cheng and Effenberger, 2015), the feedback approach is adaptive to the cavity length and reflectivity of the self-seeded RSOA. In the feedforward cancellation method, the delay and attenuation factors in the feedforward path must be measured off-line, which makes the feedforward approach less adaptive to the length and self-seeded cavity reflectivity. A new feedback crosstalk technique cancellation is shown in figure 2.9.

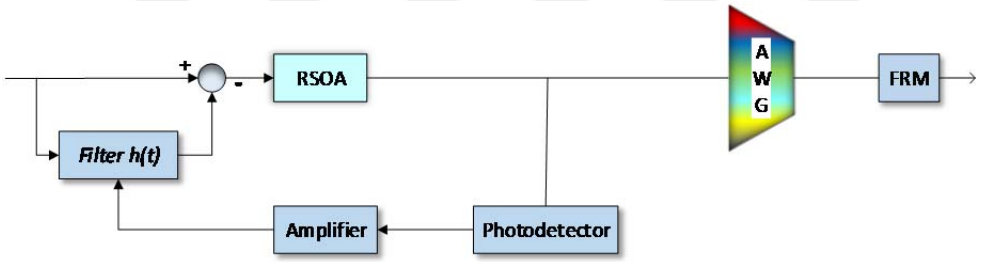



Figure 2.9. Block diagram for adaptive feedback approach (Cheng and Zhou, 2015; Cheng et al., 2016)

Adaptive In this method, the optical response h(t) of the RSOA with respect to the reflected signal can be determined, and an adaptive filter with h(t) is implemented as shown in figure 2.10. The modulating signal is passed through this adaptive filter and subsequently subtracted from the original modulating signal. Thus, the reflective intra channel crosstalk is suppressed. In (Cheng and Zhou, 2015; Cheng et al., 2016), this method is applied and concluded as follows: This method improves the average error

vector magnitude (EVM) of the 24 LTE signals from 9.4% to 7.4% (approximately 20% improvement) at -16 dBm received power, which satisfies the minimum EVM requirement of 8.0% for mobile fronthaul.

#### 2.2.1.7. Extinction Ratio

The extinction ratio (ER) is one of the important parameters that affects the transmission performances of the self-seeded RSOA. The RSOA enters deeper saturation with a stable seeding power; thus, a stronger modulation on the seeding light is suppressed and guarantees both high extinction ratio and better receiver sensitivity (Xiong and Zhong, 2013). Meanwhile, a high extinction ratio increases the re-modulation crosstalk and puts the self-seeded process at risk because of the insufficient seeded power in the spaces of the modulated seeded light (Xiong and Zhong, 2013). A low extinction ratio reduces the sensitivity of the upstream signal and fails the error-free transmission (Xiong and Zhong, 2013). In practice, the self-seeded RSOA usually operates in the saturation regime and is modulated with a low extinction ratio to alleviate the excessive penalty because of remodulation crosstalk (Xiong et al., 2013).

#### 2.2.1.8. Length of The Cavity

The advantage of the long cavity is that the distance between a shared point and ONU enables one to create more user units on the same node (Maho et al., 2016). The longitudinal modes of the cavity increase with increasing cavity length. The cavity length is limited by the chromatic dispersion in the C band, RIN and losses in the O band.

#### 2.2.1.9. Coupling Ratio

The coupling ratio of the optical coupler affects the losses of the self-seeded cavity, output power of the source, upstream transmission losses and quality of the transmitted signals (Xiong and Zhong, 2013; Maho et al., 2016). Increasing

the returned power back to the RSOA by varying the coupling ratio reduces the transmitted power to the OLT, which reduces the optical budget (Deniel et al., 2013). The loss of cavity decreases; hence, the stable seeded power on upstream transmission performance increases with varying coupling ratio in the reflective path (Wong, 2013; Xiong et al., 2013). The coupling ratio arrangement helps to improve the data modulation and receiver sensitivity (Maho et al., 2016).

#### 2.2.1.10. Longitudinal Modes

Longitudinal modes induce noise in the cavity (Maho et al., 2016). Long self-seeded sources present many longitudinal modes and cause a notably large RIN (Marazzi et al., 2014). A short cavity consists of hundreds of longitudinal modes, and their number increases to thousands with the increasing length (Maho et al., 2016).

#### 2.2.1.11. Narrow Band ASE

The narrowband amplified spontaneous emission introduces many transmission problems such as post filtering effect (PFE), Rayleigh backscattering, ASE-ASE beat noise, crosstalk and CD (Xiong and Zhong, 2013).

#### 2.2.1.12. Gain Compression

In a self-seeded system, gain compression is used to erase the returning signal. Thus, the interference with the new modulated signal is prevented (Ó Dúill et al., 2012).

#### 2.2.1.13. Filter Type

The flat-top filter output signal has a narrow spectrum full width at half maximum (FWHM); thus, the relative intensity noise increases during propagation (Parolari et al., 2012; Xiong et al., 2013; Parolari et al., 2015), and the peak wavelength is close to the cut-off of the pass band (Xiong et al., 2013). The Gaussian filter output signal has a wider FWHM, which is sensitive to chromatic dispersion during propagation (Parolari et al., 2012; Xiong et al., 2013; Parolari et

al., 2015; Maho et al., 2016). The laser wavelength for both cases is red-shifted compared to the central wavelength of the AWG channel because of Bogatov effect (Maho et al., 2016).

#### 2.2.1.14. Polarization Sensitivity

The polarization sensitivity is one of the crucial issues in the self-seeding system. Polarization occurs because of the birefringence of the drop fiber in the self-seeded cavity. A fiber mirror connected to the low-polarization-dependent-gain RSOA has been used to increase the seeding efficiency at the beginning (Wong et al., 2007; Maho et al., 2016). The cavity remains susceptible to the polarization fluctuations with time (Presi and Ciaramella, 2011). As a solution, a Faraday rotator has been added after the RSOA (Martinelli et al., 2012), and the fiber mirror has been replaced by a FRM to obtain a polarization retracing circuit, which enables high PDG RSOA usage.

### 2.2.2. Research on Self-Seeded RSOA

Experimental works have shown different results for 1.2, 2.5, 5 and 10 Gb/s. Most works have been performed in the C-band at the speed of 1.25 Gb/s. The distance for transmission is approximately 20 km.

Reflective crosstalk arises because of reflections in the self-seeded cavity, which degrades the transmission performance. The approaches to mitigate the reflective crosstalk are extinction ratio reduction (Xiong et al., 2013), modulation averaging (Komljenovic et al., 2012) and the usage of dual RSOAs (Deng et al., 2014). A new model was applied to prevent and suppress the reflective crosstalk in the self-seeding cavity (Cheng and Effenberger, 2015; Cheng et al., 2016). Compared to the other approaches for reflective crosstalk cancellation (Komljenovic et al., 2012; Xiong et al., 2013; Deng et al., 2014), this approach improves the transmission performance under relatively high extinction ratios without requiring additional optical components.

At long distances, the ASE-injected signals demonstrate various negative effects (Duarte and Romero, 2016). These impairments arise from the relative

intensity noise (Cho et al., 2013), chromatic distortion (Kim, 2012; Duarte et al., 2014), spectral-slicing of ASE-based BLS and post filtering (Duarte et al., 2014)[(Lee et al., 2010; Lee et al., 2010). Different types of BLS designs have been offered to mitigate the impairment effects but remain limited in long reach. In (Duarte and Romero, 2016), self-seeded RSOA and high-power pre-spectrum-slicing source (PSSL) were compared in terms of maximum reach transmission. In the comparison, the bit error rate was, and the power penalties were similar: 2.7 dB for self-seeded RSAO and 2.6 dB for PSSL topologies. Self-seeding and PSSL topology reached 140 km for and 80 km distance with identical BER and similar power penalties. Hence, with the self-seeding, 12 dB enhancement on power budget was achieved.

In (Duarte et al., 2013; Duarte et al., 2014), a new self-seeded WDM-PON topology was proposed, where self-seeding occurs in RSOAs at the OLT, which enables upstream transmission based on the carrier remodulation at the ONU at 1.25 Gb/s operation. In (Duarte et al., 2013), 2.5 dB power penalty was obtained with a BER of $10^{-10}$ , and the transmission length was over 20 km for the injection power of -22 dBm. (Duarte et al., 2014) aimed to reach longer distances than (Duarte et al., 2013) using electronic erasure hardware. A 2-dB power penalty was obtained with a BER of $10^{-12}$. The maximum achieved transmission length was 80 km for downstream and 60 km for bidirectional communication.

The lasing behavior of the self-seeded cavity was explained in (Saliou et al., 2015; Maho et al., 2016). By measuring the output spectrum and light-current curve of the self-seeding cavity, the lasing behavior of the self-seeded cavity and the requirements for how RSOA works like a multimode laser with low coherence were explained in (Maho et al., 2016). In (Saliou et al., 2015), the error-free transmission at 2.5 Gb/s was realized with passive optical cavities up to 26 km for access networks and active cavities up to 125 km for metropolitan DWDM networks.

In (Diallo et al., 2016), the effects of the jitter, radio frequency budget, bit error rate, round trip delay and data rate on a self-seeded DWDM system were

studied on a real fronthaul link for the first time. The RSOA can reach a bit error rate of at the speed of 2.45 Gb/s.

In (Parolari et al., 2015), colorless transmitters in self-seeded WDM PON system for both C and O bands up to 10 Gb/s were compared. The C band transmitter reached 5 km (Deniel et al., 2013), and the O band reached 26 km drop fiber (Simon et al., 2014) at the speed of 2.5 Gb/s. The limiting factors were defined as the chromatic dispersion for the C band and relative intensity noise for the O band. Increasing the speed to 10 Gb/s decreases the lengths by 400 m for the C band and 1 km for the O band because of the losses (Parolari et al., 2014). The power was limited by the power budget but after tens of kilometers of propagation in a single-mode fiber, the CD effect is removed for the O band and enables the Gb/s transmission. Unlike the C band, CD remains as a negative effect and can only reach 50 km at 2.5 Gb/s and maximum 10 km at 10 Gb/s with a bit error rate below the $3\times10^{-3}$ FEC limit.

In (Gebrewold et al., 2015), the externally seeded RSOAs, RSOA-FCLs, and sliced ASE spectrum were demonstrated and compared for the colorless transmission. The modulation speeds of the sliced ASE spectrum were approximately to 1 Gb/s for less than 10 km. The externally seeded RSOAs use expensive lasers at CO for each ONU; thus, the price increased with expensive lasers at CO. RSOA-FCL was between externally seeded RSOAs and sliced ASE spectrum in terms of the power, frequency response, signal-to-noise ratio and RIN. It is a cost-efficient solution for PON systems. Hence, RSOA-FCL is preferred for short-reach applications up to 10 Gb/s.

In (Marazzi et al., 2013; Parolari et al., 2014), 10 Gb/s was achieved with a single RSOA. In (Gebrewold et al., 2015), it was achieved with two RSOAs. In (Brunero et al., 2016), with the polarization division multiplexed WDM PON transmitters based on two self-seeded RSOAs at the ONU, 10 Gb/s was achieved with up to 20 km SSMF. In (Gebrewold et al., 2015), the subcarrier multiplexing method was used to boost the performance, and 10 Gb/s over 25 km was achieved.

In (Deniel et al., 2013; Deniel et al., 2013; Simon et al., 2014; Saliou et al., 2015), a new method called the “face-to-face configuration” was applied. In this method, two RSOAs were used to create the optical cavity. A mirror was placed behind the demultiplexer, and the shared point was removed. It reached 70 km with a speed of 2.5 Gb/s in (Simon et al., 2014); 125 km was achieved with the active cavity in (Saliou et al., 2015).

As a conclusion, although self-seeded RSOA simplifies the system, the losses occur because of the reflective path degrades the system power. Furthermore, the spent time during the seeding process also degrades the system performance.

### 2.3. Seeding Light from Central Office (Loop Back)

The researchers and service providers have attempted to remove the light sources from ONUs, since it is an expensive and risky way to require each end user to manage its own wavelength. In case of an ONU deviates from the designated wavelength, this user will not only damage itself, but it will also affect the other neighboring channels. Therefore, light sources to seed the ONUs have been suggested to be supplied from the central office.

In this method, reflecting optical sources are applied to the user ends. These sources can be reflective electro absorption modulators (REAMs), injection-locked FPLDs (Ki-Man et al., 2006), and RSOAs (Park et al., 2007) to reach high data rates (Berrettini et al., 2009; Schrenk et al., 2009; Antoniades et al., 2011). There are two ways to seed optical sources remotely. The first way is CO transmits a designated wavelength together with downstream data and upstream data is modulated on this designated wavelength. Thus, different wavelengths are used to transmit upstream and downstream data. The second way is upstream data is remodulated on the same wavelength where downstream data is modulated. Thus, a single wavelength is used to transmit upstream and downstream data. The schematic of these two methods are given in figure 2.10.

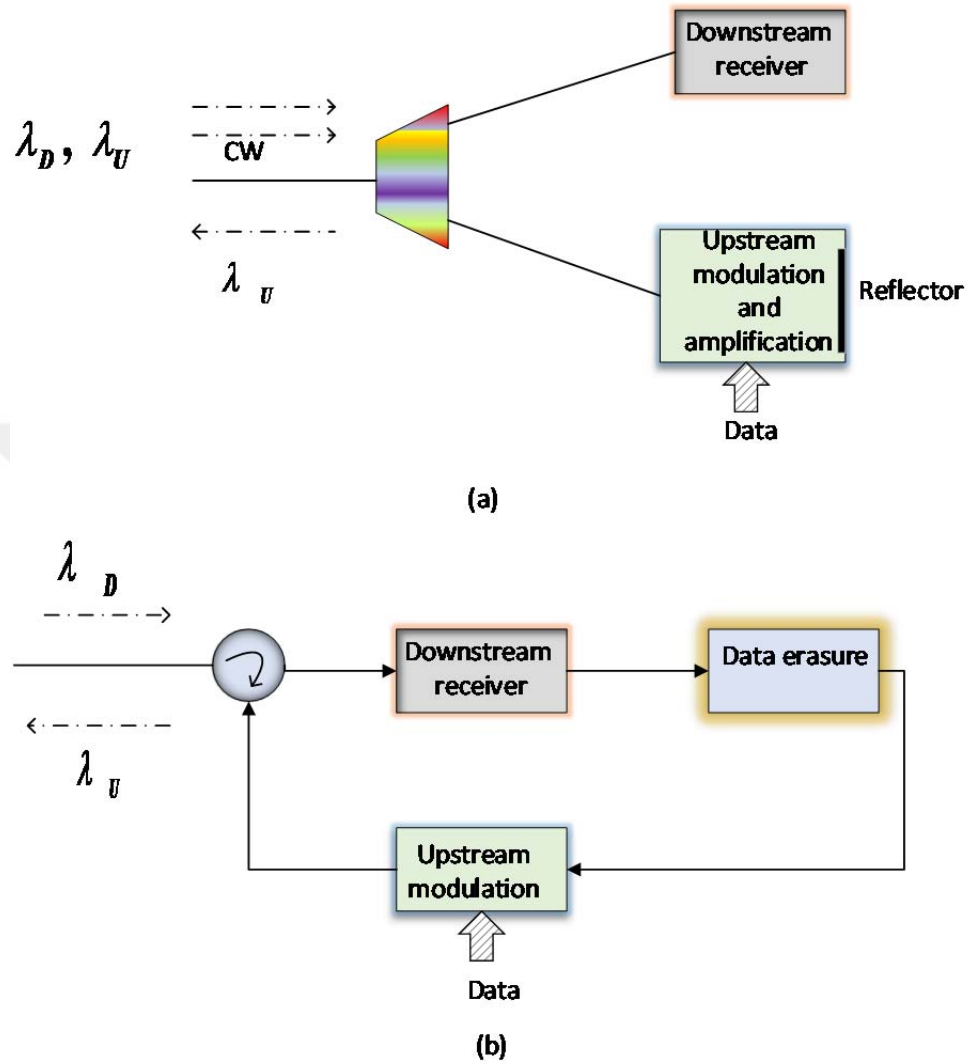



Figure 2. 10. Remotely seedings: a. separate wavelength for upstream&downstream; b. reusing of downstream carrier (Antoniades et al., 2011)

Different wavelength usage for both downstream transmission and upstream transmission increases the transceiver numbers and the cost of the system increases. Thus, remodulation method has been proposed to decrease the cost of the system.

### 2.3.1. Remodulation Technique

In this method, the downstream carrier is used at both ONU and OLT. Hence, the colorless sources can be applied to the end-users. The wavelength of the ONU is identified by the downstream carrier wavelength. The modulated downstream data is divided into two portions at the ONU side. One portion of the downstream signal is detected at the receiver part of the ONU. The other portion seeds the optical source for upstream transmission. In this way, the system expenses decrease because the need for extra fiber cable will be eliminated. However, this method causes crosstalk due to the remained downstream data. Thus, the downstream data should be erased to not overlap with upstream data. The schematic of remodulation process is shown in figure 2.11(Cho et al., 2009). Reflection-I is the reflected downstream signal. At the same time, it causes noise by mixing with the upstream signal. Reflection-IIa is the back-reflected signal to the ONU after modulation. Reflection-IIb is the mixing of the reflected signal with the upstream signal after amplifying in RSOA (Cho et al., 2009). The effects of these reflections are theoretically evaluated in (Cho et al., 2009).

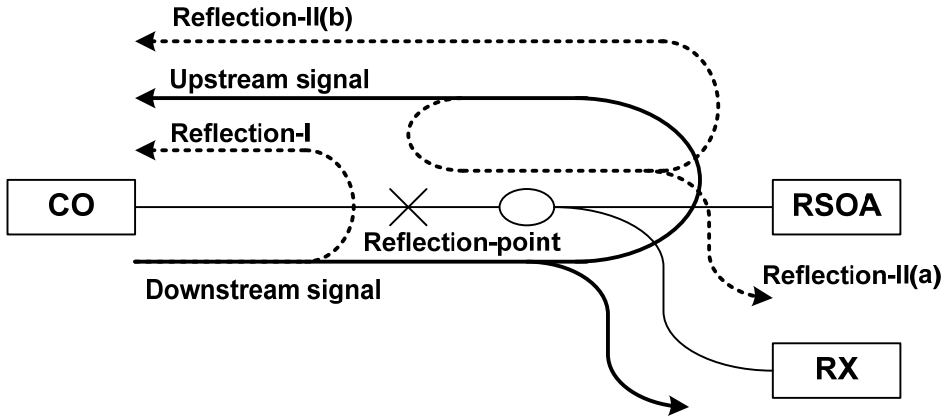



Figure 2.11. Remodulation method utilizing RSOA as a transmitter (Cho et al., 2009)

Studies on the remodulation method are ongoing so that it can be applied to access networks. The amplitude shift keying (ASK) modulation scheme is applied

to both ends (ONU and OLT) to simplify the system design. In (Takesue and Sugie, 2003), the saturated SOA is used at user end to suppress the downstream data. In (Wooram et al., 2005), RSOAs were implemented to the ONUs and better results are obtained due to the high gain saturation feature of the RSOA. Furthermore, the FPLDs are also applied to the user ends, and high data rates are achieved (Su et al., 2015).

Different modulation methods can be applied to both downstream and upstream sides to prevent data collision. For instance, applying DPSK modulation format to OLT can prevent data interference between upstream and downstream (Wai et al., 2003). However, conversion from phase to intensity will still cause crosstalk. Implementation of orthogonal modulation formats can also prevent interference between signals. In (Arellano et al., 2005), frequency-shift keying (FSK) and amplitude shift keying (ASK) modulation formats were applied to OLT and ONU respectively. In (Le et al., 2012), binary phase-shift keying (BPSK) and ASK modulation formats were applied to OLT and ONU respectively to show the transmission at high data rates. Although applying the different modulation formats increases the data rates, the required devices to apply these modulation formats are highly complex and expensive. The aim of the researchers is to provide uncomplex, upgradable, and cost-efficient communication. Therefore, the widespread use of different modulation techniques in practice will take a long time depending on the improvement of the conditions.

#### 2.3.1.1. Injection-Locking

The multimode lasers, like FPLDs, can excite in single-mode when externally injected (Yasaka et al., 1996). The injection-locked FPLD was first presented in (Hyun Deok et al., 2000). In the study, the BLS was used for seeding, and research has continued with other studies (Shin et al., 2003; Sil-Gu et al., 2008). The parameters such as injection power, injection current and, modulation index affect the efficiency of the locked-laser. The usage of BLS is affected by all these parameters and produce high-intensity noise. It also demonstrates the incoherent transmission characteristic which decreases the system data rates (Lee et

al., 2006; Park and Lee, 2008). Therefore, the usage of supercontinuum laser sources has been proposed to seed the laser in ONU. Detailed studies and explanations of this method are provided in the following chapters.

### 2.3.2. Research on Loop Back Technique

In (Koponen and Soderlund, 2004; Payoux et al., 2006), a small ER was applied to CO to solve the noise problem in this technique, and the speed was reduced in ONU. It has been shown in (Takesue and Sugie, 2003; Wooram et al., 2005) that noise is reduced by using gain saturated RSOA as a transmitter. In addition, using different coding techniques in (Guo-Wei et al., 2005; Prat et al., 2005; Prat et al., 2005; Jeung-Mo and Sang-Kook, 2006; Tian et al., 2006; Kim et al., 2007; Cho et al., 2008), the noise problem was tried to be solved. The achievements of these techniques are presented in (Arellano et al., 2006; Kim et al., 2007; Yu et al., 2007). In (Fujiwara et al., 2006; Lee et al., 2008; Cho et al., 2009), the effects of undesirable reflections caused by parameters such as Rayleigh backscattering, splices, and connectors are discussed when the remodulation technique is applied. It has been shown in (Cho et al., 2008; Urban et al., 2008; Murakami et al., 2009) that the reflections can be reduced by applying the Manchester coding and subcarrier multiplexing (SCM) method. However, it is still one of the serious limiting factors for the remodulation technique. Recently, studies on the data deletion capability of the FPLD were carried out in (Lee et al., 2006; Zhou et al., 2010).

## 2.4. Comparison of Colorless Methods

The comparison and summary of colorless sources are given in table 2.1. The table includes the main techniques of a passive optical network system where colorless sources can be applied to decrease the system cost and increase the bandwidth. In addition, the advantages and disadvantages of these sources are summarized. According to the table, the remodulation and injection locking schemes discussed in sections 2.3.1 and 2.3.1.1 are more favorable in terms of both performance and system cost.

Tablo 2.1. Comparison of colorless methods and sources (Cikan and Aksoy, 2019).

| **Scheme** | | **Optical source** | **Advantages** | **Disadvantages** |
|---|---|---|---|---|
| Self-Emitting | Spectrum-Slicing | BLS, SLED and LED | Low cost<br>No need to seed | Beat noise and fiber dispersion.<br>Rayleigh backscattering and error floor for higher speed and longer transmission.<br>Low power, and incoherent output. |
| | Tunable Laser Diode | Tunable Laser Diode | No seed needed<br>Good output power<br>Long reach | High cost<br>External modulator needed<br>Wavelength assignment algorithm is required |
| Seeding Light from Central Office | Re-Modulation | Any Type | Low cost<br>Relatively high bit rate | Back reflection<br>Extinction ratio<br>Requires centralized broadband source |
| | Injection-Locking | FP-LD | Low cost<br>Simplicity<br>Relatively high speed | Back reflection<br>SNR of the injected signal<br>Low output power |
| | Loop-Back | Any Type | Low cost | Back reflection<br>SNR of the seed light<br>Requires centralized broadband source |
| Self-Seeding | FP-LD | FP-LD | Low cost<br>No external source needed | Wavelength alignment<br>Relatively low speed |
| | RSOA | RSOA | Low cost<br>No external source needed | Low data rates<br>Transmission distance limited |

Note: A part of this chapter has been published in IEEE Canadian Journal of Electrical and Computer Engineering. Doi: 10.1109/CJECE.2018.2872433

# 3. CHARACTERISTICS AND DATA ERASURE ANALYSIS OF REFLECTIVE SEMICONDUCTOR OPTICAL AMPLIFIER

SOAs and Reflective RSOAs take significant role in PONs. SOAs have anti-reflective (AR) coatings on end facets. RSOAs employ low reflectivity coating on one side and high reflectivity (HR) coating on the other facet. The electrical signal is applied to create gain in the semiconductor active area which amplifies the input signal. The schematic of RSOA is demonstrated in figure 3.1(Dutta et al., 2013).

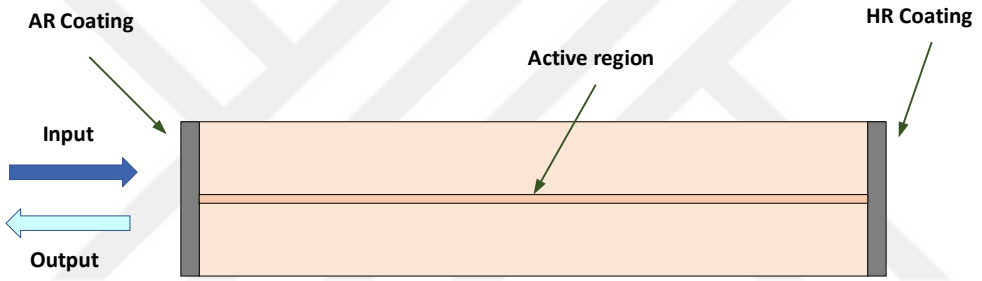



Figure 3.1. Schematic of RSOA device. One of the facets is HR and the other is AR coated (Dutta et al., 2013).

The injected signal is amplified and then reflected in the AR part. This chapter first explains the historical background of the RSOA. It begins with the discovering of the RSOA and then follows with the application of it into optical networks. The last subsection discusses the data deletion efficiency of the RSOA.

## 3.1. Historical Background of RSOA

The SOAs started to take place and brighten in optical fiber communication with the investigations and fabrication of it at 1550 nm in the 1980s (Eisenstein et al., 1985; Mahony et al., 1985). At that time, there were investigations on removing unproductive regenerators and replace them with

effective devices such as optical amplifiers which seemed very enticing. Later on, SOAs started to be applied as inline and preamplifiers. However, there was some dB difference between the transverse magnetic (TM) and transverse electric (TE) polarizations of the SOAs. Amplifying the TM and TE modes separately were proposed to solve this problem. Therefore, a FRM with a 45 degree was implemented in a side of SOA where the proposed structure was akin to RSOA (Mukai et al., 1982; Olsson, 1989). For instance, first, the light was injected into SOA and one of the polarization modes was amplified. Afterward, FRM tilted 90 degrees the light when the light was leaving on the other side of the SOA and reflected it back in the form of another mode. Thus, another mode was amplified in the cavity. This structure led the way for first step of the exploration of the RSOA.

The opinion of transfer videos over optical fiber and the distribution of fibers in the access network emerged in late of the 1980s (Murphy et al., 1988). Although the deployment of optical fiber in the access layer was a very positive change, the high-cost arose due to the whole infrastructure alteration. Therefore, the researchers and communication companies looked for ways to reduce the high cost and came up with an idea of using considerable cheap optical light sources such as reflective modulators at the user ends (Wheeler et al., 1986; Gibassier et al., 1994). Nevertheless, the implementation of modulators was not a consistent solution due to their insertion losses. As a result, a device was required which capable of operating on both as a modulator and amplifier. The RSOA was first proposed in 1986 by Wood et al [100] to overcome the limitations of SOA. The back facet of the SOA was modified as high reflective to perform amplification in the cavity. The studies on RSOAs started in this way. Afterward, the researches on improving the gain, optical, and modulation bandwidths of RSOAs have proceeded (Buldawoo et al., 1997; Chan et al., 2001).

RSOAs can operate in both nonlinear and linear systems and can be used in many optical communication applications. The functioning system primarily linked to the amplitude of the input power. In the case of RSOAs are employed as

amplifiers, the system function in their linear region. On the contrary, RSOAs nonlinear behavior has been beneficial at other signal processing practices. These signal processing practices such as demultiplexing and wavelength regeneration are reviewed in (Mecozzi and Wiesenfeld, 2001; Leuthold et al., 2004; Leuthold et al., 2010). RSOAs also show powerful nonlinear gain saturation because of the distribution of light in both directions. Hence, RSOAs are preferred in access networks for their nonlinear noise suppression feature. These devices also occupy a small area and in parallel with they can be easily integrated with other devices (Yariv, 1990). The electro-optical and coupling efficiency of RSOA has developed over the years. Although RSOAs have many advantages, the polarization dependency of gain and high noise figures limit them to be widely implemented.

The operation of the RSOA is basically controlled by two equations: optical propagation and carrier rate. In the following section, the working principle and the theory of RSOA are presented. Static and dynamic modeling of RSOA is studied in appendices A and B with detail.

### 3.2. The Theory of RSOA

The main parameters of the RSOA can be listed as optical gain, gain saturation, polarization sensitivity, and amplifier noise. The gain in an SOA is obtained through transitions between the conduction band (CB) and the valence band (VB). The difference between the energies of these two bands is called bandgap energy (Eg). In a semiconductor, the three main transition processes between bands are called as absorption, spontaneous emission, and stimulated emission.

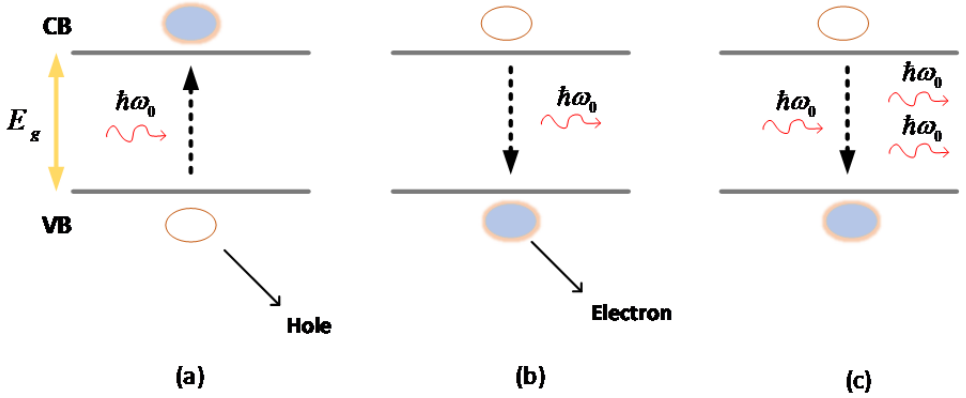



Figure 3.2. The transitions between bands in a semiconductor: (a) absorption, (b) spontaneous emission and (c) stimulated emission

Absorption occurs when the energy $\hbar\omega_0$ equal to or greater than Eg, the electron of the VB will absorb the energy of that photon and excites to CB. This process causes the generation of an electron-hole pair. Spontaneous emission occurs when an excited electron in CB is not in balance. Therefore, the electron transits into VB or somewhere in the gap band after some time in a random direction with releasing energy in the form of a photon. This process causes noise in optical amplifiers. Stimulated emission occurs when an incident photon interacts with the excited electron, causing its drop to the VB. Thus, a new photon is created with the same phase and polarization (Ramaswami et al., 2010). Amplification of the signal forms when stimulated emission is more prevailing. The stimulated emission in semiconductor devices is achieved by injecting current into SOA. When the injection current is small, only the absorption and spontaneous emission phenomena occur in the active region of the device. As the injected current increases, the phenomenon of stimulated emission grows, and a condition called transparency takes place when it is equal to the sum of absorption, spontaneous emission, and loss. The signal passes through the SOA without being amplified or attenuated at transparency conditions where the SOA behaves as a unit gain amplifier. When the injected current is high and stimulated emission is dominant

over absorption, spontaneous emission, and all losses involved, the population inversion condition occurs which enables the gain on the device (Ramaswami et al., 2010). The gain (G) of the amplifier can be expressed as in equation (3.1).

$$Gain(G) = \frac{P_{out}}{P_{in}} \tag{3.1}$$

The optical gain of an amplifier depends on the wavelength of the incident signal. The medium of the amplifier is an important factor for the optical gain wavelength. The gain coefficient can be written as in equation (3.2) in the case of a homogeneously broadened two-level system (Agrawal and Dutta, 2013).

$$g(\omega) = \frac{g_0}{1 + (\omega - \omega_0)^2 T_2^2 + \frac{P_{in}}{P_{sat}}} \tag{3.2}$$

where $g_0$ is the peak gain, ω is the frequency of the incident signal, $\omega_0$ is the frequency of transition between energy bands, $T_2$ is the dipole relaxation time and $P_{sat}$ is the saturation power (Agrawal and Dutta, 2013). Equation (3.3a) and (3.3b) demonstrate that the maximum gain occurs when the incident signal frequency encounters with the transition frequency. Figure 3.3 shows the plot of the g (ω) function, and gain spectrum G (ω) (Agrawal, 2012).

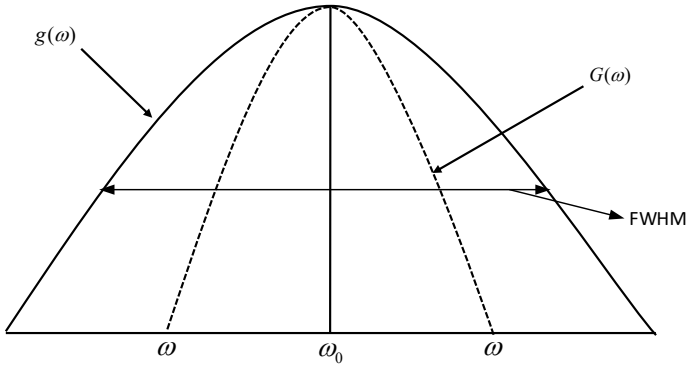



Figure 3.3. Lorentz g (ω) gain profile and corresponding gain spectrum amplifier G (ω) (Agrawal, 2012).

The gain bandwidth is defined as the Full Width at Half Maximum (FWHM) of the gain spectrum g (ω). For a Lorentzian spectrum, it is given by (Connelly, 2007):

$$\Delta\omega_g = \frac{2}{T_2} \tag{3.3a}$$

$$\Delta f_g = \frac{\Delta\omega_g}{2\pi} = \frac{1}{\pi T_2} \tag{3.3b}$$

where $\Delta f_g$ is the gain frequency.

Gain saturation occurs when the device operates in the nonlinear region (Gerd Keiser, 2013). As power increases, the availability of carriers in the active region decreases. Thus, the level of population inversion decreases which causes a reduction in the gain of the amplifier. The saturation point is where the gain falls by half (3 dB) as shown in figure 3.4 (Connelly, 2007).

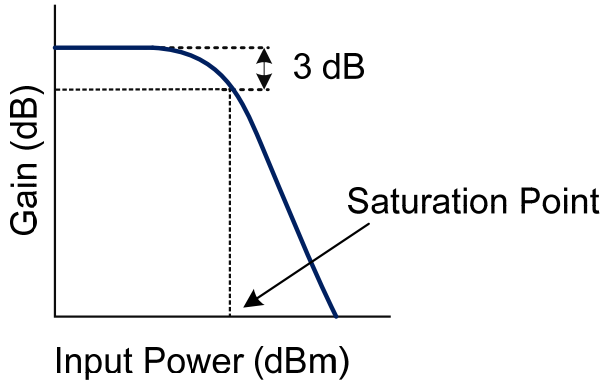



Figure 3. 4. RSOA Saturation Curve (Connelly, 2007)

When $\omega$ is equal to $\omega_0$, the equation (3.2) is simplified to:

$$G = \frac{G_0}{1 + \frac{P_{in}}{P_{sat}}} \tag{3.4}$$

Levels 0 and 1 of a digital signal have different power values, and this characteristic affects the RSOA when it is working in the saturation regime. There will be a decrease in the signal extinction ratio when the gain of level 0 is greater than level 1. The other parameters that influence the performance of the RSOA are the amplifier noise and polarization sensitivity.

The main source of noise in an SOA is the ASE (Agrawal and Dutta, 2013). ASE occurs when the spontaneously emitting photons amplify with the signal photons and this process cause noise. Another optical amplifier noise parameter is the noise figure (NF). It can be defined as (Gerd Keiser, 2013):

$$NF(dB) = 10 \log \frac{SNR_{input}}{SNR_{output}} \tag{3.5}$$

The abbreviation of SNR is the signal-to-noise ratio. The noise figure is dominantly influenced by the spontaneous emission factor $n_{sp}$, which is defined as in equation (3.6) (Connelly, 2007):

$$n_{sp} = \frac{n_2}{n_2 - n_1} \tag{3.6}$$

$n_{sp}$ is also called population inversion. $n_1$ and $n_2$ are the valence and conduction bands of the carrier density, respectively (Connelly, 2007). The relation of $n_{sp}$ with noise figure is (Agrawal and Dutta, 2013),

$$n_{sp} = \frac{NF - 1}{1 - \frac{1}{G}} \tag{3.7}$$

The minimum noise figure can be calculated using the equation (3.7). Current technology allows the population inversion value to be equal to 1 and the gain value to be much higher than 1. In this case, the minimum noise figure value is equal to 3 dB (Agrawal and Dutta, 2013).

The polarization sensitivity is another factor that affects the working principle of the RSOA. In general, the gain of an SOA depends on the polarization state of the input signal. This dependence is due to some factors, such as the waveguide structure, the anti-reflective coating material, and material gain (Senior John M, 2009). The waveguide of the amplifier is characterized by two polarizations, TE and TM transverse modes, orthogonal to each other. The polarization sensitivity of an SOA is defined as the difference between the gains of these modes.

### 3.3. Data Erasure Analysis of RSOA in Bidirectional WDM PON System

The advantages of WDM are having high capacity, security, enhanced reach, simplified operation, upgradability and service transparency. These advantages make WDM PONs as a solution for future optical networks. Although WDM-PONs have many advantages over other access technologies, it has been considered as very expensive for practical application. In a typical WDM-PON network, each ONU needs its own wavelength. This causes a hurdle for commercial deployment due to the OPEX and inventory administration costs. This issue has been identified since the early days of WDM-PON research. It is not easy to install different transmitters at subscriber premises. Once the transmitter deviates from the assigned wavelength, performances of other transmitters may affect as well. Therefore, colorless light sources are offered as solution to these problems.

It is necessary to improve colorless ONUs, in which the same basic optoelectronic hardware can be utilized. (Duarte et al., 2014). The colorless property permits the mass installation and production at all ONUs. (Gebrewold et al., 2015). Employment of colorless sources at ONUs will notably decrease the high maintenance, operation, and installation costs of WDM-PON networks. Thus, utilizing credible light sources at ONUs is a precondition for the deployment of WDM-PON (Xiong et al., 2013).

Different solutions have been demonstrated for the colorless transmitter in WDM-PON in literature. Combination of remodulation method with RSOA application to the user ends are considered as potential solution among them (Prat et al., 2005; Yu et al., 2007; Cho et al., 2009; Cho et al., 2010; Lee et al., 2010; Chi et al., 2012; Cho et al., 2012; Ó Dúill et al., 2012; Cho et al., 2013; Duarte et al., 2013; Duarte et al., 2014; Zhou and Deng, 2015; Choudhury and Khan, 2016; Jung et al., 2017).

The remodulation method simply can be explained as reusing the downstream light for upstream transmission unlike loop back scheme and it has

also known as a low-cost solution. The power splitter at ONU splits the downstream signal into two parts as upstream modulator and receiver. The use of colorless transceivers at the subscriber side, such as RSOAs (Cho et al., 2010; Lee et al., 2010; Cho et al., 2013; Duarte et al., 2014), allows easy and simple management of the transceiver inventory for the entire network, reducing OPEX and ensuring cost-effective operation. The RSOA remodulates the downstream wavelength with upstream data and then sends to the central office back (Lee et al., 2010). The RSOA should be operated in deep saturation to suppress the amplitude modulation in the upstream data and using unequal extinction ratios for the amplitude modulated traffic channels can minimize the crosstalk between US and DS data (Cho et al., 2010; Duarte et al., 2013). Sharing a single wavelength for both downstream and upstream induces the usage of productive optical spectra and allows a higher number of available channels when compared to the other loop-back scheme where distinct wavelengths for DS and US are used (Duarte et al., 2014). However, the usage of identical wavelength with downstream wavelength and upstream wavelength from RSOA degrades the performance due to the interference between US and DS carrier wavelength. This is due to the downstream data on the carrier that may not be erased fully in even in the saturation operation of RSOA. It is difficult to analyze the downstream data erasure ability of RSOA in experimental work. Hence, in this study, the data erasure analysis of RSOA in a remodulation system is investigated utilizing Optisystem software. RSOA performance and behavior are affected by several factors such as confinement factor, injection current, and injection power. In this chapter of the thesis, these parameters that affect the data deletion of the RSOA is investigated.

### 3.3.1. System Setup

The setup of the system is demonstrated in figure 3.5. The downstream signal is generated using MZ modulator at CO. The $ER_d$ value of the modulator is

applied as 5 and 10 dB. The modulated signal is sent to the ONU and reflected back to the OLT. The erasure analysis of the reflected signal is investigated by observing the changes in certain parameters.

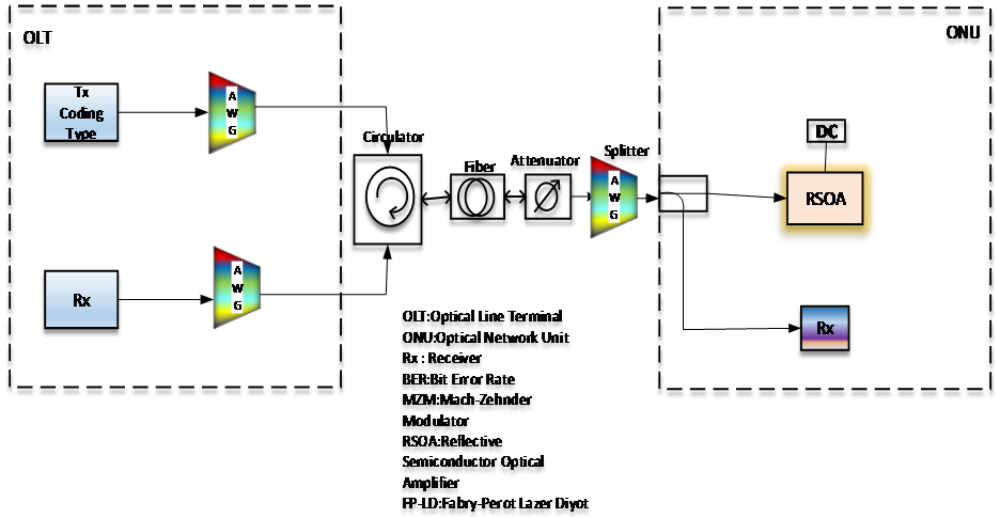



Figure 3.5. RSOA as a transmitter in bidirectional WDM PON

The attenuators are implemented to adjust the power level. The power is adjusted starting from – 20 dB up to 0 dB. The data rate of the design is 5 Gb/s at the 193.1 THz window. The specific parameters belong to RSOA is provided in table 3.1

Table 3.1. RSAO Specifications

Main Parameters

| Name | Value | Units |
|---|---|---|
| Input coupling loss | 3 | dB |
| Output coupling loss | 3 | dB |
| Input facet reflectivity | 50e-06 | |
| Output facet reflectivity | 0.99 | |

Physical Parameters

| Name | Value | Units |
|---|---|---|
| Active length | 600e-06 | m |
| Width | 0.4e-06 | m |
| Height | 0.4e-06 | m |
| Optical confinement factor | 0.4 | |
| Recombination coefficient A | 360e06 | 1/s |
| Recombination coefficient B | 0.559e-15 | $m^3/s$ |
| Recombination coefficient C | 30e-42 | $m^6/s$ |
| Group velocity | 75e06 | m/s |
| Temperature | 300 | K |
| Junction ideality factor | 2 | |

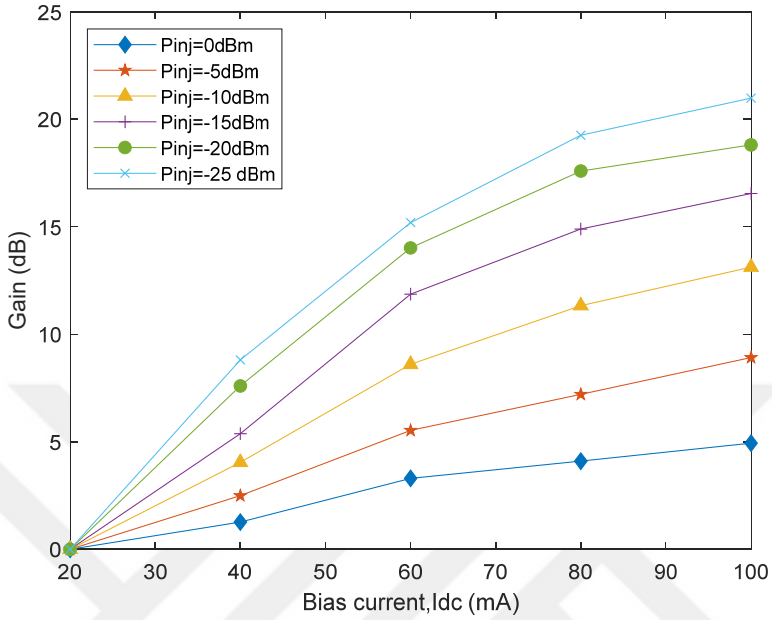
Enhanced Parameters

| Name | Value | Units |
|---|---|---|
| Gain constant $a_0$ (Differential gain coefficient) | 2.5e-21 | $m^2$ |
| Gain constant $a_2$ (Gain constant characterizing the gain- | 2.9e-32 | $m^4$ |

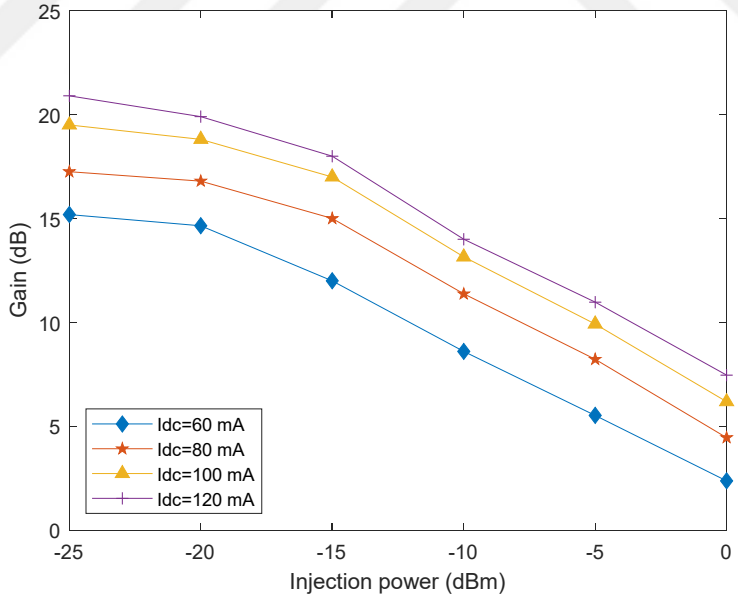
| | | |
|---|---|---|
| peak shift) | | |
| Carrier density at transparency | 1.4e24 | $m^{-3}$ |
| Nonlinear gain parameter (Equivalent effective refractive index at zero carrier Density) | 1.2e-22 | $m^3$ |
| $m_{hl}$ (Effective mass of a light hole in the valence band) | 5.06e-03 | kg |
| $A_{rad}$ (Linear radiative recombination coefficient) | 10e06 | 1/s |
| $B_{rad}$ (Bimolecular radiative recombination coefficient) | 5e-16 | $m^3/s$ |
| Active refractive index | 3.22 | |

### 3.3.2. Results and Discussion

The gain plot versus bias current and gain plot versus injection power are shown in figures 3.6a. and 3.6b, respectively. The obtained gain value is 22 dB for an -25 dB injected power and 100 mA bias current. The gain starts to saturate over 60 mA. Figure 3.6b demonstrates that the gain starts to saturate over -20 dBm injected power.




(a)




(b)

Figure 3.6. Gain plot of RSOA with regard to: a. bias current, b. injected power

The residual downstream extinction ratio with regard to biased current is shown in figure 3.7. In this plot, two different extinction ratio and injected power values are simulated to make the comparison among them.

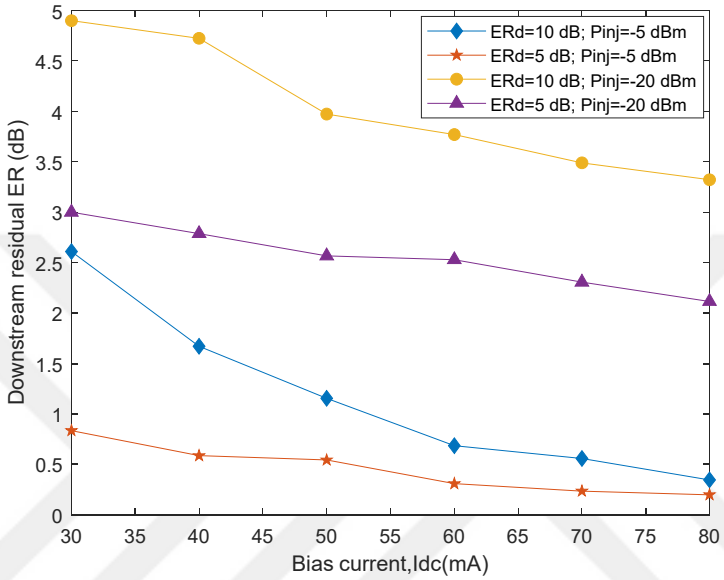



Figure 3.7. Extinction ratio versus bias current plot at different values

It is clear to observe that decreasing the $ER_d$ and increasing the $P_{inj}$ values help to erase the residual data fully. The $ER_d$ value below 0.5 value indicates that the data is erased. When the $ER_d$ is 5 dB and $P_{inj}$ value is -5 dBm, the downstream data is erased completely. The $P_{inj}$ value at -20 dBm cannot erase the data due to its working region is on the linear area.

Increasing the bias current is another important factor where that shows residual data can be erased. However, increasing the current also increases the mode competition inside the device. Therefore, the upstream BER plot with regard to increasing current is shown in Figure 3.8.

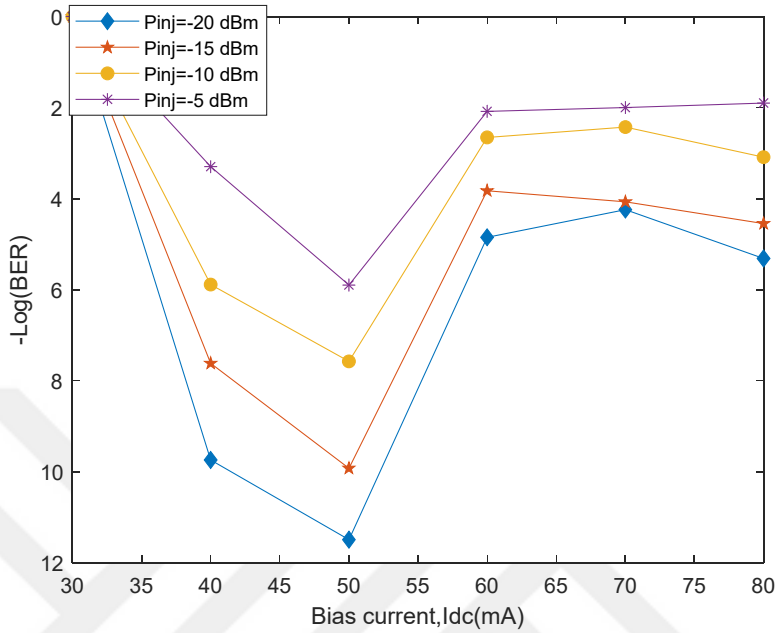



Figure 3.8. BER versus bias current plot

Figure 3.8 can be interpreted as the bias current applied to RSOA should be bigger than 50 mA to erase the downstream data.

Figure 3.9 shows that the downstream data can be completely erased at injection power of – 5 dBm. When the power applied below -15 dBm, the downstream signal is detected at CO which shows that the data is not erased at ONU.

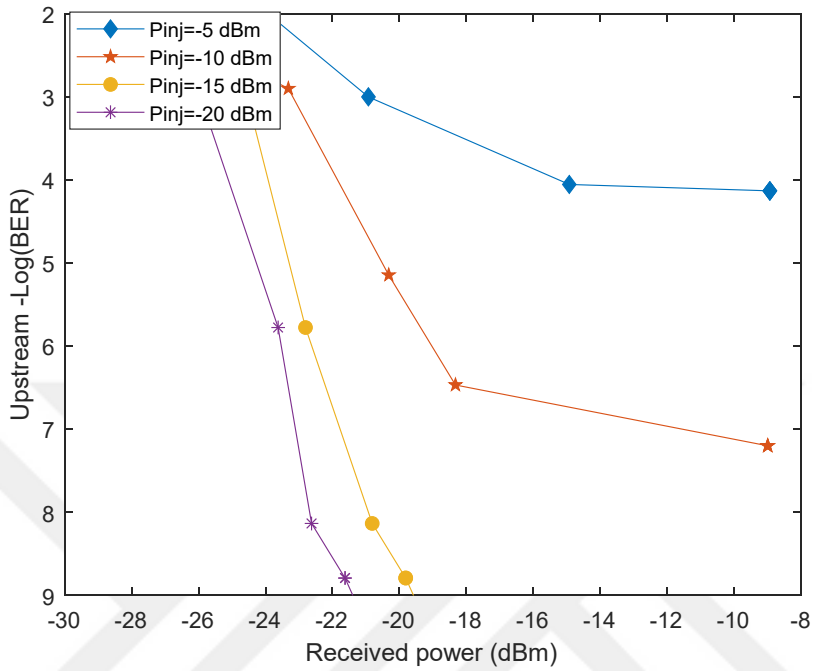



Figure 3.9. BER versus received power plot

The other factor that affects the data erasing is the confinement factor. Increasing the confinement factor helps to data be erased easily as shown in figure 3.10. Increasing the injection power at a constant confinement factor also makes the data to be erased.

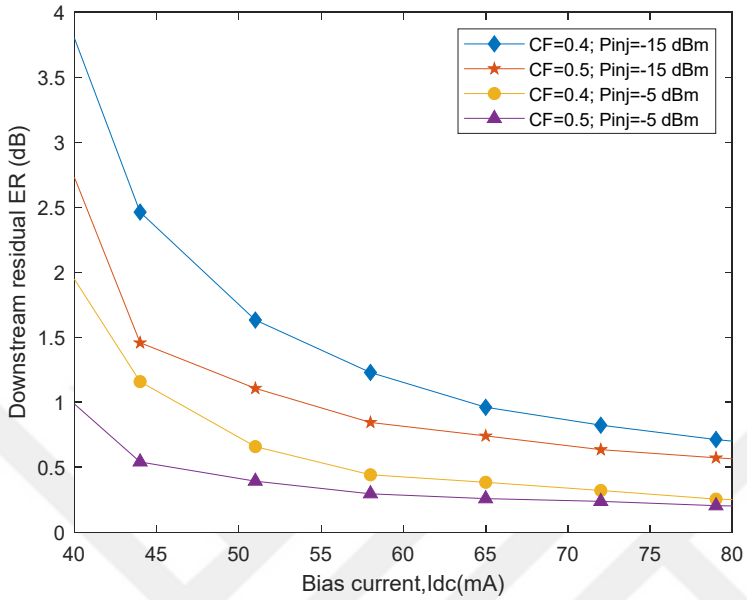



Figure 3.10. $ER_d$ versus biased current plot at different CF and $P_{inj}$ values

Increasing the CF value from 0.4 to 0.5, decreases the downstream data to reach OLT which means the data is erased. The increasing of injection power from -15 dBm to -5 dBm also erases the downstream data.

This chapter analyzed the downstream data erasure capability of the RSOA in a remodulation PON system. The simulation results demonstrated that the increasing bias current, injection power, and confinement factor are the important parameters that take the role to erase the downstream data at ONU at a remodulation system. It is determined that the increasing the parameter values as bias current over 50 mA, the confinement factor over 0.4, and the injection power over -15 dBm prevent the crosstalk between upstream and downstream data at ONU.

# 4. FABRY PEROT LASER DIODE CHARACTERISTICS

FPLD has advantages such as simplicity, low cost, high data rates, and low power consumption. Thus, it provides an efficient and powerful solution to the user ends in a WDM PON network. However, the application of the FPLD is limited due to its multimode operation. This operation can increase the intensity noise and decrease the bandwidth and power budget. To overcome these problems, the injection of the laser diode to one mode is proposed. Locking laser to a specific wavelength decreases the chirping, noise, and increase the modulation bandwidth. Thus, the data rate improves with reduced device and maintenance cost. In this section of the thesis, the FPLD is studied in detail. Firstly, the theory of the FPLD is explained. Secondly, the injection-locked FPLD is investigated.

## 4.1. The Characteristics of the FPLDs

FPLD is a type of semiconductor lasers. All around the cavity sides are doped with n-type and p-type material. The bottom and top of the FPLD is coated with electrical contacts. The mirrors are built to the side ends. The active layer of the laser is quite thin. Thus, the refractive index value of the active layer is very close to the surrounded material of the laser. Hence, lasing occurs in lateral mode and this can be minimized by using anti-reflective material.

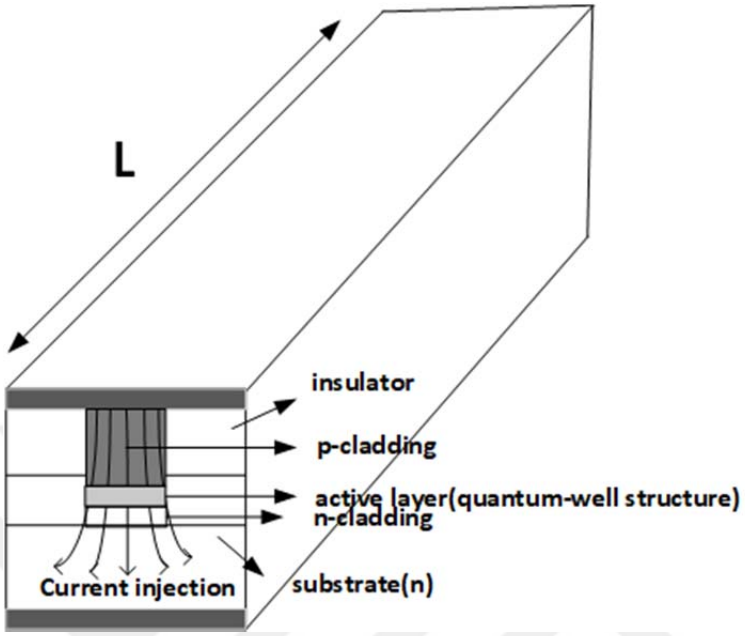



Figure 4.1. The design of the FPLD

The basic principle of the FPLD is shown in figure 4.2. The cavity of the laser includes two reflectors at the ends. The end facets are cleaved and coated. The active medium between the reflectors amplifies the light which travels between backward and forward inside the cavity. This cavity also needs to limit propagating beam diffraction. The amplification occurs over the laser's entire length through injecting current into laser diode.

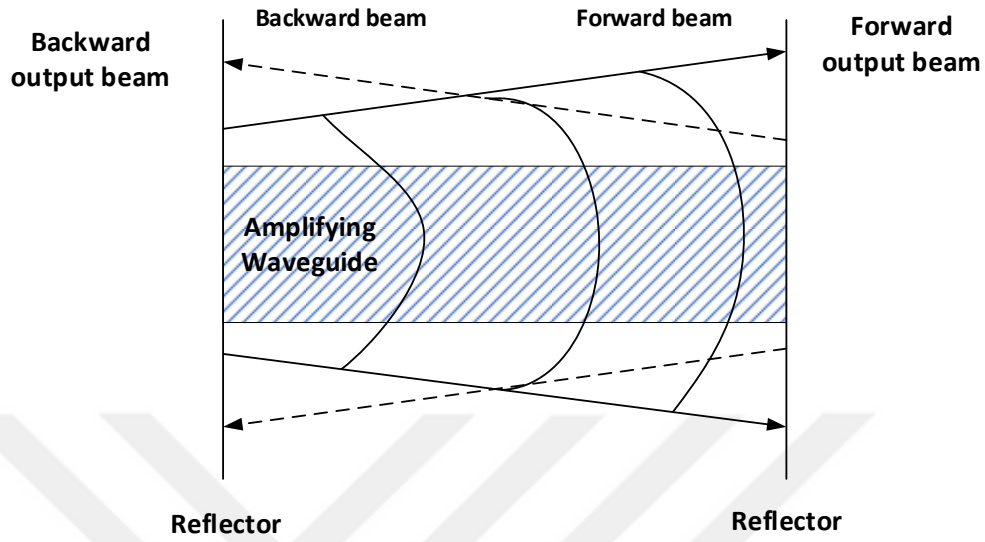



Figure 4.2. The basic schematic of FPLD: optic medium with end mirrors (Morthier and Vankwikelberge, 2013)

The center layer is separated from cladding with heterostructure. The cladding and center layers are creating a thin-film waveguide. The injected current occurs population inversion inside the central layer. The claddings confine the light in the center layer and create stimulated emission. The produced wavelengths inside the cavity depend on the length of the cavity (Kasap, 2013). These wavelengths are defined as longitudinal modes of the FPLD and can be expressed by the following formula (Chuang, 1995).

$$L = \frac{m\lambda}{2n} \tag{4.1}$$

Where, m: arbitrary integer

landa: wavelength

L: cavity length

n: refractive index

According to the formula (4.1), the eternal number of modes can be supported by the cavity. However, the semiconductor substance just provides gain in a limited range of wavelengths. The gain curve determines this range. The material of the laser such as quantum well or bulk also affects the gain curve range. The classic gain curve and the lasing modes are as shown in figure 4.3, respectively(Dutton, 1998).

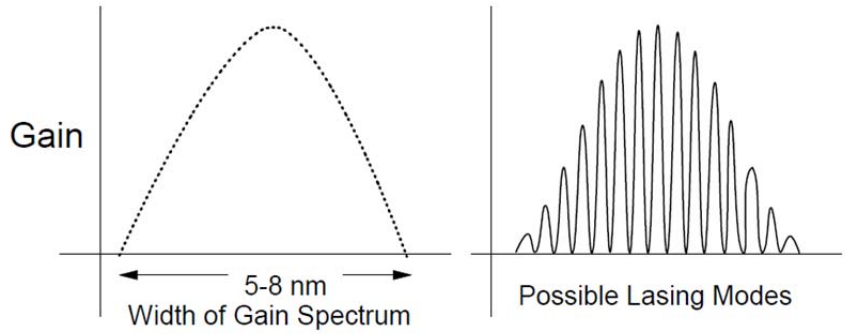



Figure 4.3. a. The gain spectrum, b. produced lasing modes

A Fabry-Perot laser can generate a wavelength spectrum. All wavelengths must be capable of resonating in the cavity and must be in the range of the gain spectrum of the cavity.

To abstain from the output power loss, it is preferred to apply the rear facet reflectivity of the Fabry-Perot laser highly around 90% and front facet around %7(Cikan and Aksoy, 2019). Hence the output power is produced primarily from the laser front facet.

The free spectral range (FSR) of the laser can be explained as the gap between consecutive modes and can be expressed as in equation (4.2).

$$\Delta\lambda = \frac{\lambda^2}{2n_g L} \tag{4.2}$$

Where, Ng: group refractive index

Landa: wavelength and these can be expressed as

$$n_g = n - \lambda \frac{\partial n}{\partial \lambda} \tag{4.3}$$

$$\lambda = \frac{c}{f} \tag{4.4}$$

The wavelength and frequency are related with the formula in equation (4.5).

$$\Delta f = -\frac{c}{\lambda^2}.\Delta\lambda \tag{4.5}$$

Frequency spacing of consecutive modes:

$$\Delta f = \frac{c}{2n_g L} \tag{4.6}$$

To summarize, the main specifications of the FPLD can be listed as follows:

- The material of the FPLD is comprised of the semiconductor.
- The coherent light is emitted.
- The laser can be modulated directly.
- The modes of the laser are generally multiple longitudinal.

### 4.2. Injection-Locked Technique

WDM PONs have many advantages over other technologies such as protocol transparency, security, and high capacity. However, WDM PON systems have expensive components. Thus, these expensive components prevent WDM PON networks to deploy widely. Colorless optical sources have been offered to solve the expensive cost issue. Although the application of colorless sources at the user ends partially solved the problem, there were still some problems that degrade the transmitter performance. Injection-locking has also been proposed to enhance the transmission performance of the transmitters. Injection-locking is an innovative method that provides high-speed transmission and overcomes the degrades in transmission performance. To set up an injection-locked system, a laser is needed (usually called as master) to inject photons into the slave laser.

There are two major effecting factors of injection locking. The first one is to enhance the slave laser characteristics. The second is to provide the synchronization of slave and master lasers. The application of injected-locked lasers instead of the tunable lasers at the user ends also decreases the cost of the system. Hence, injection-locking is very important in WDM PON network systems. This technique guarantees the single-mode operation, minimize the mode partition noises, and decrease the linewidth of the laser (Jin and Chuang, 2006). Such enhancements increase the modulation bandwidth.

In this thesis, theoretical and simulation of injection-locked FPLD (IL-FPLD) is investigated and the results are compared with the free-running FPLD. The results have demonstrated that the IL-FPLD modulation response is better than free-space laser. Additionally, IL-FPLD removes mode partition noise, chirping, and mode hopping. It can also minimize the linewidth and provide a single-mode operation. One other advantage of injection locking is the external injection minimize the nonlinearity, increase the relaxation frequency, and linearity for modulation response can be ensured at lower frequencies. This tends to decrease the intermodulation distortions considerably.

### 4.2.1. Injection Locking on FPLD

The application of IL-FPLDs at user ends is a colorless cost-efficient method. The central office transmits the light to the ONU to externally lock the laser. The refractive index of the medium and FPLD cavity length determine the longitudinal modes of the laser. The mode partition noise appears when any longitudinal modes are filtered. Free running FPLD is not suitable for carrier transmission due to the relative intensity noise (Hyun Deok et al., 2000). On the other side, the free-running FPLD locks to a specific mode by suppressing other cavity modes when externally seeded and so the intensity of the locked mode improves. FPLD operates in quasi-single mode when side mode suppression ratio (SMSR) is higher than 30 dB.

CW lasers or ASE sources can be used for externally seeded lights. Spectrum-sliced ASE sources are incoherent, provide stable output power and cost efficient. Notably, the unpolarized feature of the ASE sources yields advantages while operating with polarization-dependent Fabry Perot lasers. Nevertheless, the ASE source causes RIN and decreases the data rate of the externally seeded source. The intensity noise of the spectrum sliced is transmitted to the externally seeded source and degrades the laser performance(Cheng et al., 2006). Phase noise and the filtering effect of IL-FPLD degrade the WDM PON network performance (Lee et al., 2006; Kim et al., 2007). Spectrum sliced ASE injected FPLD reached to 1.25 Gb/s over 45 km with using RZ modulation (Kim, 2010). The transmission performance of the network increased to 2.5 Gb/s after implementing the noise suppressor to the end of the externally seeded source (Jeong and Lee, 2009).

The performance of the IL-FPLD increases when seeded by a coherent CW source. The needed seeding power is less for coherent sources when compared with the incoherent sources. Coherent seeding source provide low-intensity noise and thus the data rate of IL-FPLD increases up to 10 Gb/s (Xu et al., 2007). However, the tuning range between the seeding source and the seeded source must be arranged carefully to provide smooth transmission. Spectrum sliced FPLD can also

be used as a seeding master source and demonstrate the average performance between CW seeding and ASE seeding sources. It shows high mode partition noise and this limits the FPLD to be used as a carrier. The work of FPLD as a master laser is demonstrated in (Kwon et al., 2005) and 2.5 Gb/s data rate to a distance of 25 km was achieved.

### 4.2.2. Weak Resonant Cavity FPLD

IL-FPLD is negatively affected from rayleigh backscattering induced penalty due to the central office performs the externally seeding. The increase of the linewidth of the seeding source decreases the penalty. In this case, ASE seeded IL-FPLD more resistant to the back-reflection penalty (Moon et al., 2007). On the other hand, coherent light seeded IL-FPLD is exposed to a penalty due to back-reflection (Moon et al., 2007).

Bias current and temperature are impactful factors on wavelength fluctuation for both FPLD and the seeding source in practical systems. There can be still light fluctuation on the central wavelength even with the usage of the temperature controller in the system. Thus, injection locking range increment can be attractive in practical applications. Decreasing the facet reflectivity of the FPLD like around 1 % induce the laser to produce lower resonance and thereupon to lase in weak mode. Therefore, the injection locking range of the weak resonant cavity FPLD (WRC FPLD) is larger, unlike typical FPLD (Lin et al., 2011). WRC FPLD can operate almost uncooled, which removes the need of longitudinal mode alignment with seeding source. This performance resembles externally seeded RSOA where wavelength alignment is not needed (Lin et al., 2009; Xiong et al., 2012).

### 4.2.3. Theoretical Model of IL-FPLD

The dynamic theoretical model of IL-FPLD was studied in (Lang, 1982; Mogensen et al., 1985). The significant researches on the improvement of

modulation bandwidth (Lau et al., 2008), nonlinear noise suppression (Seo et al., 2001), and minimizing the intensity noise (Simpson et al., 1995) were performed.

The rate equation of a free-running laser is given in equation (4.7) (Lau, 2006).

$$\frac{\partial E(t)}{\partial t} = \frac{1}{2} g \Delta N (1 + j\alpha) E(t) \tag{4.7}$$

$$\Delta N = N(t) - N_{th} \tag{4.8}$$

In which, $E(t)$ : electric field,

$g$ : linear gain coefficient

$\Delta N$ : carrier number above threshold

$\alpha$ : linewidth enhancement factor

The rate equation model of IL-FPLD was studied in (Kun-Youl et al., 2005). The dynamic rate equations of FPLD can be presented as follows:

$$\frac{\partial E_0}{\partial t} = \frac{1}{2}(1 + j\alpha)(G_0 - \gamma) E_0(t) + F_E^0(t) + k_c E_{inj} e^{j2\pi\Delta f} \tag{4.9}$$

$$\frac{\partial E_i}{\partial t} = \frac{1}{2}(1 + j\alpha)(G_i - \gamma) E_i(t) + F_E^i(t) \tag{4.10}$$

$$\frac{\partial N}{\partial t} = \frac{I}{qV} - \gamma_e N - \sum_i G_i \left| E_i \right|^2 \tag{4.11}$$

And,

$$G_i = \frac{\Gamma v_g \alpha (N - N_0)}{\left[1 + \left(\frac{2i\Delta f_{mode}}{\Delta f_g}\right)^2\right].(1 + \varepsilon \sum |E_i|^2)} \tag{4.12}$$

$$\gamma = v_g(\alpha_{int} + \alpha_m) \tag{4.13}$$

$$\alpha_m = \frac{1}{2L}.\ln\left(\frac{1}{R_f R_b}\right) \tag{4.14}$$

$$\gamma_e = A_{nr} + BN + CN^2 \tag{4.15}$$

$$\Delta f = f_{inj} - f_0^{th} \tag{4.16}$$

$$k_c = \frac{v_g(1-R_f)}{2L\sqrt{R_f}}.\sqrt{\frac{\eta(\sqrt{R_f}+\sqrt{R_b})(1-\sqrt{R_f R_b}}{\sqrt{R_b}(1-R_f)\ln\left(\frac{1}{\sqrt{R_f R_b}}\right)}} \tag{4.17}$$

Where, $|E(t)|^2$ is photon density, $\gamma$ is the loss factor, $\gamma_e$ is the carrier recombination rate, $k_c$ is the coupling efficiency, and $F_E^i(t)$ is the spontaneous emission noise.

The parameters of FPLD applied in simulations of the thesis are given in table 4.1.

Table 4.1. FPLD Spesifications

Main Parameters

| Name | Value | Units |
|---|---|---|
| Frequency | 193.1 | THz |
| Bias current | 30 | mA |
| Front facet reflectivity | [0,1] | |
| Rear facet reflectivity | [0,1] | |
| Laser model | Spatially averaged multimode | |

Physical Parameters

| Name | Value | Unit |
|---|---|---|
| Active Layer Parameters | | |
| Active length | 0.06 | cm |
| Active layer width | 15e-05 | cm |
| Active layer depth | 20e-06 | cm |
| Group index | 3.5 | |
| Quantum efficiency | 0.4 | |
| Gain bandwidth | 5 | THz |
| Mode confinement factor | 0.4 | |
| Carrier Parameters | | |
| Recombination model | Lifetime | |
| Carrier lifetime | 1.86e-09 | s |
| Recombination coefficient A | 100e06 | 1/s |
| Recombination coefficient B | 0.2e-09 | $cm^3/s$ |
| Recombination coefficient C | 40e-30 | $cm^6/s$ |

The output-spectra comparison of wavelength-locked with ASE sliced and free-running FPLD is demonstrated in figure 3.4 (Park and Lee, 2008)

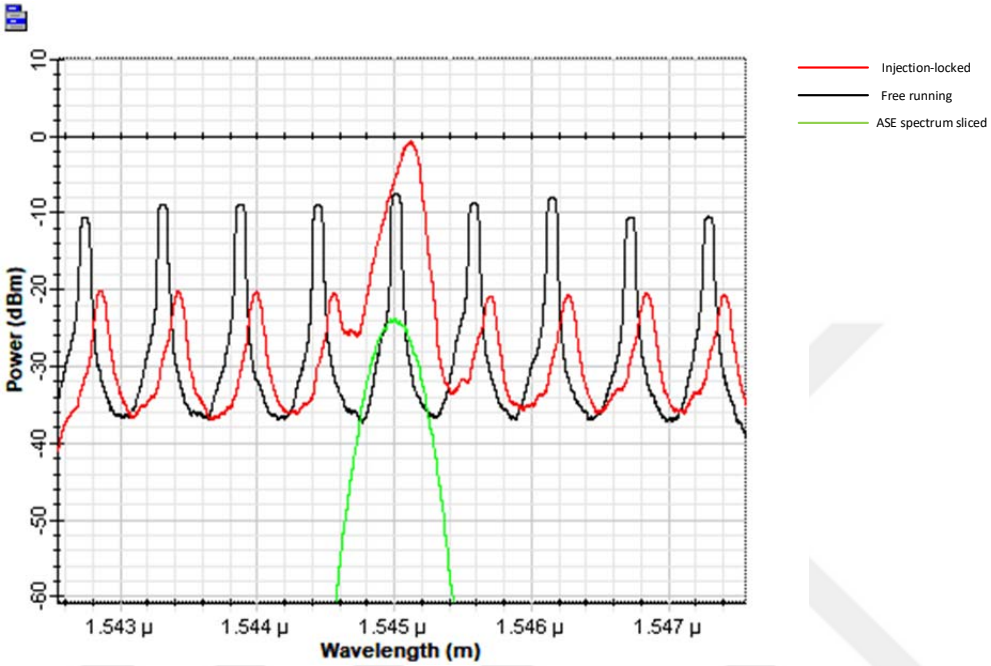



Figure 4.4. Simulation result of ASE spectrum sliced, free running and injection locked FPLD (Park and Lee, 2008)

# 5. DATA ERASURE ANALYSIS OF FPLD BASED ON REMODULATION BIDIRECTIONAL PON SYSTEM

The data-erasing mechanism is a promising cost-efficient option for future broadband access networks. This chapter analyzes the data erasure efficiency of the FPLD at a speed of 5 Gb/s based on bidirectional WDM PONs using the carrier remodulation technique. The effects of many parameters such as the biasing current, extinction ratio, confinement factor, and injection power demonstrate the data erasure efficiency of the FPLD in the upstream bidirectional remodulation PON system are discussed. The novelty of this study is the very high front facet reflectance results are demonstrated for the first time and comparison with commercial front facet reflectance are shown. A range of injection power from -25 dBm to 0 dBm and an FPLD bias current of 20-100 mA were applied to the system. The injection power below 0 dBm and bias current above 30 mA provide successful transmission of upstream data. The FPLD can suppress the residual downstream extinction ratio <0.5 dB, which removes the need of additional data erasure usage.

## 5.1. Overview

In recent years, there is an exponentially increasing demand for broadband and high-data-rate applications. The PON has emerged to provide a significantly higher bandwidth for the access network, and access services have offered WDM PON as a final solution for future broadband communication(Banerjee et al., 2005). The most critical problem in the application of practical WDM PON networks is to apply low-cost transmitters at optical network units(ONUs)(Kazovsky et al., 2007; Yeh et al., 2008). To solve this problem, WDM PONs have offered solutions such as the use of colorless transmitters because of the advantages of colorless technology, such as the low cost, jitter, latency, and dedicated bandwidth(Lin et al., 2009; Lin et al., 2010; Cikan and Aksoy, 2019). Identical ONUs, which are called

colorless sources, are applied to reduce both capital expenditure (CapEx) and operational expenditure (OpEx)(Maher et al., 2010).

There are many methods to apply colorless ONUs, such as spectrum slicing(Healey et al., 2001; Soo-Jin et al., 2004; Payoux et al., 2005; Lin et al., 2009; Antoniades et al., 2011), optical loopback solutions(Ki-Man et al., 2006; Park et al., 2007; Berrettini et al., 2009; Schrenk et al., 2009; Antoniades et al., 2011) and mode control method(Lin et al., 2015; Tsai et al., 2016). A wavelength-filtered broad-optical-spectrum light source is used for each ONU in the spectrum slicing method. In the optical loopback method, ONUs are remotely fed with generated optical carriers at the OLT or some point of the network (Ki-Man et al., 2006; Park et al., 2007; Berrettini et al., 2009; Schrenk et al., 2009; Antoniades et al., 2011).

Generally, in an optical loopback method, ONUs have reflective facets. The FPLD(Ki-Man et al., 2006), RSOA(Park et al., 2007) and REAMs can be used as optical sources to satisfy high data rates at the ONUs (Berrettini et al., 2009; Schrenk et al., 2009). To remotely seed an ONU, a separate wavelength is sent with a downstream channel. Thus, the ONUs perform upstream transmission over this particular wavelength. The usage of different wavelengths for upstream and downstream requires an increased number of transceivers and induces high cost.

Alternatively, the upstream data can be modulated to the same wavelength with the carried downstream data. The ONUs remodulate the upstream data on the downstream optical carrier with this method(Antoniades et al., 2011), but the usage of an identical wavelength for both upstream and downstream (bidirectional communication) causes physical impairments(Antoniades et al., 2011). There are two main solutions to solve this problem. The first solution is the use of orthogonal modulation formats in bidirectional fibers (Wai et al., 2003; Prat et al., 2005; Martinez et al., 2008). However, applying different modulation systems to the optical ends increases the cost. The second solution is to erase the downstream data to separate it from the upstream data and remodulate the downstream optical carrier

with the upstream data(Takesue and Sugie, 2003). Therefore, the data-erasing mechanism is a promising cost-efficient option for future broadband access networks(Chi et al., 2012; Li et al., 2015).

In this work, a remodulation scheme for bidirectional fiber is investigated to perform low cost WDM PONs. There are many studies on the use of injection-locked FPLD in carrier remodulation schemes(Chan et al., 2002; Wai et al., 2003; Sang-Mook et al., 2005; Jeung-Mo and Sang-Kook, 2006; Kim and Han, 2006; Kim, 2008; Lu et al., 2016). However, the data erasure of downstream data in the FPLD has been discussed only once in the literature to the best of our knowledge(Su et al., 2015), where the current biasing and injection power( $P_{inj}$ ) parameters were considered to explain the data erasure efficiency inside the FPLD. In this study, the data erasure efficiency is studied with more details, where many parameters such as the confinement factor, extinction ratio, current levels, injection power, and effects of the facet reflectivity to the system are discussed. In addition, the results for very high front facet reflective are demonstrated for the first time.

### 5.2. System Setup

The remodulation system setup is shown in figure 5.1.

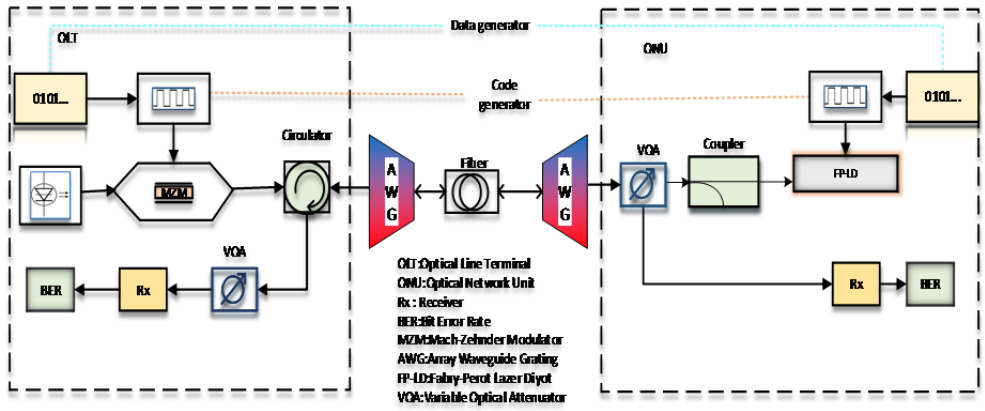



Figure 5.1. Carrier remodulation system based on bidirectional WDM PON using FPLD at ONU

The system consists of three main parts. At the OLT side: The downstream data was modulated by the Mach-Zehnder (MZ) modulator, which uses non-return-to-zero (NRZ) data to generate signals to transmit the optical carrier with the downstream data. The AWG multiplexes the signals generated from the downstream transmitters; then, these signals are sent to the AWG at the optical ends using bidirectional optical fibers. The AWG at a remote node performs demultiplexing and sends demultiplexed signals to the ONUs.

The downstream signal is divided into two portions by the optical coupler at the ONU. The lower intensity fraction was sent to the receiver, and the remained power signal was directed to the transmitter at the upstream to be used as an optical carrier. Hence, the remaining signal is erased in the FPLD, and the upstream data are remodulated on the downstream carrier. The usage of the same carrier for both upstream and downstream directions helps to remove the separate signal carrier usage for upstream.

Downstream and upstream signals are separated using a circulator at the OLT to prevent crosstalk in the bidirectional fiber. The power levels of the system are controlled with two VOAs at the OLT and ONU. The data-erasing ability of the FPLD was observed by a BER analyzer.

The gain-saturated RSOA can also be implemented as an upstream transmitter, but the modulation bandwidth of the RSOA is limited and cannot provide high-speed data transmission(Sang-Mook et al., 2005; Kim and Han, 2006; Kim, 2008) . The injection-locked FPLD has an inherent data suppression effect, which largely decreases its ASE noise compared to a gain-saturated SOA(Lin et al., 2011; Chi et al., 2012; Lu et al., 2016).

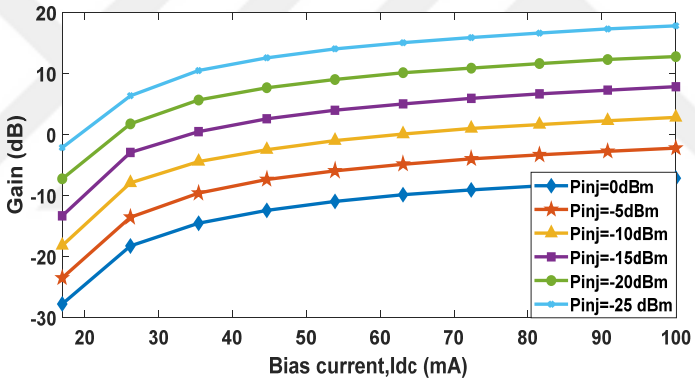
The cavity length of the colorless FPLD is 600 $\mu m$ , the confinement factor (CF) is 0.4, and two different reflection facets of %0.2 and %93 were applied to the FPLD. These two reflective facets of FPLDs were compared for each parameter that measures the erasure efficiency of the FPLD. The smaller facet reflectance demonstrates a weaker effect at cavity, which benefits from a wide injection locking range and low injection power requirement(Su et al., 2015). The colorless FP-LD was biased from 20 to 100 mA to simultaneously provide the data erasing and carrier reuse for optimization. The downstream injection power was detuned from -25 to 0 dBm using the VOA. The system data rate was set as 5 Gbps in 1550 nm window.

The data-erasing ability of the internal FPLD is demonstrated by using the Optisystem 15 evaluation software. The figures of merits were analyzed, including the downstream residual ER, upstream injection power, FPLD bias current, CF and received power measurement at the OLT. In addition, the reflective facets of the FPLD were changed, and the erasure efficiency of these FPLDs were compared.

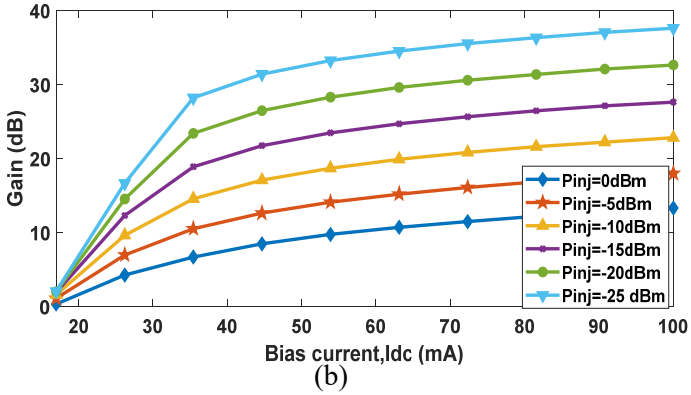
### 5.3. Results and Discussion

The gain versus bias current curve of the FPLD is demonstrated in figure 5.2. All figures were evaluated with high and low reflective facets of the FPLD to demonstrate the effectiveness of the reflective facets of the FPLD in data erasure. The reflective facet of FPLD was employed as %0.2, which is the practical value for a WRC FPLD, and the results were demonstrated in parts b of the figures. In

addition, the reflective facet of the FPLD was increased to %93 to observe the effect of the increased reflective facet on the data erasure in the FPLD. The modulation peak current of higher reflective facet FPLD is increased to 10 mA. Figure 5.2 shows that the maximum gain is approximately 17.8 and 37 dB for the higher and lower reflective facets, respectively, at the injection power of -25 dBm. For both reflective facets, absorption occurs for up to 10 mA, linear gain occurs for $I_{bias}$ up to 30 mA, and the optical gain saturates immediately above the threshold current, which is approximately 30 mA. The reduced facet reflectance design creates a weak resonant feature and shows a higher gain spectrum at identical injection power levels.



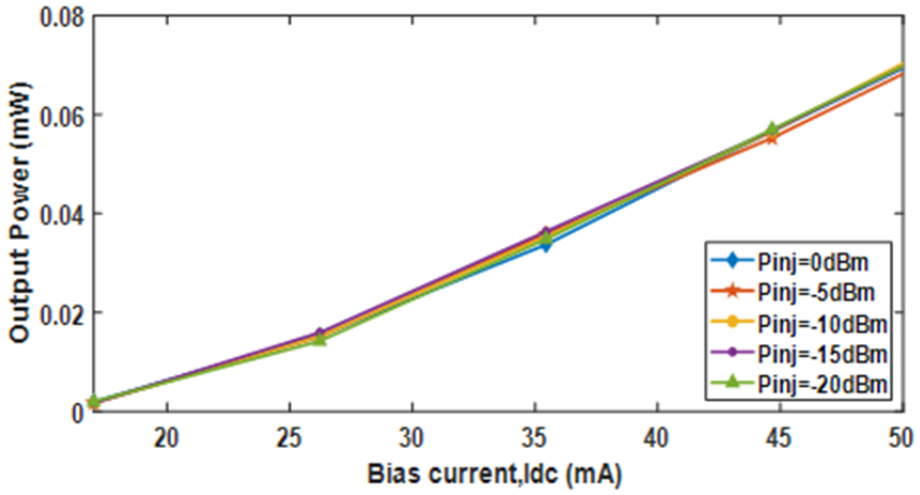

(a)



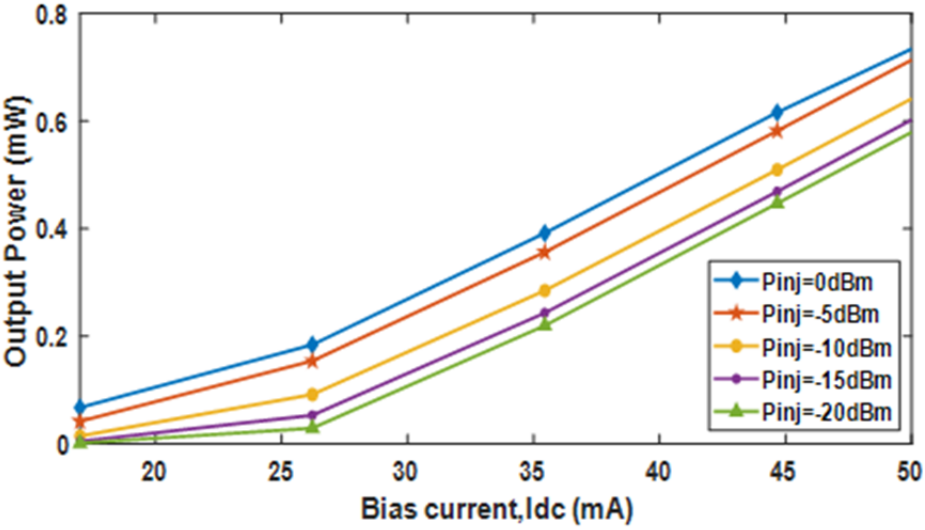

(b)

Figure 5.2. FPLD gain characteristics; a: reflective facet %93; b: reflective facet %0.2

The plot of output power versus current of the colorless FPLD by injecting different power levels is shown in figure 5.3. The on-off-keying(OOK) data do not enable the FPLD to significantly change its power over the current response, so the power limits the switching in a finite range and suppresses the downstream data(Lu et al., 2016). This phenomenon effectively ensures that the upstream modulation is protected from interference with the residual downstream data in a colorless injection-locked FPLD. The stimulated emission of the desired mode increases with externally injected photons and supports the gain competition of the upstream FPLD. Thus, the threshold current decreases, and the output power increases(Lu et al., 2016). The output power of the upstream FPLD only increases from 0.56 to 0.72 mW at the bias current of 50 mA with 15 dB increment in injection power. Interestingly, the very highly reflective facet FPLD outputs overlap and demonstrate identical output power results for any injection power. Thus, higher facet FPLD designs are not affected by any $P_{inj}$ level.




(a)




(b)

Figure 5.3. Power versus current response of FPLD; a: reflective facet %93; b: reflective facet %0.2

The modulation bandwidth of the FPLD improves with increased injection power. The injection-locked FPLD relaxation oscillation frequency can also be

lightly increased due to both enhancements in relative strength of the coupling and increase in gain coefficients(Su et al., 2015).

The other method to analyze the data erasure ability of FPLD is to check the residual ER of the 5-Gb/s NRZ OOK downstream data encoded on the carrier. Adjustments must be made at the FPLD to minimize the residual ER of the downstream data. By sufficiently increasing the DC bias in the FPLD, we can erase the downstream data, and the remained data can be observed as the intensity noise for the upstream transmission. Therefore, different levels of injection powers and bias currents were applied to the system to demonstrate the erasure efficiency of the FPLD. The eye diagrams were also demonstrated to observe the transmission capability of the upstream transmitter after erasure, as shown in figure 5.4. For the FLPD with lower reflective facets, the bias current increase from 25 to 55 mA dramatically suppresses the residual ER of the downstream data from 4.8 to 0.7 dB at the injection power level of 0 dBm as shown in figure 5.4b. Furthermore, the residual ER can be reduced to below 0.1 dB by decreasing the downstream injection power to -20 dBm. The reason is that the inherent mode competition dominates the transient behaviour of the FPLD and ultimately minimizes the corresponding shift of the power to the current transfer function at the lasing condition to confine the power switching range(Su et al., 2015). A highly-reflective-facet FPLD suppresses the residual ER at the same rate of downstream data from 5 to 0.7 dB, which is independent from any injection current level. When a low bias current is applied, the residual ER of the suppressed downstream data lightly increases for the lower reflective facet because the incompletely erased downstream data under the weak data suppression effect slightly increases the intensity noise(Su et al., 2015). By increasing bias current of FPLD to above 35 mA, we notably reduced the residual ER of the downstream data delivered by the MZ modulator to <1 dB. As a result, the FPLD that operates at high bias current can improve its data erasing effect without decreasing the injection power because an inadequate injection power can degrade the upstream transmission performance.

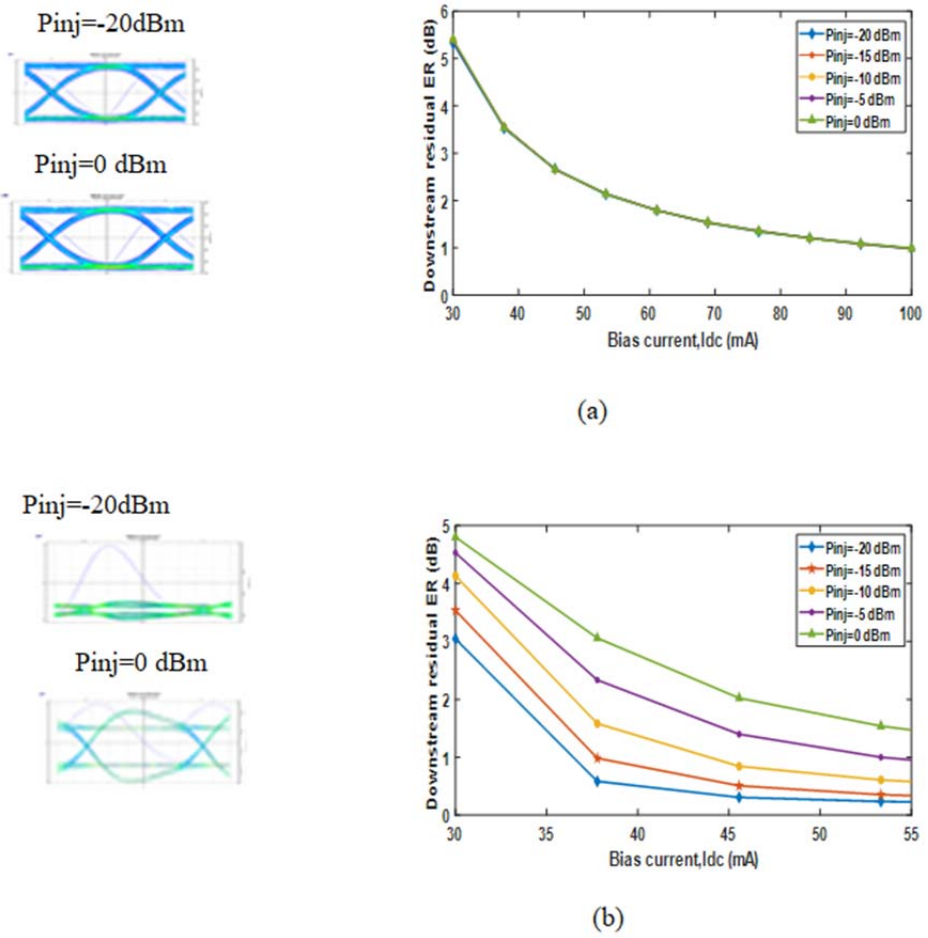



Figure 5.4. Eye diagrams and downstream residual ER&FPLD bias current plot at different injection power levels; a: reflective facet %93; b: reflective facet %0.2

In figure 5.5, the residual downstream ER at the upstream is plotted for two different downstream ER values as 10 and 5 dB and injection powers as -5 and -20 dBm. The eye diagrams were also demonstrated to observe the transmission capability of the transmitter after erasure. As expected, the higher facet reflective FPLD overlapped and showed identical responses for each downstream extinction ratio value. In figure 5.5 (b), in the lower facet reflective case, decreasing the

downstream extinction ratio decreases the residual downstream ER for identical injection power levels. The residual upstream ER drops below 0.3 dB when the injection power levels are below -20 dBm.

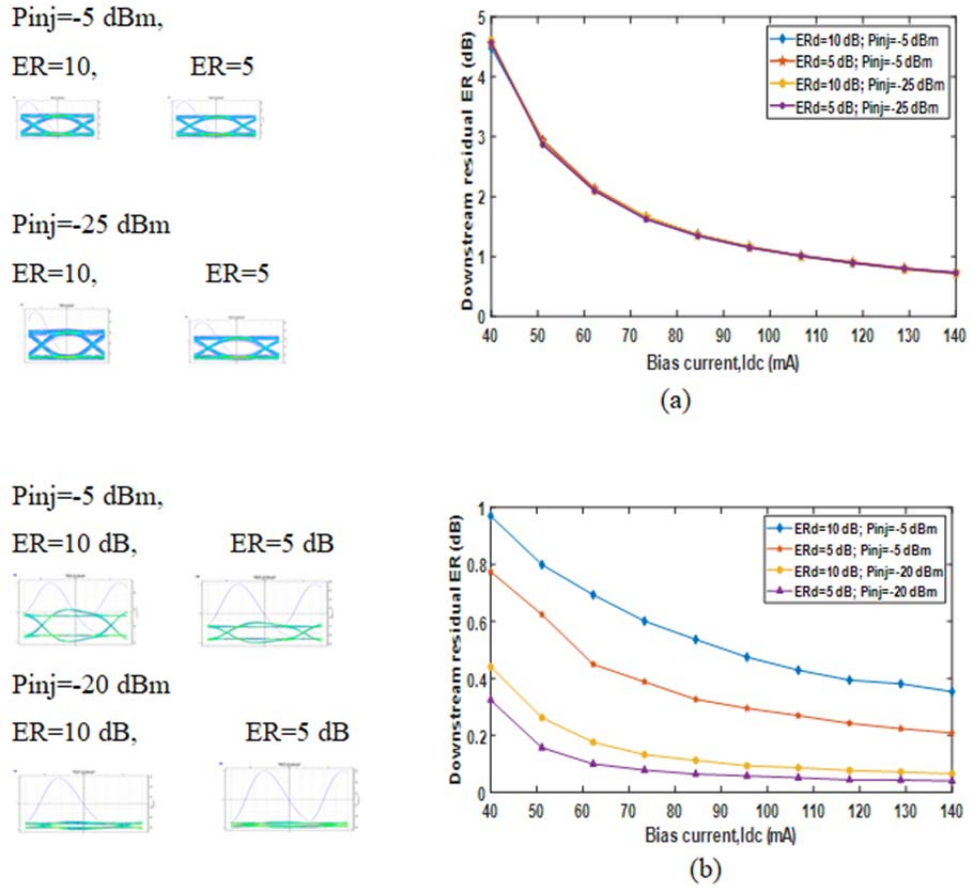



Figure 5.5. Eye diagrams and downstream residual extinction ratio result for different ER and Pinj levels

Downstream data can be entirely erased for bias currents above 50 mA. The $ER_{up}$ value decreases to <0.5 dB for injection powers of -5 and – 20 dBm.

The highly biased FPLD can improve the data erasing effect at the same injection power level and provide a larger modulation bandwidth for the upstream

transmission. However, the inherent mode competition is also improved to decrease the side mode suppression ratio (SMSR)(Su et al., 2015). Thus, the upstream back-to-back BER analyses for different current biases and injection power levels are demonstrated in figure 5.6.

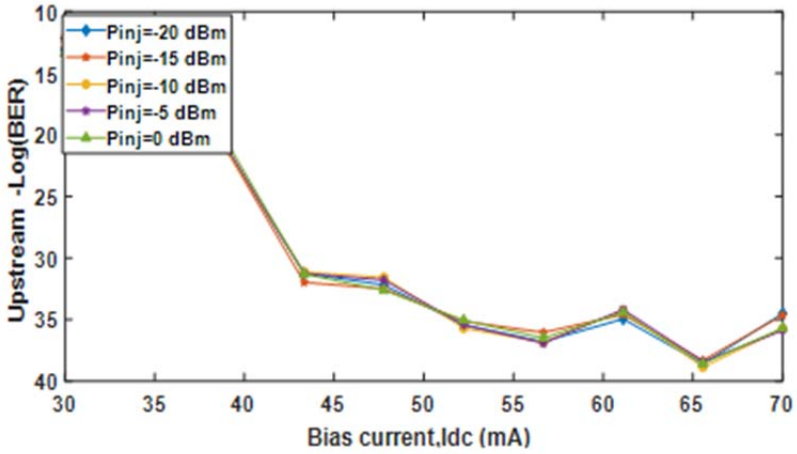
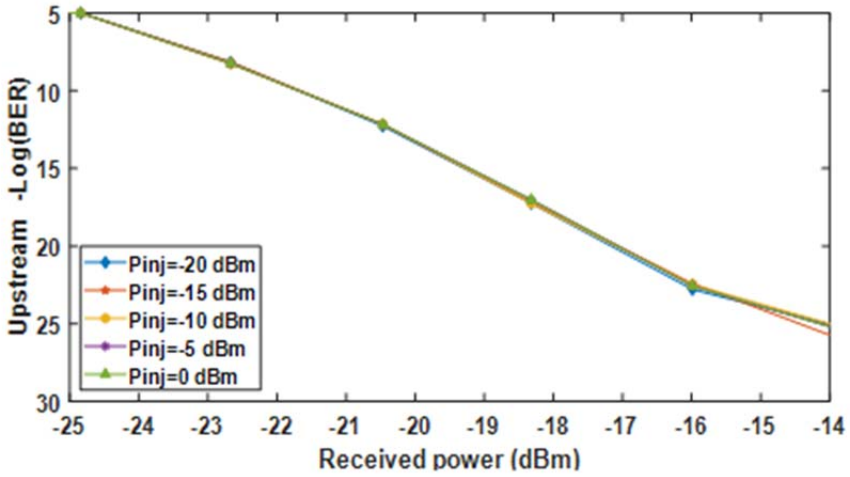


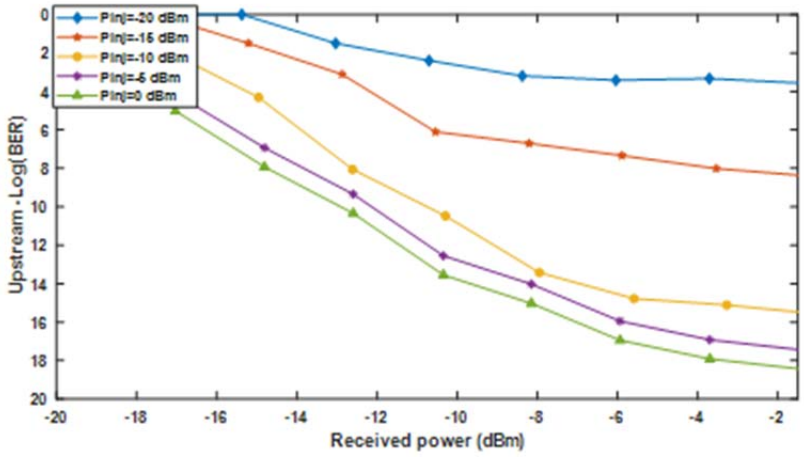

Figure 5. 6. BER result at OLT for several injection power levels

As clear from figure 5.7 b, the injection-locked colorless FPLD cannot have a wide modulation bandwidth with a suppressed RIN for better transmission when the biased current level is low. However, higher biasing causes mode competition, decreases the SMSR and degrades the transmission quality. Thus, the smallest BER values obtained when the FPLD is biased between 60-63 mA. The BER performance also increases with increasing injection power level from -20 to 0 dBm because the SMSR also increases. The FPLD biased at 60 mA successfully transmits 5 Gb/s NRZ OOK data with the $ER_d$ of 10dB at an injection power of 0 dBm, as shown in figure 5.7.

As stated in figure 5.7, the BER values show the error-free region (BER< $10^{-9}$) for injection power above -15 dBm for the FPLD-biased current of 50 mA. There is a proportional rate between received power and upstream BER results at the OLT.




(a)



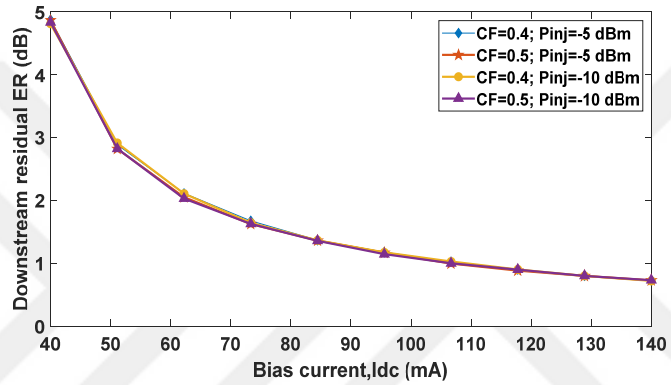

(b)

Figure 5.7. Upstream BER results vs. received power at OLT for 50 mA FPLD biased current

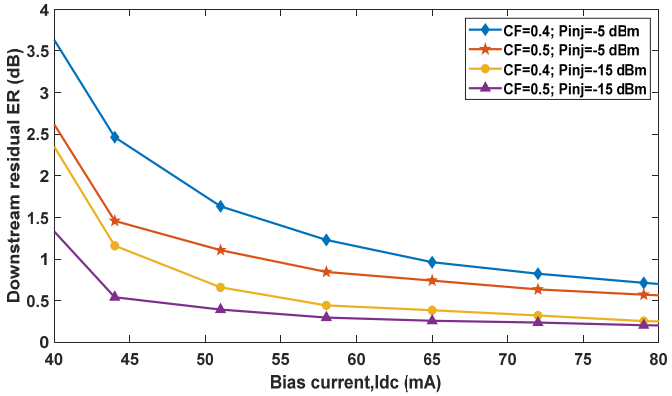
When the BER value decreases, the received power at the OLT increases and provides an error-free transmission. Increasing the injection power levels

provides better upstream transmission, and increasing the biased current increases the performance of the system.

The effects of the confinement factor for upstream transmission is shown in figure 5.8. The downstream ER was taken as 10 dB, and the downstream residual ER values were measured at different CF and $P_{inj}$ values by sweeping the biased FPLD current for many values.




(a)




(b)

Figure 5 8. Downstream ER vs. Bias current for different values of CF and Pinj

The results show that increasing the confinement factor increases the residual downstream data erasure. Applying lower injection power also increases the data erasure efficiency of the FPLD. The results show the best performance when the CF is 0.5 and $P_{inj}$ of -15 dBm.

As conclusion, this chapter has deeply analyzed the data erasure efficiency of the injection locked colorless FPLD based on the remodulation WDM PON system by considering parameters such as the downstream residual extinction ratio, confinement factor, different upstream injection power levels, different upstream bias current levels, bit error rate at upstream, and comparing two different reflective facets of FPLD. The speed rate of the system is 5 Gb/s. The colorless FP-LD was biased from 20 to 100 mA to simultaneously provide the data erasing and carrier reuse for optimization. The downstream injection power was detuned from -25 to 0 dBm using the VOA. The reflective facet of FPLD was employed as %93 and %0.2 respectively. Interestingly, the very highly reflective facet FPLD outputs overlap and demonstrate identical output results for any injection power and current levels. Thus, higher facet FPLD designs are not affected by any injected power and current levels. The downstream residual ER can be suppressed below 0.5 dB by increasing the FPLD bias current. Increasing the confinement factor also increases the data erasure capability of the FPLD due to the residual power in the medium. The optimum biasing current level was determined to be 50-62 mA for this system.

Note: This chapter has been published in Journal of Modern Optics. Doi: https://doi.org/10.1080/09500340.2019.1699182

# 6. DATA ERASURE IN FABRY-PEROT DIODE LASERS: EFFECTS OF FACET REFLECTIVITY

In this chapter, the effects of facet reflectivity on the data erasure ability of IL-FPLD, based on a remodulation method in WDM PON, were investigated. For this purpose, the feasible front facet reflectivity of FPLD was determined as between 0.2% and 7%, depending on the specified injected power interval. Firstly, the system carried out analysis without applying data at the user end to comprehensively demonstrate how much downstream data was completely erased in FPLD. Then, 2.5 Gb/s NRZ data was applied and the results compared with the erased downstream signal without data. The results show that upstream transmission improved with an increase in facet reflectivity between 0.2% and 7%.

## 6.1. Overview

PON has become the broad bandwidth supplier for access networks. Types of PON, such as WDM, TDM and OFDM, are used in communication systems to fulfil higher data rate demands. WDM PON is preferred as a solution among these due to its high capacity and low-cost user solutions(Banerjee et al., 2005; Lin et al., 2010; Cikan and Aksoy, 2019). Colorless transmitters have been proposed to use at the user end of WDM PON systems because of their advantages, including latency, jitter, the low cost, and the dedicated bandwidth (Yeh et al., 2008; Cikan and Aksoy, 2019). One of the methods of applying colorless transmitters is the spectrum slicing method (Healey et al., 2001; Soo-Jin et al., 2004; Payoux et al., 2005; Antoniades et al., 2011; Cikan and Aksoy, 2020). This method is limited to lower data rates(Gong-Ru et al., 2004), incoherent output, and low power (Kazovsky et al., 2011). Another method, known as the injection locking method, provides both a high modulation bandwidth and injection locking. The remodulation method has also attracted considerable interest amongst colorless solutions. Using separate wavelengths for upstream and downstream transmissions

has a high cost. Therefore, the remodulation method was developed to use the same wavelength for both upstream and downstream transmissions. However, using an identical carrier for both downstream and upstream transmissions can create physical impairments(Antoniades et al., 2011). Orthogonal modulation formats can prevent physical impairment but using different modulation methods at both ends also increases the cost (Wai et al., 2003; Prat et al., 2005; Martinez et al., 2008). Another method can be used to erase downstream modulated data and separate it from the carrier. This data erasing method can occur in two ways. The first option is using an external eraser, but this also has a high cost. The second option is erasing the downstream data in an optical colorless source at the ONU and modulating the upstream data on the same carrier coming from the CO. But this process is not so easy, because downstream data in a colorless source may not be erased completely, and this causes downstream data to overlap with upstream data.

Generally, FPLD or gain-saturated RSOA can be used to provide high data rates at ONU as colorless transmitters(Ki-Man et al., 2006; Park et al., 2007; Berrettini et al., 2009; Schrenk et al., 2009). However, RSOA cannot provide high-speed data transmission due to its limited modulation bandwidth (Sang-Mook et al., 2005; Kim and Han, 2006; Kim, 2008). IL-FPLD has an inherent data suppression ability, which decreases its ASE noise compared with a gain-saturated SOA (Lin et al., 2011; Chi et al., 2012; Lu et al., 2016). Finite AR coating also retains its low longitudinal mode within FPLD, so coherence can be higher than with RSOA coating(Lin et al., 2013).

The remodulation method using injection locked FPLD has been studied in many works(Chan et al., 2002; Wai et al., 2003; Sang-Mook et al., 2005; Jeung-Mo and Sang-Kook, 2006; Kim and Han, 2006; Kim, 2008; Lu et al., 2016). In addition, a new type of mode-locked long cavity laser diode has emerged, which provides a wider gain spectrum and partial coherence. This is called WRC-FPLD (Peng et al., 2008; Lin et al., 2009; Lin et al., 2010; Chi et al., 2012; Lin et al., 2013). The transmission performance of FPLD by changing the front facet

reflectivity has been studied in (Lin et al., 2009; Lin et al., 2010; Lin et al., 2010; Chi et al., 2012; Lin et al., 2012; Chen et al., 2013; Lin et al., 2013; Lin et al., 2013; Yeh et al., 2013). The data erasure efficiency of FPLD has been discussed in only two reports (Su et al., 2015; Cikan and Aksoy, 2020). The effects of parameters like CF and current levels on the data erasure efficiency of FPLD were demonstrated in (Cikan and Aksoy, 2020). However, the effects of front facet reflectivity on the data erasure efficiency of WRC FPLD has not been discussed yet (to the best of our knowledge). In this study, for the first time, the effects of front facet reflectivity on the data erasure efficiency of WRC FPLD are demonstrated and discussed. The results show that the facet reflectivity of WRC FPLD must be tuned carefully, considering parameters such as injection power ( $P_{inj}$ ), CF, cavity length, etc. to completely erase the downstream data. The effect of facet reflectivity on FPLD's data erasure efficiency was analyzed by comparing, quality(Q) factor, downstream residual extinction ratio ( $ER_d$ ) and, upstream residual extinction ratio ( $ER_u$ ) parameters.

### 6.2. System Setup

Figure 6.1 shows the setup of remodulation scheme based on WDM PON. The system was designed by using the Optisystem-16 evaluation software. A CW laser is employed to carry 5 Gb/s of NRZ data from the OLT to the ONU. AWG is employed to multiplex and demultiplex the signals. An optical coupler (OC) divided the downstream signal into two portions at the ONU: a lower power was sent to the receiver part of the ONU, and a higher intensity fraction signal was sent into FPLD. The VOA was employed to control the amount of power injected into FPLD. In previous reports(Su et al., 2015; Cikan and Aksoy, 2020), NRZ data was applied to both sides (the ONU and the OLT) to analyze the erasure efficiency of FPLD at 0.2% reflective facet only. However, applying upstream data into FPLD at

the ONU can prevent the clear observation of data erasure efficiency of the laser source.

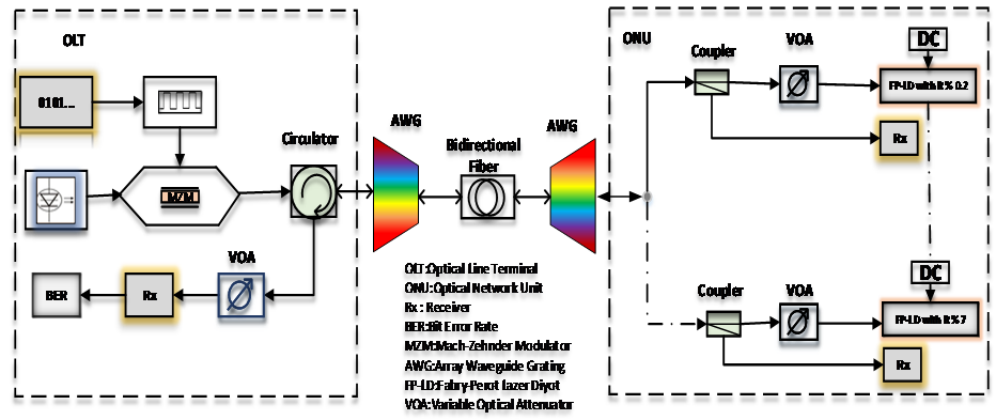


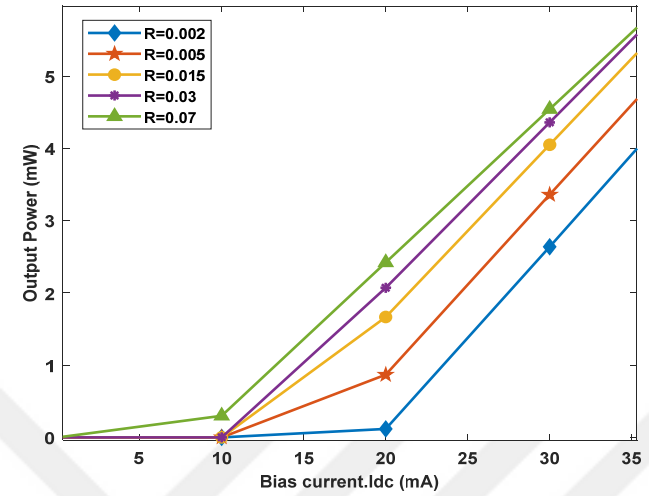

Figure 6.1. Remodulation technique based WDM PON system employing FPLD at ONU

First, the data erasure ability of FPLD for a range of facet reflectivity was studied without applying data (instead of an upstream data set at the ONU). Because of this, we could analyze how much downstream data was erased completely in FPLD and how much data was left and transmitted to the receiver part of the CO. Then, 2.5 Gb/s of NRZ data was applied to verify the efficiency of the upstream transmission, depending on the amount of erased downstream signal, which changes with facet reflectivity levels. The applied parameters of FPLD are cavity length of 600 $\mu m$ , CF of 0.4, 99% back facet reflectivity and, a range of front facet reflectivity between 0.2% and 90%. We analyzed the downstream residual extinction ratio, Q factor and BER results of the upstream transmission to observe the data erasure efficiency of WRC FPLD. The FPLD's threshold current value decreases with an increase in front facet reflectivity. Therefore, the biased current was applied as twice the threshold current for each FPLD. The biased current swept from 0 mA to 60 mA to allow us to observe the output power and

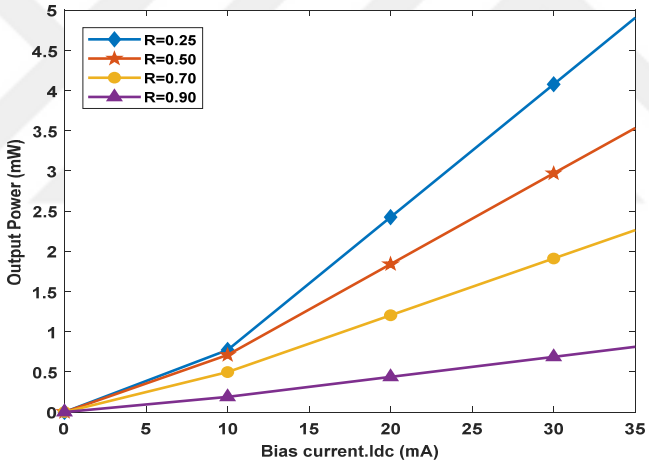
behaviour of the laser. VOA was applied from -20 dB to 0 dB to tune the injection power into FPLD.

### 6.3. Results and Discussion

Figure 6.2 shows the output power versus bias current plot of free-running FPLD. The front facet reflectivity of FPLD was employed as 0.2%, 0.5%, 1.5%, 3%, 7%, 8%, 9%, 12%, 15%, 25%, 50%, 70%, and 90%, with the threshold current values as 29.68 mA, 26.52 mA, 23 mA, 20.95 mA, 18.58 mA, 18.22 mA, 17.91 mA, 17.63 mA, 17.16 mA, 16.59 mA, 15.33 mA, 13.72 mA, 12.97 mA, and 12.43 mA, respectively. Free running FPLD was inspected by separating the facet response of the laser into three parts because the output power response changed depending on facet reflectivity values. Smaller front facet reflectivity of FPLD shows weaker cavity effects, which provides wide injection locking range and gain spectrum value. Therefore, it is easier for a longitudinal mode of FPLD with a smaller facet reflectivity to coincide with an incoming mode from CO. Although decreasing facet reflectivity provides advantages, WDM PON transmission worsens as smaller facet reflectivity causes higher mirror losses(Lin et al., 2009; Lin et al., 2013; Su et al., 2015; Cikan and Aksoy, 2020).




(a)

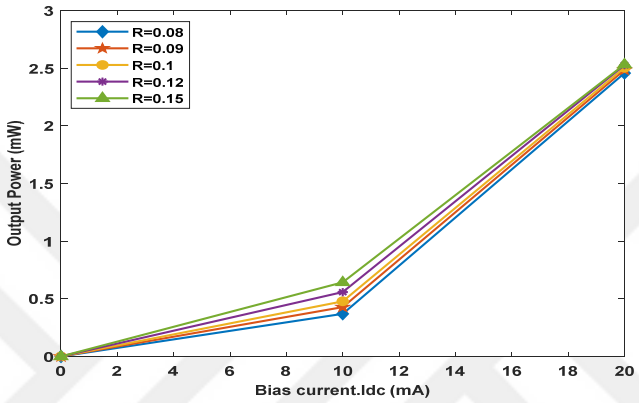



(b)

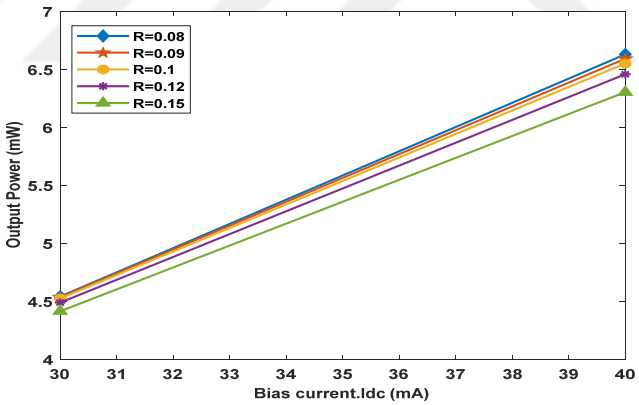
Figure 6.2. Output power& biased current plot of free running FPLD: a. Front facet reflectivity between 0.2%-7%; b. Front facet reflectivity between 25%-90%.

Figure 6.2. a depicts the output power versus bias current plot of free running FPLD with a front facet reflectivity between 0.2% and 7%. The graph demonstrates higher output power when FPLD has higher front facet reflectivity. Although the threshold current decreases at reflective facet between 25% and %90,

the output power also decreased as demonstrated in Figure 6.2.b. The output behaviour of the laser changed for reflective facets between 8% and 15%, as shown in Figure 6.3. The output power versus the current plot demonstrated different behaviour for bias current smaller and bigger than 20 mA.



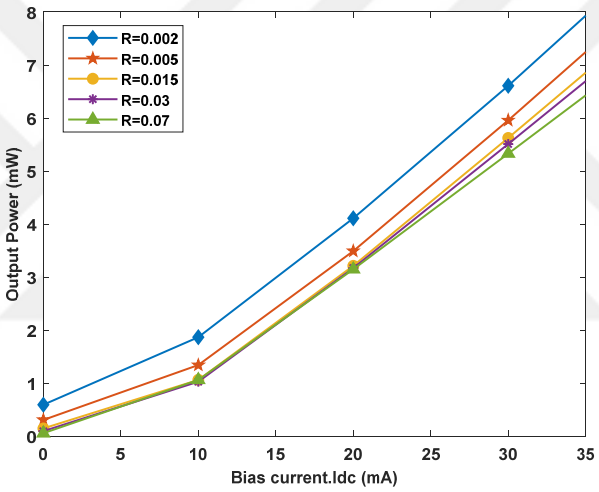

(a)



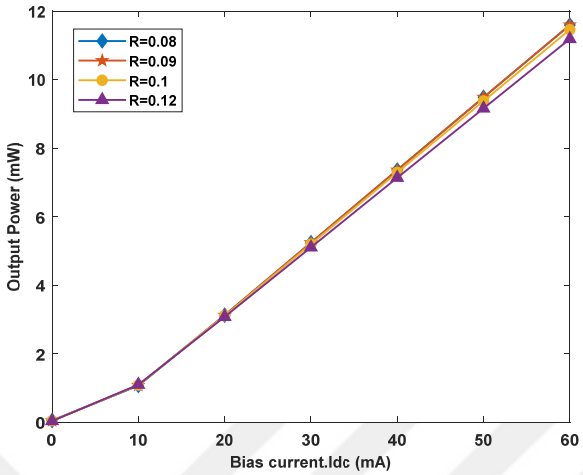

(b)

Figure 6.3. Output power& biased current plot of free running FPLD at front facet reflectivity between 0.8%-15%; a. Biased current smaller than 20 mA; b. Biased current bigger than 20 mA

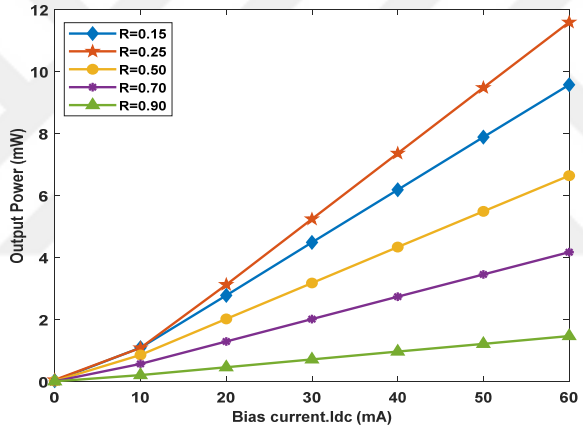
The results also demonstrated reverse behaviour when compared with lower facet reflectivity results for reflectivity values bigger than 25% independent from applied biased current, due to the low injection locking spectrum. Figure 6.4 shows the power-to-current response of injection locked (CW-injected) FPLD at different facet reflectivity levels. Injection-locked FPLD effectively suppresses relative intensity noise. When FPLD was injection locked with a laser source, the reflectivity values between 0.2% and 7% demonstrate reverse behaviour compared with free-running FPLD at 0 dB $P_{inj}$ .




(a)



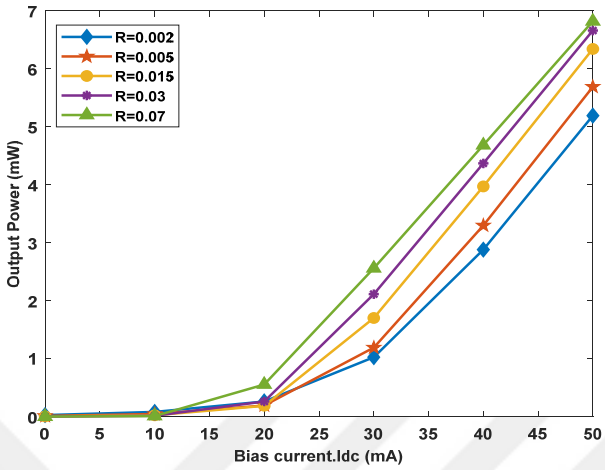

(b)



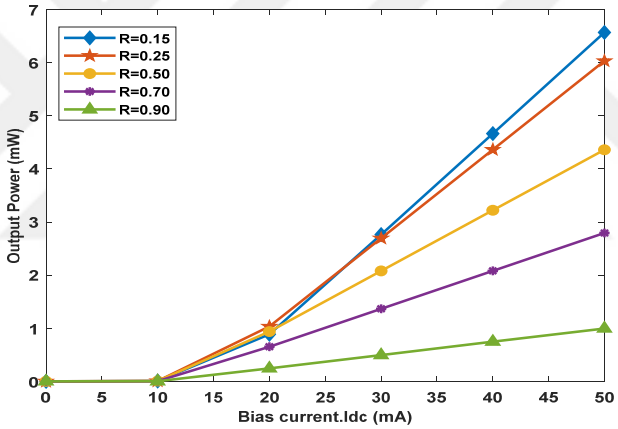

(c)

Figure 6.4. Output power& biased current plot of injection locked FPLD: a. Front facet reflectivity between 0.2%-7%; b. Front facet reflectivity between 8%-12%; c. Front facet reflectivity between 15%-90%.

If the CF value is decreased from 0.4 to 0.3 and the injected power is decreased from 0 dBm to below -10 dBm, reflective facet behaviour occurs as demonstrated in figure 6.5. According to the results, factors such as CF and the injected optical power affect the behaviour of WRC FPLD. When CF and injected power were decreased, the reflective facet values between 0.2% and 7% show a similar but bigger output power than free-running FPLD.




(a)



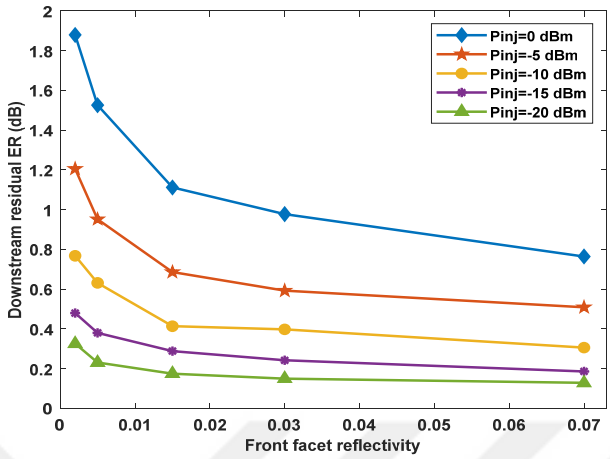

(b)

Figure 6.5. Output power& biased current plot of injection locked FPLD with <-10 dB: a. Front facet reflectivity between 0.2%-7%; b. Front facet reflectivity between 15%-90%.

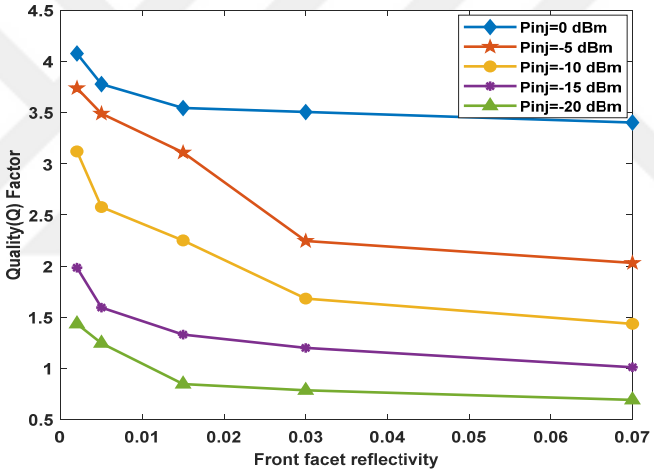
According to the obtained results, the facet reflectivity behaviour of FPLD variations can be divided into three parts: the first part is facet reflectivity between 0.2% and 7%, the second part is between 8% and 12%, and the third part is between 15% and 90%. Thus, the facet reflectivity values should be arranged carefully depending on factors like CF and injected powers. Decreasing the injection power without changing CF also gives these results, as shown in figure

6.5. One of the most important methods to analyze the data erasure ability of FPLD is to control residual downstream ER value. This value must be less than 0.5 dB for the laser to erase the downstream data and encode new upstream data on the downstream carrier.

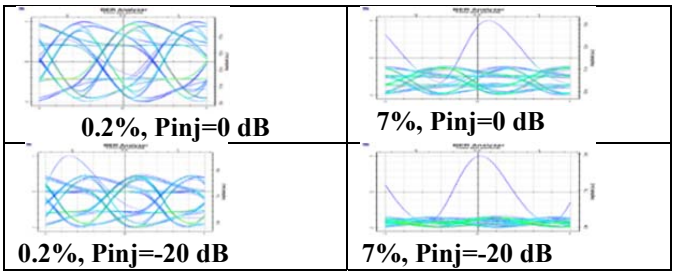
As is clear from the plots above (Figures 2, 3, 4, and 5), the outputs of the laser changed depending on many parameters, including CF, injected power, facet reflectivity and biased current. Because the facet reflectivity between 8% and 12% were affected largely from the applied biased current, these intervals are not a good choice for remodulation based WDM PON applications. Furthermore, when FPLD is injection locked, all output power results of these intervals overlap, as shown in figure 6.4. The facet reflectivity values between 15% and 90% are also not suitable for practical applications due to their narrow injection locking range and low output power. A highly asymmetrical coating lowers unwanted backward reflection at the front facet and prevents power consumption at the rear facet(Lin et al., 2009). Hence, facet reflectivity of WRC FPLD between 0.2% and 7% are the most suitable interval for WDM PON applications. $ER_d$ and upstream Q factor plots are demonstrated in figures 6.6 a and 6.6 b. $ER_d$ is 0.47dB at a $P_{inj}$ value of -15 dB and 0.32 at $P_{inj}$ value of -20 dB for 0.2% facet reflectivity. When the $P_{inj}$ value increased to above -15dB, the residual $ER_d$ was 1.5 for a $P_{inj}$ of 0 dB, 0.9 for a $P_{inj}$ of -5dB, and 0.6 for a $P_{inj}$ of -10dB for 0.5% reflective facets. Therefore, $P_{inj}$ values should be at least -15dB for 0.2% and 0.5% facet reflectivity. Q factor should be at least 3 before FEC and 6 after FEC for telecommunication applications. The Q factors of the 0.2% reflective facet values were 4, 3.7, 3.12, 1.98, and 1.43 for $P_{inj}$ values of 0 dB, -5 dB, -10 dB, -15 dB, and -20 dB, respectively. The Q factors of 0.5% facet reflectivity were 3.7, 3.4, 2.5, 1.5, and 1.2 for $P_{inj}$ values of 0 dB, -5 dB, -10 dB, -15 dB, and -20 dB, respectively. Thus, the residual downstream data was erased below -15 dB for 0.2% and 0.5% facet reflectivity.




(a)



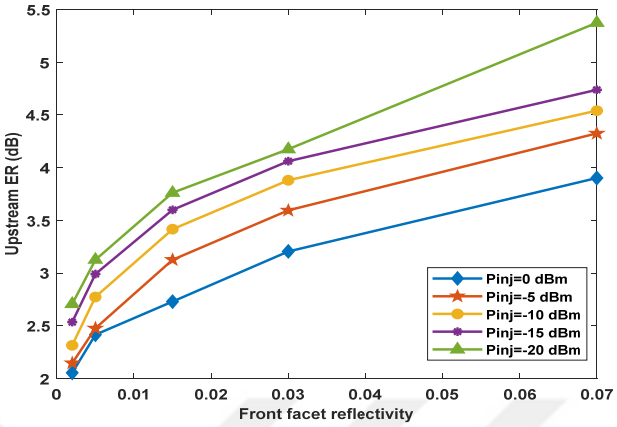

(b)



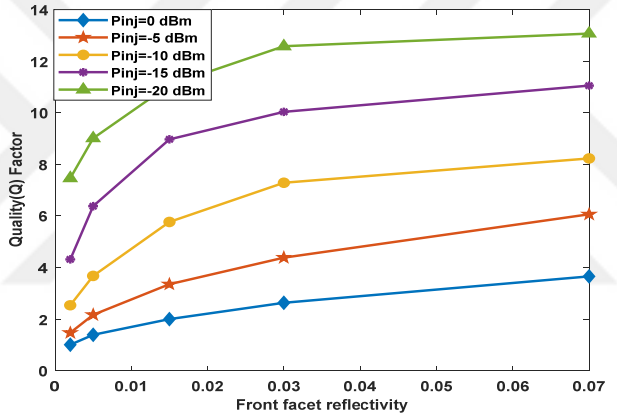

(c)

Figure 6.6. WRC FPLD without data: a. Front facet reflectivity & Downstream residual ER; b. Front facet reflectivity & Q factor; c. Eye diagrams

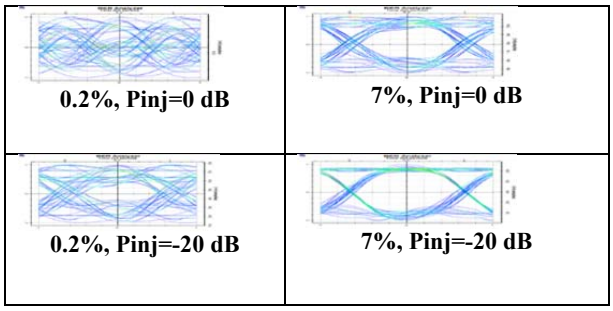
When the reflectance of front facet increased to 1.5%, the $ER_d$ value was 1.11 dB and the Q factor was 3.5 for a 0 dB $P_{inj}$ value. $ER_d$ decreased to 0.6 dB, 0.4 dB, 0.2 dB, and 0.1 dB, and the Q factor decreased to 3.1, 2.2, 1.3, and 0.8 for $P_{inj}$ values of -5 dB, -10 dB, -15 dB, and -20 dB, respectively. Therefore, the $P_{inj}$ value should be at least -10 dB for a 1.5% facet reflectivity. The $ER_d$ and Q factor decreased to 0.39 dB and 1.6, respectively, at a $P_{inj}$ value of -10 dB for a 3% facet reflectivity. The $ER_d$ and Q factor decreased to 0.5 dB and 2, respectively, at a $P_{inj}$ value of -5 dB for a 7% facet reflectivity. Therefore, the maximum power injection value should be -15 dB for 0.2% and 0.5% reflective front facets, -10 dB for 1.5% and 3% reflective front facets, and -5 dB for a 7% reflective facet. Eye diagrams of 0.2% and 7% facet reflectivity are also given to compare the erased data at $P_{inj}$ values of 0 dB and -20 dB. The downstream data was erased more in the colorless source with reflectivity value increased from 0.2% to 7%. Thus, it is expected to be increased upstream transmission with increasing facet reflectivity when data applied into FPLD.




(a)




(b)




(c)

Figure 6.7. WRC FPLD with 2.5 Gb/s NRZ data: a. Front facet reflectivity & Downstream residual ER; b. Front facet reflectivity & Q factor; c. Eye diagrams

Figure 6.7.a and 6.7.b demonstrate the $ER_u$ and Q factor results when 2.5 Gb/s of NRZ upstream data was applied into WRC FPLD. Eye diagrams were also provided at $P_{inj}$ values of 0 dB and -20 dB. The decrease in the reflectance of the front facet weakens the efficiency of the PON transmission due to the mirror loss and reduced cavity resonance. Upstream Q factors of 0.2% facet reflectivity are 1, 1.4, 2.5, 4, and 7 for $P_{inj}$ values of 0 dB, -5 dB, -10 dB, -15 dB, and -20 dB, respectively. BER value is also $<10^{-9}$ at a $P_{inj}$ value of -20 dB. Thus, data transmitted better at a -20 dB $P_{inj}$ value. Other facet reflectivity values demonstrated similar behaviour as well. Q factor goes above 6 and BER decreases below $10^{-9}$ at $P_{inj}$ values of -15 dB, -10 dB, -10 dB, and -5 dB for front facet reflectance of 0.5%, 1.5%, 3% and 7%, respectively.

As conclusion, in this paper, the data erasure efficiency of FPLD was investigated by considering the front facet reflectivity of FPLD. First, the data erasure ability of FPLD in a remodulation based PON system was analyzed without applying data, by changing the front facet reflectivity of the laser, and the amount of erased downstream data was observed. Then, 2.5 Gb/s of NRZ data was applied and the results compared with the erased downstream signal without data. Facet reflectivity levels of WRC FPLD between 0.2% and 7% were determined as the optimum reflectivity values for remodulation based WDM PON applications. However, as a lower reflectivity of AR coating causes a greater loss of mirror and creates a reduced resonance of cavity, increasing facet-reflectivity, especially at 7%, gave better results. Eye diagrams of 0.2% and 7% facet reflectivity are also given to compare the erased and transmitted data at $P_{inj}$ values of 0 dB and -20 dB. As a result, the 7% front facet reflectivity value of FPLD demonstrated a much better upstream transmission because it erased downstream data precisely.

## 6. DATA ERASURE IN FABRY-PEROT DIODE LASERS: EFFECTS OF FACET REFLECTIVITY

Nisa NACAR ÇIKAN

Note: This chapter has been published in Journal of Modern Optics. Doi: https://doi.org/10.1080/09500340.2020.1759716

# 7. CONLUSION

WDM PON technology has been noted as a potential technology for communication networks to fulfill the gradually rising demand on bandwidth. However, widespread implementation of WDM PON technology has been halted due to maintenance and establishment costs. Studies and researches are continuing to make this technology mature and affordable. TDM PON technology has become insufficient to meet the highly increased bandwidth demand with new developing technologies such as IoT has been emerged. Therefore, it has become necessary to deploy WDM PON technology, which supports high capacity, symmetric data traffic, affordable and commercially applicable, in access networks. In this dissertation, studies have been carried out to make WDM PON technology cost-effective and commercially applicable. Accordingly, the thesis is basically discussed under two main headings. First, the system is designed using Optisystem software to implement cost-effective colorless ONUs in access networks. Secondly, the redundant data erasure capabilities of these light sources are analyzed in a remodulation based WDM PON.

In Chapter 2, a general classification of colorless sources and a comparison of them are presented. The colorless WDM PON technology has been investigated in three main categories as self-emitting, self-seeded, and seeding light from central office(loop-back) technologies. The researchers and service providers have attempted to remove the light sources from ONUs, since it is an expensive and risky way to require each end user to manage its own wavelength. In case of an ONU deviates from the designated wavelength, this user will not only damage itself, but it will also affect the other neighboring channels. Therefore, light sources to seed the ONUs have been suggested to be supplied from the central office. The remodulation method has been proposed among colorless technologies because of its specification of having a single wavelength usage to transmit upstream and downstream data.

In Chapter 3, the historical background of the RSOA is explained. It begins with the discovering of the RSOA and then follows with the application of it into optical networks. Then the data erasure analysis of the RSOA has been discussed. The simulation results demonstrated that the increasing bias current, injection power, and confinement factor are the important parameters that take the role to erase the downstream data at ONU at a remodulation system. It is determined that the increasing the parameter values as bias current over 50 mA, the confinement factor over 0.4, and the injection power over -15 dBm prevent the crosstalk between upstream and downstream data at ONU.

In Chapter 4 and 5, the mathematical model of FPLD and IL-FPLD are presented to explain the laser's working principle. The data erasure efficiency of the IL colorless FPLD based on the remodulation WDM PON system has been analyzed by considering parameters such as the downstream residual extinction ratio, confinement factor, different upstream injection power levels, different upstream bias current levels, bit error rate at upstream, and comparing two different reflective facets of FPLD. The speed rate of the system is 5 Gb/s. The colorless FP-LD was biased from20 to 100mA to simultaneously provide the data erasing and carrier reuse for optimization. The downstream injection power was detuned from −25 to 0 dBm using the VOA. The reflective facet of FPLD was employed as %93 and %0.2 respectively. Interestingly, the very highly reflective facet FPLD outputs overlap and demonstrate identical output results for any injection power and current levels. Thus, higher facet FPLD designs are not affected by any injected power and current levels. The downstream residual ER can be suppressed below 0.5 dB by increasing the FPLD bias current. Increasing the confinement factor also increases the data erasure capability of the FPLD due to the residual power in the medium. The optimum biasing current level was determined to be 50-62mA for this system.

In Chapter 6, the data erasure efficiency of FPLD was investigated by considering the front facet reflectivity of FPLD. First, the data erasure ability of

FPLD in a remodulation based PON system was analyzed without applying data, by changing the front facet reflectivity of the laser, and the amount of erased downstream data was observed. Then, 2.5 Gb/s of NRZ data was applied and the results compared with the erased downstream signal without data. Facet reflectivity levels of WRC FPLD between 0.2% and 7% were determined as the optimum reflectivity values for remodulation based WDM PON applications. However, as a lower reflectivity of AR coating causes a greater loss of mirror and creates a reduced resonance of cavity, increasing facet-reflectivity, especially at 7%, gave better results. Eye diagrams of 0.2% and 7% facet reflectivity are also given to compare the erased and transmitted data at Pinj values of 0 dB and −20 dB. As a result, the 7% front facet reflectivity value of FPLD demonstrated a much better upstream transmission because it erased downstream data precisely.

For future work, a colorless source application at ONUs is a fascinating solution in remodulation based WDM-PON systems. Special new methods should be improved to suppress the crosstalk that occurs during the remodulation process and develop the coherence degrees. In summary, the high-speed running of FPLDs and RSOAs is a research way worthwhile for future studies.

**REFERENCES**


Agrawal, G. P. (2012). Fiber-Optic Communication Systems, Wiley.

Agrawal, G. P. and Dutta, N. K. (2013). Semiconductor Lasers, Springer US.

Akulova, Y. A., Fısh, G. A., Pıng-Chıek, K., Schow, C. L., Kozodoy, P., Dahl, A. P., Nakagawa, S., Larson, M. C., Mack, M. P., Strand, T. A., Coldren, C. W., Hegblom, E., Pennıman, S. K., Wıpıejewskı, T. and Coldren, L. A., (2002). "Widely tunable electroabsorption-modulated sampled-grating DBR laser transmitter." IEEE Journal of Selected Topics in Quantum Electronics 8(6): 1349-1357.

Amıtabha Banerjee, Y. P., Frederıck Clarke, Huan Song, Sunhee Yang, Glen Kramer, Kwangjoon Kım, And Bıswanath Mukherjee, (2005). "Wavelength-division-multiplexed passive optical network (WDM-PON) technologies for broadband access: a review [Invited]." Journal of Optical Networking 4(11): 737-758.

Antonıades, N. N., Ellınas, G. and Roudas, I. (2011). WDM Systems and Networks: Modeling, Simulation, Design and Engineering, Springer New York.

Arellano, C., Bock, C., Prat, J. and Langer, K. (2006). RSOA-based optical network units for WDM-PON. 2006 Optical Fiber Communication Conference and the National Fiber Optic Engineers Conference.

Arellano, C., Polo, V., Bock, C. and PRAT, J. (2005). Bidirectional single fiber transmission based on a RSOA ONU for FTTH using FSK-IM modulation formats. OFC/NFOEC Technical Digest. Optical Fiber Communication Conference, 2005.

Arya, V. and Jacobs, I., (1997). "Optical preamplifier receiver for spectrum-sliced WDM." Journal of Lightwave Technology 15(4): 576-583.

Banerjee, A., Park, Y., Clarke, F., Song, H., Yang, S., Kramer, G., Kım, K. and Mukherjee, B., (2005). "Wavelength-division-multiplexed passive optical network (WDM-PON) technologiesfor broadband access: a review [Invited]." Journal of Optical Networking 4(11): 737-758.

Banerjee, A., Park, Y., Clarke, F. W., Song, H., Yang, S. and Kramer, G., (2005). "Wavelength-division-multiplexed passive optical network (WDM-PON) technologies for broadband access: a review (Invited)." Journal of Optical Networking 4: 737-758.

Berrettını, G., Melonı, G., Gıorgı, L., Ponzını, F., Cavalıere, F., Ghıggıno, P., Potı, L. and Bogonı, A. (2009). Colorless WDM-PON performance improvement exploiting a Service-ONU for multiwavelength distribution. 2009 Conference on Optical Fiber Communication - incudes post deadline papers.

Bobrovs, V., Spolıtıs, S., Trıfonovs, I. And Ivanovs, G. (2013). Spectrum sliced WDM-PON system as energy efficient solution for optical access systems. 2013 IEEE Latin-America Conference on Communications.

Boıvın, L., Taccheo, S., Doerr, C. R., Schıffer, P., Stulz, L. W., Monnard, R. and LIN, W., (2000). "400 Gbit/s transmission over 544 km from spectrum-sliced supercontinuum source." Electronics Letters 36(4): 335-336.

Brıand, J., Payoux, F., Chanclou, P. and Joındot, M., (2007). "Forward error correction in WDM PON using spectrum slicing." Optical Switching and Networking 4: 131-136.

Brunero, M., Paroları, P., Brenot, R. and Martınellı, M. (2016). 20-Gb/s polarization division multiplexed WDM PON transmitter based on self seeded RSOAs. 18th Italian National Conference on Photonic Technologies (Fotonica 2016).

Buldawoo, N., Mottet, S., Gall, F. L., Sıgogne, D., Meıchenın, D. and Chelles, S. (1997). A semiconductor laser amplifier-reflector for the future FTTH applications. Integrated Optics and Optical Fibre Communications, 11th International Conference on, and 23rd European Conference on Optical Communications (Conf. Publ. No.: 448).

Buus, J. and Murphy, E. J., (2006). "Tunable lasers in optical networks." Journal of Lightwave Technology 24(1): 5-11.

Chan, L. Y., Chan, C. K., Tong, D. T. K., Tong, F. and Chen, L. K., (2002). "Upstream traffic transmitter using injection-locked Fabry-Perot laser diode as modulator for WDM access networks." Electronics Letters 38(1): 43-45.

Chan, L. Y., Chan, C. K., Tong, T. K., Cheung, S. Y., Tong, F. and Chen, L. K. (2001). Demonstration of data remodulation for upstream traffic in WDM access networks using injection-locked FP laser as modulator. OFC 2001. Optical Fiber Communication Conference and Exhibit. Technical Digest Postconference Edition (IEEE Cat. 01CH37171).

Chen, H., Yeh, C., Chow, C., Sung, J., Lıu, Y. and Chen, J., (2013). "Investigation of Using Injection-Locked Fabry–Pérot Laser Diode With 10% Front-Facet Reflectivity for Short-Reach to Long-Reach Upstream PON Access." IEEE Photonics Journal 5(3): 7901208-7901208.

Cheng, N. and Effenberger, F. J. (2015). Feedforward cancellation of remodulation crosstalk in WDM PON using self-seeded RSOAs. 2015 Opto-Electronics and Communications Conference (OECC).

Cheng, N. and Zhou, L. (2015). Efficient mobile fronthaul for 24×20MHz LTE signals using self-seeded RSOA with adaptive crosstalk cancellation.

Cheng, N., Zhou, L., Lıu, X. and Effenberger, F. J., (2016). "Reflective Crosstalk Cancellation in Self-Seeded WDM PON for Mobile Fronthaul/Backhaul." Journal of Lightwave Technology 34(8): 2056-2063.

Cheng, X., Wen, Y. J., Dong, Y., Xu, Z., Shao, X., Wang, Y. and LU, C., (2006). "Optimization of Spectrum-Sliced ASE Source for Injection-Locking a Fabry–PÉrot Laser Diode." IEEE Photonics Technology Letters 18(18): 1961-1963.

Chı, Y.-C., Lı, Y.-C., Wang, H.-Y., Peng, P.-C., Lu, H.-H. and Lın, G.-R., (2012). "Optical 16-QAM-52-OFDM transmission at 4 Gbit/s by directly modulating a coherently injection-locked colorless laser diode." Optics Express 20(18): 20071-20077.

Chı, Y., Lın, C., Lın, S. and Lın, G., (2012). "The Reuse of Downstream Carrier Data Erased by Self-Feedback SOA for Bidirectional DWDM-PON Transmission." Journal of Lightwave Technology 30(19): 3096-3102.

Cho, K., Lee, Y., Choı, H., Murakamı, A., Agata, A., Takushıma, Y. and Chung, Y., (2009). "Effects of reflection in RSOA-based WDM PON utilizing remodulation technique." Journal of Lightwave Technology 27.

Cho, K., Murakamı, A., Lee, Y., Agata, A., Takushıma, Y. and Chung, Y., (2008). "Demonstration of RSOA-based WDM PON Operating at Symmetric Rate of 1.25 Gb/s with High Reflection Tolerance."

Cho, K. Y., Lee, Y. J., Choı, H. Y., Murakamı, A., Agata, A., Takushıma, Y. and Chung, Y. C., (2009). "Effects of Reflection in RSOA-Based WDM PON Utilizing Remodulation Technique." Journal of Lightwave Technology 27(10): 1286-1295.

Cho, S., Lee, H. H., Lee, J. H., Lee, J. H., Myong, S. I. and Lee, S. S. (2012). A loop-back WDM-PON technology based on RSOA using wavelength reuse scheme and it's commercialization status in Korea. The 10th International Conference on Optical Internet (COIN2012).

Cho, S., Lee, J., Lee, J., Lee, E., Lee, H., Jung, E., Choı, B., Kım, D., Kwon, O. and Lee, S. S. (2010). Demonstrations of RSOA based loop-back WDM-PON with 100 Gb/s (80 × 1.25 Gb/s) capacity employing spectrum sliced incoherent light injection. 36th European Conference and Exhibition on Optical Communication.

Cho, S., Lee, J. H., Lee, H. H., Myong, S. I., Lee, J. H. and Lee, S. S., (2013). "Loop-back WDM-PON with 100 Gb/s capacity using spectrally sliced ASE injected RSOA." IEEE/OSA Journal of Optical Communications and Networking 5(5): 447-456.

Cho, S. I., Lee, S.-S. and Shın, D.-W., (2010). "Improving upstream transmission performance using a receiver with decision threshold level adjustment in a loopback WDM-PON." Optical Fiber Technology 16: 129-134.

Choudhury, P. and Khan, T., (2016). "Symmetric 10Gb/s wavelength reused bidirectional RSOA based WDM-PON with DPSK modulated downstream and OFDM modulated upstream signals." Optics Communications 372: 180-184.

Chuang, S. L. (1995). Physics of Optoelectronic Devices, Wiley.

Chung, Y. C., Lee, J. S., Derosıer, R. M. and Dıgıovannı, D. J., (1994). "1.7 Gbit/s transmission over 165 km of dispersion-shifted fibre using spectrum-sliced fibre amplifier light source." Electronics Letters 30(17): 1427-1428.

Cıkan, N. and Aksoy, M., (2019). "Data erasure analysis of FPLD based on remodulation bidirectional PON system." Journal of Modern Optics 67: 1-7.

Cıkan, N. N. and Aksoy, M., (2019). "A Review of Self-Seeded RSOA Based on WDM PON." Canadian Journal of Electrical and Computer Engineering 42(1): 2-9.

Cıkan, N. N. and Aksoy, M., (2020). "Data erasure analysis of FPLD based on remodulation bidirectional PON system." Journal of Modern Optics 67(2): 139-145.

Cısco. (2020, March 9). "Cisco Annual Internet Report (2018–2023) White Paper". https://www.cisco.com/c/en/us/solutions/collateral/executive-perspectives/annual-internet-report/white-paper-c11-741490.html.

Connelly, M. J. (2007). Semiconductor Optical Amplifiers, Springer US.

Consortıum, I. E. (2007). Annual Review of Communications: Volume 59, International Engineering Consortium.

Deng, M., Lıng, Y., Chen, X., Gıddıngs, R., Hong, Y., Yı, X., Qıu, K. and Tang, J., (2014). "Self-seeding-based 10Gb/s over 25km optical OFDM transmissions utilizing face-to-face dual-RSOAs at gain saturation." Optics express 22: 11954-11965.

Denıel, Q., Salıou, F., Chanclou, P. and Erasme, D. (2013). Self-seeded RSOA based WDM-PON transmission capacities. 2013 Optical Fiber Communication Conference and Exposition and the National Fiber Optic Engineers Conference (OFC/NFOEC).

Denıel, Q., Salıou, F., Chanclou, P., Erasme, D. and Brenot, R. (2013). Up to 45km-long amplified self-seeded RSOA based external cavity for 2.5Gb/s WDM PON transmission. 2013 Optical Fiber Communication Conference and Exposition and the National Fiber Optic Engineers Conference (OFC/NFOEC).

Denıel, Q., Salıou, F., Le, S. D., Chanclou, P., Erasme, D. and Brenot, R. (2013). Amplified RSOA self-tuning laser for WDM PON using saturated SOA for noise reduction and data cancellation. 39th European Conference and Exhibition on Optical Communication (ECOC 2013).

Dıallo, T., Pızzınat, A., Salıou, F., Chanclou, P., Sımon, G. And Aupetıt-Berthelemot, C., (2016). "Self-Seeded DWDM Solution for Fronthaul Links in Centralized-Radio Access Network." Journal of Lightwave Technology 34(21): 4965-4971.

Duarte, U. R., Penze, R. S., Pereıra, F. R., Padela, F. F., Rosolem, J. B. and Romero, M. A., (2013). "Combined Self-Seeding and Carrier Remodulation Scheme for WDM-PON." Journal of Lightwave Technology 31(8): 1323-1330.

Duarte, U. R. and Romero, M. A., (2016). "Enhancement of maximum reach on spectrum-sliced ASE systems employing self-seeded reflective-SOAs transmitters." Electronics Letters 52(2): 130-131.

Duarte, U. R., Romero, M. A., Rosolem, J. B., Penze, R. S. And Leonardı, A. A. (2014). Enhancement of chromatic dispersion and post-filtering effects tolerances on spectrum-sliced WDM-PONs using self-seeded reflective-SOAs. 2014 International Telecommunications Symposium (ITS).

Duarte, U. R., Rosolem, J. B., Penze, R. S. and Romero, M. A., (2014). "Analysis of ASE-related impairments on wavelength-reuse WDM-PONs based on self-seeded reflective SOAs." IEEE/OSA Journal of Optical Communications and Networking 6(9): 773-781.

Duıll, S. O., Marazzı, L., Paloları, P., Koos, C., Freude, W. and Leuthold, J. (2012). Modulation cancellation properties of reflective SOAs. 2012 38th European Conference and Exhibition on Optical Communications.

Dutta, N. K., Wang, Q. and Scıentıfic, W. (2013). Semiconductor Optical Amplifiers, World Scientific.

Dutton, H. J. R. (1998). Understanding Optical Communications, Prentice Hall PTR.

Eısensteın, G., Jopson, R. M., Lınke, R. A., Burrus, C. A., Koren, U., Whalen, M. S. and Hall, K. L., (1985). "Gain measurements of InGaAsP 1.5 μm optical amplifiers." Electronics Letters 21(23): 1076-1077.

Elbers, J. (2010). Optical access solutions beyond 10G-EPON/XG-PON. 2010 Conference on Optical Fiber Communication (OFC/NFOEC), collocated National Fiber Optic Engineers Conference.

Europe, F. C. (2014). FTTH Handbook, FTTH Council Europe.

Fattal, D., Fıorentıno, M., Tan, M., Houng, D., Wang, S. and Beausoleıl, R., (2008). "Design of an efficient light-emitting diode with 10 GHz modulation bandwidth." Applied Physics Letters 93: 243501-243501.

Feldman, R. D., Harstead, E. E., Jıang, S., WooD, T. H. and Zırngıbl, M., (1998). "An evaluation of architectures incorporating wavelength division multiplexing for broad-band fiber access." Journal of Lightwave Technology 16(9): 1546-1559.

Frıgo, N. J., Iannone, P. P., Magıll, P. D., Darcıe, T. E., Downs, M. M., Desaı, B. N., Koren, U., Koch, T. L., Dragone, C., Presby, H. M. and Bodeep, G. E., (1994). "A wavelength-division multiplexed passive optical network with cost-shared components." IEEE Photonics Technology Letters 6(11): 1365-1367.

Fujıwara, M., Jun-Ichı, K., Suzukı, H. and Iwatsukı, K., (2006). "Impact of backreflection on upstream transmission in WDM single-fiber loopback access networks." Journal of Lightwave Technology 24(2): 740-746.

Gebrewold, S. A., Bonjour, R., Barbet, S., Maho, A., Brenot, R., Chanclou, P., Brunero, M., Marazzı, L., Paroları, P., Totovıć, A., Gvozdıc, D., Hıllerkuss, D., Hafner, C. And Leuthold, J., (2015). "Self-Seeded RSOA-Fiber Cavity Lasers vs. ASE Spectrum-Sliced or Externally Seeded Transmitters—A Comparative Study." Applied Sciences 5: 1922-1941.

Gebrewold, S. A., Bonjour, R., Hıllerkuss, D., Hafner, C., Leuthold, J. and Brenot, R. (2015). Adaptive subcarrier multiplexing maximizing the performance of a bandwidth-limited colorless self-seeded reflective-SOA. 2015 International Conference on Photonics in Switching (PS).

Gerd Keıser (2013). Optical Fiber Communication - SIE, Tata McGraw-Hill Education.

Gıbassıer, C., Abıven, J., Ramus, C., Huet, F. and Saulnıer, J., (1994). "Simultaneous two-way light intensity modulation optical transmission at the same bit rate without a light source in the subscriber terminal." Electronics Letters 30(14): 1162-1163.

Gong-Ru, L., Yu-Huang, L. and Yung-Cheng, C., (2004). "Theory and experiments of a mode-beating noise-suppressed and mutually injection-locked Fabry-Perot laser diode and erbium-doped fiber amplifier link." IEEE Journal of Quantum Electronics 40(8): 1014-1022.

Gumaste, A. and Antony, T. (2004). First Mile Access Networks and Enabling Technologies, Cisco Press.

Guo-Weı, L., Nıng, D., Chun-Kıt, C. and Lıan-Kuan, C. (2005). Use of downstream inverse-RZ signal for upstream data re-modulation in a WDM passive optical network. OFC/NFOEC Technical Digest. Optical Fiber Communication Conference, 2005.

Han, K. H., Son, E. S., Choı, H. Y., Lım, K. W. and Chung, Y. C., (2004). "Bidirectional WDM PON using light-emitting diodes spectrum-sliced with cyclic arrayed-waveguide grating." IEEE Photonics Technology Letters 16(10): 2380-2382.

Healey, P., Townsend, P., Ford, C., Johnston, L., Townley, P., Lealman, I., Rıvers, L., Perrın, S. and Moore, R., (2001). "Spectral slicing WDM-PON using wavelength-seeded reflective SOAs." Electronics Letters 37(19): 1181-1182.

Hong, J., Kım, H. and Makıno, T., (1998). "Enhanced wavelength tuning range in two-section complex-coupled DFB lasers by alternating gain and loss coupling." Journal of Lightwave Technology 16(7): 1323-1328.

Hyun Deok, K., Seung-Goo, K. and Chang-Hee, L., (2000). "A low-cost WDM source with an ASE injected Fabry-Perot semiconductor laser." IEEE Photonics Technology Letters 12(8): 1067-1069.

Ieee Sa. (2004). "IEEE 802.3ah-2004". https://standards.ieee.org/standard/802_3ah-2004.html.

ITU-T. (2019, April 11). "G.983.1 : Broadband optical access systems based on Passive Optical Networks (PON)". https://www.itu.int/rec/T-REC-G.983.1-200501-I/en.

ITU-T. (2020,February 10). "G.984.1: Gigabit-capable passive optical networks (GPON): General characteristics". https://www.itu.int/rec/T-REC-G.984.1-200803-I/en.

Iwatsukı, K. and Kanı, J., (2009). "Applications and Technical Issues of Wavelength-Division Multiplexing Passive Optical Networks With Colorless Optical Network Units [Invited]." IEEE/OSA Journal of Optical Communications and Networking 1(4): C17-C24.

Jeong, G., Lee, J., Park, M. Y., Kım, C. Y., Cho, S., Lee, W. and Kım, B. W., (2006). "Over 26-nm Wavelength Tunable External Cavity Laser Based on Polymer Waveguide Platforms for WDM Access Networks." IEEE Photonics Technology Letters 18(20): 2102-2104.

Jeong, J. S. and Lee, C. (2009). Optical noise suppression techniques for wavelength-locked Fabry-Perot laser diode. 2009 15th Asia-Pacific Conference on Communications.

Jeung-Mo, K. and Sang-Kook, H., (2006). "A novel hybrid WDM/SCM-PON sharing wavelength for up- and down-link using reflective semiconductor optical amplifier." IEEE Photonics Technology Letters 18(3): 502-504.

Jıe Hyun, L., Mahn Yong, P., Cheol Young, K., Seung-Hyun, C., Wooram, L., Geon, J. and Byoung Whı, K., (2005). "Tunable external cavity laser based on polymer waveguide platform for WDM access network." IEEE Photonics Technology Letters 17(9): 1956-1958.

JIN, X. and Chuang, S.-L., (2006). "Bandwidth Enhancement of Fabry-Perot Quantum-well Lasers by Injection-locking." Solid-state Electronics - SOLID STATE ELECTRON 50: 1141-1149.

Jung, D. K., Shın, S. K., Lee, C. and Chung, Y. C., (1998). "Wavelength-division-multiplexed passive optical network based on spectrum-slicing techniques." IEEE Photonics Technology Letters 10(9): 1334-1336.

Jung, D. K., Shın, S. K., Woo, H. G. and Chung, Y. C., (2000). "Wavelength-tracking technique for spectrum-sliced WDM passive optical network." IEEE Photonics Technology Letters 12(3): 338-340.

Jung, S., Mun, K., Kang, S. and Han, S. K., (2017). "Optical signal suppression by a cascaded SOA/RSOA for wavelength reusing reflective PON upstream transmission." Optics Express 25: 22851.

Kamınow, I., Lı, T. and Wıllner, A. E. (2013). Optical Fiber Telecommunications Volume VIB: Systems and Networks, Elsevier Science.

Kaneko, S., Jun-Ichı, K., Iwatsukı, K., Ohkı, A., Sugo, M. and Kameı, S., (2006). "Scalability of spectrum-sliced DWDM transmission and its expansion using forward error correction." Journal of Lightwave Technology 24(3): 1295-1301.

Kang, J., Kım, T., Choı, I., Lee, S. and Han, S., (2007). "Self-seeded reflective semiconductor optical amplifier based optical transmitter for up-stream WDM-PON link." IET Optoelectronics 1(2): 77-81.

Kasap, S. O. (2013). Optoelectronics and Photonics: Principles and Practices, Pearson.

Kashıma, N., (2006). "Dynamic properties of FP-LD transmitters using side-mode injection locking for LANs and WDM-PONs." Journal of Lightwave Technology 24(8): 3045-3058.

Kawanıshı, S., Takara, H., Uchıyama, K., Shake, I. and Morı, K. (1999). 3 Tbit/s (160 Gbit/s/spl times/19 ch) OTDM/WDM transmission experiment. OFC/IOOC . Technical Digest. Optical Fiber Communication Conference, 1999, and the International Conference on Integrated Optics and Optical Fiber Communication.

Kazovsky, L. G., Cheng, N., Shaw, W. T., Gutıerrez, D. and Wong, S. W. (2011). Broadband Optical Access Networks, Wiley.

Kazovsky, L. G., Shaw, W.-T., Gutıerrez, D., Cheng, N. and Wong, S.-W., (2007). "Next-Generation Optical Access Networks." Journal of Lightwave Technology 25(11): 3428-3442.

Keatıng, A. J., Holloway, W. T. and Sampson, D. D., (1995). "Feedforward noise reduction of incoherent light for spectrum-sliced transmission at 2.5 Gb/s." IEEE Photonics Technology Letters 7(12): 1513-1515.

Kı-Man, C., Jın-Serk, B. and Chang-Hee, L., (2006). "Color-free operation of dense WDM-PON based on the wavelength-locked fabry-Pe/spl acute/rot laser diodes injecting a low-noise BLS." IEEE Photonics Technology Letters 18(10): 1167-1169.

Kım, B.-W., (2008). "RSOA-Based Wavelength-Reuse Gigabit WDM-PON." Journal of the Optical Society of Korea 12(4): 337-345.

Kım, C., (2012). "Impact of seed source power on dispersion-limited maximum reach in WDM-PONs using broadband light source seeded optical sources." Optics express 20: 3473-3478.

Kım, C. H., Lee, J. H., Jung, D. K., Han, Y. and Lee, S. B. (2007). Performance comparison of directly-modulated, wavelength-locked Fabry-Pérot laser diode and EAM-modulated, spectrum-sliced ASE source for 1.25 Gb/s WDM-PON. OFC/NFOEC 2007 - 2007 Conference on Optical Fiber Communication and the National Fiber Optic Engineers Conference.

Kım, H. (2010). An ASE-injected FP-LD-based return-to-zero transmitter for long-reach WDM-PONs. 2010 Conference on Optical Fiber Communication (OFC/NFOEC), collocated National Fiber Optic Engineers Conference.

Kım, S., Jun, S., Takushıma, Y., Son, E. and Chung, Y., (2007). "Enhanced performance of RSOA-based WDM PON by using Manchester coding." Journal of Optical Networking 6.

Kım, S., Son, E., Jun, S. and Chung, Y., (2007). "Effects of Downstream Modulation Formats on the Performance of BidirectionalWDM-PON using RSOA."

Kım, T. and Han, S., (2006). "Reflective SOA-Based Bidirectional WDM-PON Sharing Optical Source for Up/Downlink Data and Broadcasting Transmission." IEEE Photonics Technology Letters 18(22): 2350-2352.

Komljenovıc, T., Babıc, D. and Sıpus, Z., (2012). "47-km 1.25-Gbps transmission using a self-seeded transmitter with a modulation averaging reflector." Optics express 20: 17386-17392.

Koonen, T., (2006). "Fiber to the Home/Fiber to the Premises: What, Where, and When?" Proceedings of the IEEE 94(5): 911-934.

Koponen, J. J. and Soderlund, M. J. (2004). A duplex WDM passive optical network with 1:16 power split using reflective SOA remodulator at ONU. Optical Fiber Communication Conference, 2004. OFC 2004.

Koyama, F. (1997). High power superluminescent diodes for multi-wavelength light sources. Conference Proceedings. LEOS '97. 10th Annual Meeting IEEE Lasers and Electro-Optics Society 1997 Annual Meeting.

Koyama, F., Yamatoya, T. and Iga, K. (2000). Highly gain-saturated GaInAsP/InP SOA modulator for incoherent spectrum-sliced light source. Conference Proceedings. 2000 International Conference on Indium Phosphide and Related Materials (Cat. No.00CH37107).

Kun-Youl, P., Sıl-Gu, M., Kı-Man, C. and Chang-Hee, L., (2005). "A theoretical model of a wavelength-locked Fabry-Pe/spl acute/rot laser diode to the externally injected narrow-band ASE." IEEE Photonics Technology Letters 17(9): 1797-1799.

Kwon, H.-C., Kang, J.-M. and Han, S. K., (2005). "WDM-PON downstream optical link using wavelength-locked FP-LD by spectrally-sliced FP-LD."

Lam, C. F. (2011). Passive Optical Networks: Principles and Practice, Elsevier Science.

Lang, R., (1982). "Injection locking properties of a semiconductor laser." IEEE Journal of Quantum Electronics 18(6): 976-983.

Lau, E. K., (2006). High-Speed Modulation of Optical Injection-Locked Semiconductor Lasers.

Lau, E. K., Sung, H. and Wu, M. C., (2008). "Frequency Response Enhancement of Optical Injection-Locked Lasers." IEEE Journal of Quantum Electronics 44(1): 90-99.

Le, Q. T., Zogal, K., Lerber, T. V., Gıerl, C., Emsıa, A., Brıggmann, D. and Kueppers, F. (2012). Direct DPSK modulation of chirp managed lasers for symmetrical 10-Gbit/s WDM-PONs. 2012 38th European Conference and Exhibition on Optical Communications.

Lee, C., Sorın, W. V. and Kım, B. Y., (2006). "Fiber to the Home Using a PON Infrastructure." Journal of Lightwave Technology 24(12): 4568-4583.

Lee, H., Cho, S. H., Lee, J. H. and Lee, S. S. (2010). Excess Intensity Noise Suppressed 100-GHz Spectrum-Sliced WDM-PON with Pre-Spectrum-Sliced Seed Light Source.

Lee, H. H., Cho, S. and Lee, S. S., (2010). "Efficient Excess Intensity Noise Suppression of 100-GHz Spectrum-Sliced WDM-PON With a Narrow-Bandwidth Seed Light Source." IEEE Photonics Technology Letters 22(20): 1542-1544.

Lee, J. H., Cho, S., Jang, Y. S. and Lee, S. (2010). Enhancement of power budget in RSOA based loop-back type WDM-PON by using the cascaded RSOAs. 2010 12th International Conference on Transparent Optical Networks.

Lee, J. H., Cho, S., Lee, H., Jung, E., Yu, J., Kım, B., Lee, S., Koh, J., Sung, B., Kang, S., Kım, J., Jeong, K. and Lee, S. S., (2010). "First Commercial Deployment of a Colorless Gigabit WDM/TDM Hybrid PON System Using Remote Protocol Terminator." Journal of Lightwave Technology 28(4): 344-351.

Lee, J. H., Kım, C. H., Han, Y. and Lee, S. B., (2006). "WDM-Based Passive Optical Network Upstream Transmission at 1.25 Gb/s Using Fabry–PÉrot Laser Diodes Injected With Spectrum-Sliced, Depolarized, Continuous-Wave Supercontinuum Source." IEEE Photonics Technology Letters 18(20): 2108-2110.

Lee, J. S., Chung, Y. C. and Dıgıovannı, D. J., (1993). "Spectrum-sliced fiber amplifier light source for multichannel WDM applications." IEEE Photonics Technology Letters 5(12): 1458-1461.

Lee, Y. J., Cho, K. Y., Murakamı, A., Agata, A., Takushıma, Y. and Chung, Y. C. (2008). Reflection tolerance of RSOA-based WDM PON. OFC/NFOEC 2008 - 2008 Conference on Optical Fiber Communication/National Fiber Optic Engineers Conference.

Leuthold, J., Bonk, R., Vallaıtıs, T., Marculescu, A., Freude, W., Meuer, C., Bımberg, D., Brenot, R., Lelarge, F. and Duan, G.-H. (2010). Linear and nonlinear semiconductor optical amplifiers.

Leuthold, J., Jaques, J. and Cabot, S. (2004). All-optical wavelength conversion and regeneration.

Lı, Y.-C., Chı, Y.-C., Tsaı, C.-T., Cheng, M.-C. and Lın, G.-R., (2015). "Reusing Downstream Carrier in Colorless Laser Diode for Full-Duplex 64-QAM OFDM." Journal of Lightwave Technology 33(9): 1780-1787.

Lın, C. (2006). Broadband Optical Access Networks and Fiber-to-the-Home: Systems Technologies and Deployment Strategies, Wiley.

Lın, C., Chı, Y., Tsaı, C., Wang, H. and Lın, G., (2015). "39-GHz Millimeter-Wave Carrier Generation in Dual-Mode Colorless Laser Diode for OFDM-MMWoF Transmission." IEEE Journal of Selected Topics in Quantum Electronics 21(6): 609-618.

Lın, G.-R., Cheng, T.-K., Chı, Y.-C., Lın, G.-C., Wang, H.-L. and Lın, Y.-H., (2009). "200-GHz and 50-GHz AWG channelized linewidth dependent transmission of weak-resonant-cavity FPLD injection-locked by spectrally sliced ASE." Optics Express 17(20): 17739-17746.

Lın, G.-R., Wang, H.-L., Lın, G.-C., Huang, Y.-H., Lın, Y.-H. and Cheng, T.-K., (2009). "Comparison on Injection-Locked Fabry–Perot Laser Diode With Front-Facet Reflectivity of 1% and 30% for Optical Data Transmission in WDM-PON System." Journal of Lightwave Technology 27(14): 2779-2785.

Lın, G., Cheng, T., Lın, Y., Lın, G. and Wang, H., (2010). "A Weak-Resonant-Cavity Fabry–Perot Laser Diode With Injection-Locking Mode Number-Dependent Transmission and Noise Performances." Journal of Lightwave Technology 28(9): 1349-1355.

Lın, G., Lıao, Y., Chı, Y., Kuo, H., Lın, G., Wang, H. and Chen, Y., (2010). "Long-Cavity Fabry–Perot Laser Amplifier Transmitter With Enhanced Injection-Locking Bandwidth for WDM-PON Application." Journal of Lightwave Technology 28(20): 2925-2932.

Lın, G., Wang, H., Lın, G., Huang, Y., Lın, Y. and Cheng, T., (2009). "Comparison on Injection-Locked Fabry–Perot Laser Diode With Front-Facet Reflectivity of 1% and 30% for Optical Data Transmission in WDM-PON System." Journal of Lightwave Technology 27(14): 2779-2785.

Lın, S.-Y., Su, Y.-C., Lı, Y.-C., Wang, H.-L., Lın, G.-C., Chen, S.-M. and Lın, G.-R., (2013). "10-Gbit/s direct modulation of a TO-56-can packed 600-μm long laser diode with 2% front-facet reflectance." Optics Express 21(21): 25197-25209.

Lın, S., Chı, Y., Lıao, Z., Wang, H., Lın, G. and LIN, G. (2012). Wdm-Pon transmission using WRC-FPLDs with AR coating reflectance of 0.5% and 1.2%. 2012 17th Opto-Electronics and Communications Conference.

Lın, S., Chı, Y., Su, Y., Lıao, J., Wang, H., Lın, G. and Lın, G., (2013). "Coherent Injection-Locking of Long-Cavity Colorless Laser Diodes With Low Front-Facet Reflectance for DWDM-PON Transmission." IEEE Journal of Selected Topics in Quantum Electronics 19(4): 1501011-1501011.

Lın, Y.-H., Lın, C.-J., Lın, G.-C. and Lın, G.-R., (2011). "Saturated signal-to-noise ratio of up-stream WRC-FPLD transmitter injection-locked by down-stream data-erased ASE carrier." Optics Express 19(5): 4067-4075.

Lın, Y.-H., Lın, C.-J., Lın, G.-C. and Lın, G.-R., (2011). "Saturated signal-to-noise ratio of up-stream WRC-FPLD transmitter injection-locked by down-stream data-erased ASE carrier." Optics express 19: 4067-4075.

Lıou, K., Glance, B., Koren, U., Burrows, E. C., Raybon, G., Burrus, C. A. and Dreyer, K., (1996). "Monolithically integrated semiconductor LED-amplifier for applications as transceivers in fiber access systems." IEEE Photonics Technology Letters 8(6): 800-802.

Lıou, K., Koren, U., Burrows, E. C., Zyskınd, J. L. and Dreyer, K., (1997). "A WDM access system architecture based on spectral slicing of an amplified LED and delay-line multiplexing and encoding of eight wavelength channels for 64 subscribers." IEEE Photonics Technology Letters 9(4): 517-519.

Lorılewısmedıa. (2020). "What Happens in an Internet Minute". https://lorilewismedia.com/.

Lu, F., Chı, Y., Xu, M., Cheng, L., Wang, J., Tsaı, C., Lın, G. and Chang, G. (2016). Cost-effective bi-directional mobile fronthaul employing WRC-FPLD for beyond LTE-Advanced services. 2016 Optical Fiber Communications Conference and Exhibition (OFC).

Maher, R., Barry, L. P. and Anandarajah, P. M. (2010). Cost efficient directly modulated DPSK downstream transmitter and colourless upstream remodulation for full-duplex WDM-PONs. 2010 Conference on Optical Fiber Communication (OFC/NFOEC), collocated National Fiber Optic Engineers Conference.

Maho, A., Sımon, G., Barbet, S., Lelarge, F., Salıou, F., Chanclou, P., Paroları, P., Marazzı, L., Brunero, M., Martınellı, M., Grebewold, S. A., Leuthold, J. and Brenot, R., (2016). "Demystification of the Self-Seeded WDM Access." Journal of Lightwave Technology 34(2): 776-782.

Mahony, M. J. O., Marshall, I. W., Devlın, W. J. and Regnault, J. C., (1985). "Low-reflectivity semiconductor laser amplifier with 20 dB fibre-to-fibre gain at 1500 nm." Electronics Letters 21(11): 501-502.

Management Associatıon, I. R. (2010). Networking and Telecommunications: Concepts, Methodologies, Tools, and Applications: Concepts, Methodologies, Tools, and Applications, IGI Global.

Marazzı, L., Bolettı, A., Paroları, P., Gatto, A., Brenot, R. and Martınellı, M., (2014). "Relative intensity noise suppression in reflective SOAs." Optics Communications 318: 186–188.

Marazzı, L., Paroları, P., Brenot, R., De Valıcourt, G. and Martınellı, M., (2012). "Network-embedded self-tuning cavity for WDM-PON transmitter." Optics express 20: 3781-3786.

Marazzı, L., Paroları, P., Brunero, M., Gatto, A., Martınellı, M., Brenot, R., Barbet, S., Gallı, P. and Gavıolı, G., (2013). "Up to 10.7-Gb/s High-PDG RSOA-Based Colorless Transmitter for WDM Networks." IEEE Photonics Technology Letters 25(7): 637-640.

Martınellı, M., Marazzı, L., Paroları, P., Brunero, M. and Gavıolı, G., (2012). "Polarization in Retracing Circuits for WDM-PON." IEEE Photonics Technology Letters 24(14): 1191-1193.

Martınez, J. J., Gregorıo, J. I. G., Lucıa, A. L., Velasco, A. V., Aguado, J. C. and Bınue, M. Á. L., (2008). "Novel WDM-PON Architecture Based on a Spectrally Efficient IM-FSK Scheme Using DMLs and RSOAs." Journal of Lightwave Technology 26(3): 350-356.

Mccoy, A. D., Thomsen, B. C., Ibsen, M. and Rıchardson, D. J., (2004). "Filtering effects in a spectrum-sliced WDM system using SOA-based noise reduction." IEEE Photonics Technology Letters 16(2): 680-682.

Mecozzı, A. and Wıesenfeld, J. A. Y., (2001). "The Roles of Semiconductor Optical Amplifiers in Optical Networks." Optics and Photonics News 12: 36-42.

Mıchıe, C., Kelly, T. and Andonovıc, I. (2009). Reflective Semiconductor Optical Amplifiers in passive optical networks. 2009 14th OptoElectronics and Communications Conference.

Mogensen, F., Olesen, H. and Jacobsen, G., (1985). "Locking conditions and stability properties for a semiconductor laser with external light injection." IEEE Journal of Quantum Electronics 21(7): 784-793.

Moon, J., Choı, K., Mun, S. and Lee, C., (2007). "Effects of Back-Reflection in WDM-PONs Based on Seed Light Injection." IEEE Photonics Technology Letters 19(24): 2045-2047.

Morthıer, G. and Vankwıkelberge, P. (2013). Handbook of Distributed Feedback Laser Diodes, Second Edition, Artech House.

Mr. G. Pesavento, T., Inc., Mr. J.C. Kuo, Teknovus, Inc., And Mr. T. Koyama, Nec Electronıcs,. (2007). "[S3AM-P03] IEEE Access Standards, 802.3ah GE-PON Status". https://www.itu.int/itudoc/itu-t/workshop/optical/s3amp03.html.

Mukaı, T., Yamamoto, Y. and Kımura, T., (1982). "S/N and error rate performance in AlGaAs semiconductor laser preamplifier and linear repeater systems." IEEE Journal of Quantum Electronics 18(10): 1560-1568.

Murakamı, A., Jeon, H. C., Cho, K. Y., Agata, A., Takushıma, Y., Chung, Y. C. and Horıuchı, Y. (2009). Reflection tolerance enhancement of RSOA-based WDM PON by using optical frequency dithering. 2009 Conference on Optical Fiber Communication - incudes post deadline papers.

Murphy, E. J., Ocenasek, J., Sandahl, C. R., Lısco, R. J. and Chen, Y. C., (1988). "Simultaneous single-fibre transmission of video and bidirectional voice/data using LiNbO/sub 3/ guided-wave devices." Journal of Lightwave Technology 6(6): 937-945.

Noh, Y., Lee, H.-J., Ju, J. J., Kım, M.-S., Oh, S. and Oh, M.-C., (2008). "Continuously tunable compact lasers based on thermo-optic polymer waveguides with Bragg gratings." Optics express 16: 18194-18201.

Ó Dúıll, S., Marazzı, L., Paroları, P., Brenot, R., Koos, C., Freude, W. and Leuthold, J., (2012). "Efficient modulation cancellation using reflective SOAs." Optics express 20: B587-594.

Oksanen, M., Hııronen, O. P., Tervonen, A., Pıetılaınen, A., Gotsonoga, E., Jarvınen, H., Aarnıo, J., Grohn, A., Karhınıemı, M., Moıtchanov, V., Oıkkonen, M., Tahkokorpı, M. and Wallenıus, T. (2002). Spectral slicing passive optical access network trial.

Olsson, N. A., (1989). "Lightwave systems with optical amplifiers." Journal of Lightwave Technology 7(7): 1071-1082.

Pachnıcke, S., Zhu, J., Lawın, M., Wonfor, A., Eıselt, M., Penty, R. V., Cush, R., Turner, R., Fırth, P., Wale, M. J., Whıte, I. H. And Elbers, J. (2014). First demonstration of a full C-Band tunable WDM-PON system with novel high-temperature DS-DBR lasers. OFC 2014.

Park, K.-Y. and Lee, C.-H., (2008). "Intensity Noise in a Wavelength-Locked Fabry–Perot Laser Diode to a Spectrum Sliced ASE." Quantum Electronics, IEEE Journal of 44: 209-215.

Park, K. and LEE, C., (2008). "Intensity Noise in a Wavelength-Locked Fabry–Perot Laser Diode to a Spectrum Sliced ASE." IEEE Journal of Quantum Electronics 44(3): 209-215.

Park, K. J., Shın, S. K., Jı, H. C., Woo, H. G. and Chung, Y. C. (2000). A multi-wavelength locker for WDM system. Optical Fiber Communication Conference. Technical Digest Postconference Edition. Trends in Optics and Photonics Vol.37 (IEEE Cat. No. 00CH37079).

Park, S., Choı, Y., Oh, J., Koo, S. and LEE, D., (2007). "An Evolution Scenario of a Broadband Access Network Using R-SOA-Based WDM-PON Technologies." Journal of Lightwave Technology 25(11): 3479-3487.

Park, S., Jung, D., Shın, D., Shın, H. S., Yun, I., Lee, J., Oh, Y. K. and Oh, Y., (2007). "Colorless Operation of WDM-PON Employing Uncooled Spectrum-Sliced Reflective Semiconductor Optical Amplifiers." IEEE Photonics Technology Letters 19: 248-250.

Paroları, P., Marazzı, L., Brunero, M., Gallı, P., Gavıolı, G. and Martınellı, M. (2012). Embedded modulable self-tuning cavity for WDM-PON transmitter. 2012 14th International Conference on Transparent Optical Networks (ICTON).

Paroları, P., Marazzı, L., Brunero, M., Gatto, A., Martınellı, M., Chanclou, P., Denıel, Q., Salıou, F., Le, S., Brenot, R., Barbet, S., Lelarge, F., Gebrewold, S. A., Ó Dúill, S., Hıllerkuss, D., Leuthold, J., Gavıolı, G. and Gallı, P., (2014). "Self-Tuning Transmitter For Fibre-To-The-Antenna Pon Networks." Optical Switching and Networking 14.

Paroları, P., Marazzı, L., Brunero, M., Martınellı, M., Brenot, R., Maho, A., Barbet, S., Gavıolı, G., Sımon, G., Le, S. D., Salıou, F. and Chanclou, P., (2015). "C- and O-band operation of RSOA WDM PON self-seeded transmitters up to 10 Gb/s [Invited]." IEEE/OSA Journal of Optical Communications and Networking 7(2): A249-A255.

Paroları, P., Marazzı, L., Brunero, M., Martınellı, M., Brenot, R., Maho, A., Barbet, S., Gavıolı, G., Sımon, G., Salıou, F. and Chanclou, P., (2014). "10-Gb/s Operation of a Colorless Self-Seeded Transmitter Over More Than 70 km of SSMF." IEEE Photonics Technology Letters 26(6): 599-602.

Payoux, F., Chanclou, P., Moıgnard, M. and Brenot, R. (2005). Gigabit optical access using WDM PON based on spectrum slicing and reflective SOA. 2005 31st European Conference on Optical Communication, ECOC 2005.

Payoux, F., Chanclou, P., Soret, T., Genay, N. and Brenot, R. (2006). Demonstration of a RSOA-based wavelength remodulation scheme in 1.25 Gbit/s bidirectional hybrid WDM-TDM PON. 2006 Optical Fiber Communication Conference and the National Fiber Optic Engineers Conference.

Pendock, G. J. and Sampson, D. D., (1996). "Transmission performance of high bit rate spectrum-sliced WDM systems." Journal of Lightwave Technology 14(10): 2141-2148.

Peng, G.-H., Chı, Y.-C. and Lın, G.-R., (2008). "DWDM channel spacing tunable optical TDM carrier from a mode-locked weak-resonant-cavity Fabry-Perot laser diode based fiber ring." Optics Express 16(17): 13405-13413.

Prat, J., Arellano, C., Polo, V. and Bock, C., (2005). "Optical network unit based on a bidirectional reflective semiconductor optical amplifier for fiber-to-the-home networks." IEEE Photonics Technology Letters 17(1): 250-252.

Prat, J., Polo, V., Bock, C., Arellano, C. and Olmos, J. J. V., (2005). "Full-duplex single fiber transmission using FSK downstream and IM remote upstream Modulations for fiber-to-the-home." IEEE Photonics Technology Letters 17(3): 702-704.

Presı, M., Chıuchıarellı, A., Corsını, R. and Cıaramella, E. (2013). Self-seeding of semiconductor lasers for next-generation WDM Passive Optical Networks. 2013 15th International Conference on Transparent Optical Networks (ICTON).

Presı, M. and Cıaramella, E., (2011). "Stable self-seeding of Reflective-SOAs for WDM-PONs."

Ramaswamı, R., Sıvarajan, K. and Sasakı, G. (2009). Optical Networks: A Practical Perspective, Elsevier Science.

Ramaswamı, R., Sıvarajan, K. N. and Sasakı, G. H. (2010). Optical Networks: A Practical Perspective, Elsevier/Morgan Kaufmann.

Reeve, M. H., Hunwıcks, A. R., Zhao, W., Methley, S. G., Bıckers, L. and Hornung, S., (1988). "LED spectral slicing for single-mode local loop applications." Electronics Letters 24(7): 389-390.

Roppelt, M., Eıselt, M., Grobe, K. and Elbers, J. (2012). Tuning of an SG-Y branch laser for WDM-PON. OFC/NFOEC.

Roppelt, M., Pohl, F., Grobe, K., Eıselt, M. and Elbers, J. (2011). Tuning methods for uncooled low-cost tunable lasers in WDM-PON. 2011 Optical Fiber Communication Conference and Exposition and the National Fiber Optic Engineers Conference.

Salıou, F., Sımon, G., Chanclou, P., Brunero, M., Marazzı, L., Paroları, P., Martınellı, M., Brenot, R., Maho, A., Barbet, S., Gavıolı, G., Parladorı, G., Gebrewold, S. and Leuthold, J., (2015). "125-km Long Cavity Based on Self-Seeded RSOAs Colorless Sources for 2.5-Gb/s DWDM Networks." Journal of Lightwave Technology 33(8): 1602-1607.

Sampson, D. D. and Holloway, W. T., (1994). "100 mW spectrally-uniform broadband ASE source for spectrum-sliced WDM systems." Electronics Letters 30(19): 1611-1612.

Sang-Mook, L., Kı-Man, C., Sıl-Gu, M., Jung-Hyung, M. and Chang-Hee, L., (2005). "Dense WDM-PON based on wavelength-locked Fabry-Pe/spl acute/rot laser diodes." IEEE Photonics Technology Letters 17(7): 1579-1581.

Sang-Mook, L., Kı-Man, C., Sıl-Gu, M., Jung-Hyung, M. and Chang-Hee, L. (2005). Dense WDM-PON based on wavelength locked Fabry-Perot lasers. OFC/NFOEC Technical Digest. Optical Fiber Communication Conference, 2005.

Schrenk, B., Chatzı, S., Bonada, F., Lazaro, J., Klonıdıs, D., Tomkos, I. and Prat, J. (2009). C+L band remote node for amplification in extended reach full-duplex 10Gb/s WDM/TDM Passive Optical Networks.

Schrenk, B., Chatzı, S., Bonada, F., Lazaro, J. A., Klonıdıs, D., Tomkos, I. and Prat, J. (2009). C+L band remote node for amplification in extended reach full-duplex 10Gb/s WDM/TDM Passive Optical Networks. 2009 35th European Conference on Optical Communication.

Senıor John M (2009). Optical Fiber Communications: Principles and Practice, Pearson Education.

Seo, J., Seo, Y. and Choı, W. (2001). Nonlinear distortion suppression in directly modulated DFB lasers by sidemode optical injection. 2001 IEEE MTT-S International Microwave Sympsoium Digest (Cat. No.01CH37157).

Shın, D. J., Jung, D. K., Lee, J. K., Lee, J. H., Choı, Y. H., Bang, Y. C., Shın, H. S., Lee, J., Hwang, S. T. and Oh, Y. J., (2003). "155 Mbit/s transmission using ASE-injected Fabry-Perot laser diode in WDM-PON over 70/spl deg/C temperature range." Electronics Letters 39(18): 1331-1332.

Sıl-Gu, M., Jung-Hyung, M., Hoon-Keun, L., Jun-Young, K. and Chang-Hee, L. (2008). A WDM-PON with a 40 Gb/s capacity based on wavelength-locked Fabry-Perot laser diodes. 2008 34th European Conference on Optical Communication.

Sımon, G., Salıou, F., Chanclou, P., Denıel, Q., Erasme, D. and Brenot, R. (2014). 70km external cavity DWDM sources based on O-band self seeded RSOAs for transmissions at 2.5Gbit/s. OFC 2014.

Sımpson, T. B., Lıu, J. M. and Gavrıelıdes, A., (1995). "Bandwidth enhancement and broadband noise reduction in injection-locked semiconductor lasers." IEEE Photonics Technology Letters 7(7): 709-711.

Sıngal, T. L. (2016). Optical Fiber Communications: Principles and Applications, Cambridge University Press.

Soo-Jın, P., Chang-Hee, L., Kı-Tae, J., Hyung-Jın, P., Jeong-Gyun, A. and Kıl-Ho, S., (2004). "Fiber-to-the-home services based on wavelength-division-multiplexing passive optical network." Journal of Lightwave Technology 22(11): 2582-2591.

Stern, J. R., Hoppıtt, C. E., Payne, D. B., Reeve, M. H. and Oakley, K. (1988). TPON-a passive optical network for telephony. 1988 Fourteenth European Conference on Optical Communication, ECOC 88 (Conf. Publ. No.292).

Su, Y., Chı, Y., Chen, H. and Lın, G., (2015). "Data Erasing and Rewriting Capabilities of a Colorless FPLD Based Carrier-Reusing Transmitter." IEEE Photonics Journal 7(3): 1-12.

Takesue, H. and Sugıe, T. (2002). Data Rewrite of Wavelength Channel Using Saturated SOA Modulator for WDM Metro/Access Networks with Centralized Light Sources. 2002 28TH European Conference on Optical Communication.

Takesue, H. and Sugıe, T., (2003). "Wavelength Channel Data Rewrite Using Saturated SOA Modulator for WDM Networks With Centralized Light Sources." Journal of Lightwave Technology 21(11): 2546.

Takesue, H. and Sugıe, T., (2003). "Wavelength channel data rewrite using saturated SOA modulator for WDM networks with centralized light sources." Journal of Lightwave Technology 21(11): 2546-2556.

Tallı, G., Cotter, D. and Townsend, P. D., (2006). "Rayleigh backscattering impairments in access networks with centralised light source." Electronics Letters 42(15): 877-878.

Tıan, Y., Yı, L., Tıan, X., He, H., Xu, X., Su, Y. and Leng, L. (2006). Optical VPN in PON Based on DPSK Erasing/Rewriting and DPSK/IM formatting using a Single Mach-Zehnder Modulator. 2006 European Conference on Optical Communications.

Trojer, E., Dahlfort, S., Hood, D. and Mıckelsson, H. Current and next-generation PONs : A technical overview of present and future PON technology.

Tsaı, C.-T., Lın, C.-H., Lın, C.-T., Chı, Y.-C. and Lın, G.-R., (2016). "60-GHz Millimeter-wave Over Fiber with Directly Modulated Dual-mode Laser Diode." Scientific Reports 6(1): 27919.

Urban, P. J., Koonen, A. M. J., Khoe, G. D. and Waardt, H. D. (2008). Mitigation of Reflection-induced Crosstalk in a WDM Access Network. OFC/NFOEC 2008 - 2008 Conference on Optical Fiber Communication/National Fiber Optic Engineers Conference.

VENGHAUS, H. and GROTE, N. (2012). Fibre Optic Communication: Key Devices, Springer Berlin Heidelberg.

Wagner, S. S. and Chapuran, T. E., (1990). "Broadband high-density WDM transmission using superluminescent diodes." Electronics Letters 26(11): 696-697.

Wagner, S. S., Kobrınskı, H., Robe, T. J., Lemberg, H. L. and Smoot, L. S., (1988). "Experimental demonstration of a passive optical subscriber loop architecture." Electronics Letters 24(6): 344-346.

Waı, H., Chun-Kıt, C., Lıan-Kuan, C. and Tong, F., (2003). "An optical network unit for WDM access networks with downstream DPSK and upstream remodulated OOK data using injection-locked FP laser." IEEE Photonics Technology Letters 15(10): 1476-1478.

Ward, A. J., Robbıns, D. J., Busıco, G., Barton, E., Ponnampalam, L., Duck, J. P., Whıtbread, N. D., Wıllıams, P. J., Reıd, D. C. J., Carter, A. C. and Wale, M. J., (2005). "Widely tunable DS-DBR laser with monolithically integrated SOA: design and performance." IEEE Journal of Selected Topics in Quantum Electronics 11(1): 149-156.

Wheeler, J. K., Ocenasek, J. and Bohn, P. P., (1986). "Two-way transmission using electro-optical modulator." Electronics Letters 22(9): 479-481.

Wong, E., (2012). "Next-Generation Broadband Access Networks and Technologies." Journal of Lightwave Technology 30(4): 597-608.

Wong, E. (2013). Self-seeding reflective semiconductor optical amplifiers for WDM Access Networks (invited). 2013 9th International Conference on Information, Communications & Signal Processing.

WONG, E., LEE, K. and ANDERSON, T., (2006). "Low-cost WDM passive optical network with directly-modulated self-seeding reflective SOA." Electronics Letters 42(5): 299-301.

Wong, E., Lee, K. L. and Anderson, T. B., (2007). "Directly Modulated Self-Seeding Reflective Semiconductor Optical Amplifiers as Colorless Transmitters in Wavelength Division Multiplexed Passive Optical Networks." Journal of Lightwave Technology 25(1): 67-74.

Woodward, S. L., Iannone, P. P., Reıchmann, K. C. and Frıgo, N. J., (1998). "A spectrally sliced PON employing Fabry-Perot lasers." IEEE Photonics Technology Letters 10(9): 1337-1339.

Wooram, L., Mahn Yong, P., Seung Hyun, C., Jıhyun, L., Kım, C., Geon, J. and Byoung Whı, K., (2005). "Bidirectional WDM-PON based on gain-saturated reflective semiconductor optical amplifiers." IEEE Photonics Technology Letters 17(11): 2460-2462.

Xıong, F. and Zhong, W. (2013). Performance of self-seeded RSOAs in WDM-PONs. CLEO: 2013.

Xıong, F., Zhong, W. and Kım, H., (2012). "A Broadcast-Capable WDM-PON Based on Polarization-Sensitive Weak-Resonant-Cavity Fabry–Perot Laser Diodes." Journal of Lightwave Technology 30(3): 355-361.

Xıong, F., Zhong, W., Zhu, M., Kım, H., Xu, Z. and Lıu, D., (2013). "Characterization of Directly Modulated Self-Seeded Reflective Semiconductor Optical Amplifiers Utilized as Colorless Transmitters in WDM-PONs." Journal of Lightwave Technology 31(11): 1727-1733.

Xu, Z., Wen, Y., Zhong, W.-D., Chae, C.-J., Cheng, X.-F., Wang, Y., Lu, C. and Shankar, J., (2007). "High-speed WDM-PON using CW injection-locked Fabry-Perot laser diodes." Optics express 15: 2953-2962.

Yarıv, A. (1990). Optical Electronics, Oxford University Press.

Yasaka, H., Yoshıkunı, Y., Sato, K., Ishıı, H. and Sanjoh, H. (1996). Multiwavelength light source with precise frequency spacing using mode-locked semiconductor laser and arrayed waveguide grating filter. Optical Fiber Communications, OFC.

Yeh, C., Chıen, H. and CHI, S. (2008). Cost-Effective Colorless RSOA-Based WDM-PON with 2.5 Gbit/s Uplink Signal. OFC/NFOEC 2008 - 2008 Conference on Optical Fiber Communication/National Fiber Optic Engineers Conference.

Yeh, C., Chow, C., Wu, Y., Huang, S., Lıu, Y. and Pan, C., (2013). "Performance of Long-Reach Passive Access Networks Using Injection-Locked Fabry–Perot Laser Diodes With Finite Front-Facet Reflectivities." Journal of Lightwave Technology 31(12): 1929-1934.

Yoon, K.-H., Oh, S., Kım, K., Kwon, O. K., Oh, D., Noh, Y. and Lee, H.-J., (2010). "2.5-Gb/s hybridly-integrated tunable external cavity laser using a superluminescent diode and a polymer Bragg reflector." Optics express 18: 5556-5561.

Yu, J.-H., Kım, N. and Kım, B., (2007). "Remodulation schemes with reflective SOA for colorless DWDM PON." Journal of Optical Networking 6: 1041-1054.

Zaıtsu, M., Takeda, K., Takenaka, M., Tanemura, T. and Nakano, Y., (2010). "All-Optical Flip-Flop with Optical Clock Signal Using Mach-Zehnder Interferometer Bistable Laser Diode." Optics InfoBase Conference Papers.

Zhan, W., Tanemura, T., Yamauchı, S., Mukaıkubo, M. and Nakano, Y., (2015). "Uncooled (2U 50 °C) operation of self-seeded RSOA for low-cost colorless WDM-PON transmitter." 2015 European Conference on Optical Communication (ECOC): 1-3.

Zhou, L., Cheng, X., Yeo, Y. and Ngoh, L. H. (2010). Hybrid WDM-TDM PON architectures and DWBA algorithms. 2010 5th International ICST Conference on Communications and Networking in China.

Zhou, X. and Deng, N. (2015). A 25-Gb/s 20-km wavelength reused WDM system for mobile fronthaul applications. 2015 European Conference on Optical Communication (ECOC).

Zırngıbl, M., Joyner, C. H., Stulz, L. W., Dragone, C., Presby, H. M. and Kamınow, I. P., (1995). "LARnet, a local access router network." IEEE Photonics Technology Letters 7(2): 215-217.

Zırngıbl, M., Joyner, C. H., Stulz, L. W., Koren, U., Chıen, M., Young, M. G. and Mıller, B. I., (1994). "Digitally tunable laser based on the integration of a waveguide grating multiplexer and an optical amplifier." IEEE Photonics Technology Letters 6(4): 516-518.

## BIOGRAPHY

Nisa NACAR ÇIKAN earned her bachelor's degree in Electrical and Electronics Engineering from Mustafa Kemal University as the top student (with the highest grade) in 2006. She worked as a Transmission Engineer in Turk Telekom after graduation and left the company in 2008.

She holds an M.S. degree in electrical engineering from the Polytechnic Institute of New York University, New York, NY, USA, in 2011. She focused on communication and Rf design during her studies at NYU-Poly.

She worked as a teaching assistant at Drexel University between 2011-2014. She worked on RF component design with a team during her research at Drexel University. Her studies with the research team included designing the schematics and layout of microstriplines, striplines, couplers, amplifiers, filters, phase shifters, switches using CAD tools. They fabricated the implemented design on printed circuit boards and tested the designed printed circuit boards on Network Analyzer.

She also worked on the characterization of Analog Radio over Fiber Link, Flash ADC, and hybrid type of photonic analog to digital converters during her research at Drexel University.

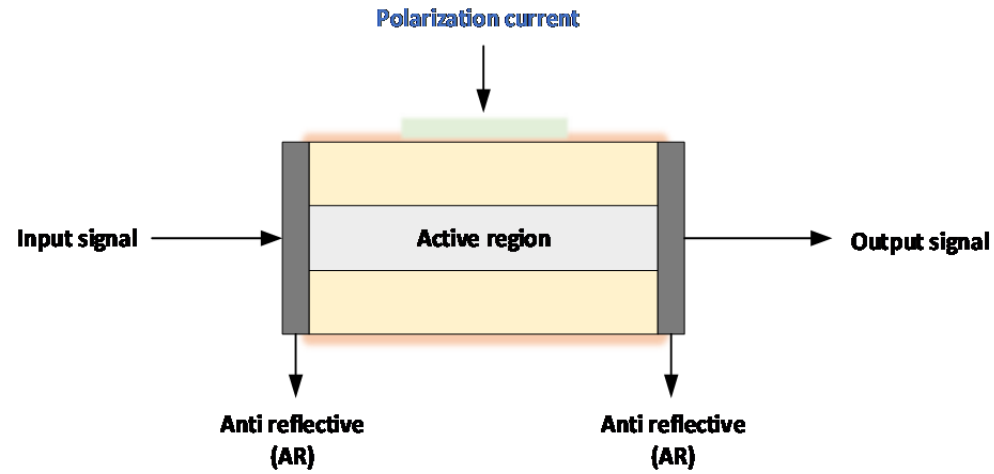
She currently works as Research Assistant at the Department of Electrical and Electronics Engineering, Cukurova University, Adana, Turkey.

Her current research interests include broadband networks, passive optical networks, optical long-haul transmissions, future internet, and fiber optic communications.

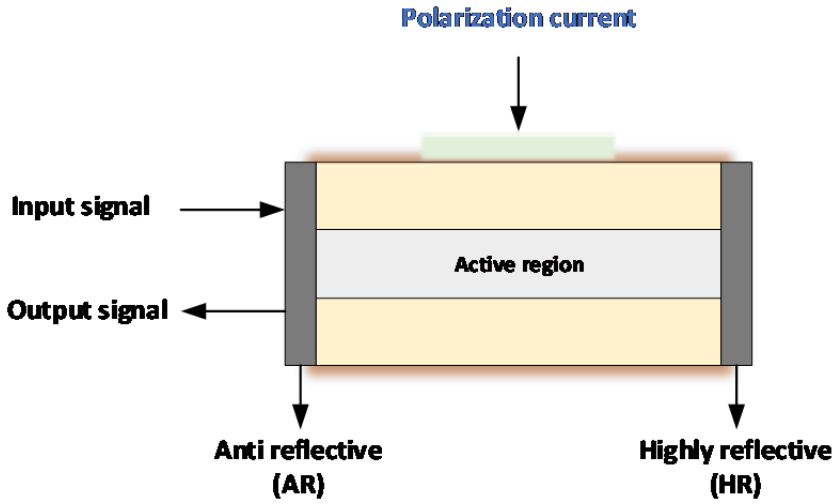
# APPENDIX

**A. Theory Behind RSOA**

RSOA's operating principle is similar to SOA with one side coated with a reflective layer. In typical SOAs, the reflectivity value of both mirrors is about 0.01%, whereas in RSOAs one side coated with a reflective layer. It is required that one of the mirrors faces has high reflectivity (90%) thus ensuring that the signal exits through the same input region (Michie et al., 2009).




(a)




(b)

Figure Appendix A.1: (a) SOA; (b) RSOA

The characteristic of the RSOA is defined by the rate equation. This equation is investigated in three parts as propagating wave, carrier, and gain.

## A.1 Wave Equation

Maxwell equation is needed to be used to define the propagation of light in the amplifier. Maxwell equations are listed in equations between A.1 to A.4.

$$\nabla \times E = -\frac{\partial B}{\partial t} \quad \text{A.1}$$

$$\nabla \times H = J + \frac{\partial D}{\partial t} \quad \text{A.2}$$

$$\nabla . D = \rho v \quad \text{A.3}$$

$$\nabla . B = 0 \quad \text{A.4}$$

where,

E: electric field

B: magnetic flux density

H: magnetic field

J: current density

D: electric displacement

: charge density

These equations can be expresses as following in a nonmagnetic dielectric medium.

$$B = \mu_0 H \quad \text{A.5}$$

$$D = \varepsilon_0 E + P \quad \text{A.6}$$

$$J = \sigma E \quad \text{A.7}$$

where,

$\mu_0$ : vacuum permeability,

$\varepsilon_0$ : vacuum permittivity,

$P$ : electric polarization,

$\sigma$ : conductivity

Now, if we assume the medium is isotropic and homogeneous, and no free charge,

$$\nabla\times\nabla\times E=-\mu_0\frac{\partial}{\partial t}(\nabla\times H)=-\mu_0\frac{\partial J}{\partial t}-\mu_0\frac{\partial^2 D}{\partial t^2}=-\mu_0\sigma\frac{\partial E}{\partial t}-\mu_0\varepsilon_0\frac{\partial^2 E}{\partial t^2}-\mu_0\frac{\partial^2 P}{\partial t^2} \quad \text{A.8}$$

In other term,

$$\nabla\times\nabla\times E=\nabla(\nabla.E)-\nabla^2 E \quad \text{A.9}$$

In the case of free of charge $pv=0$ and thus, $\nabla.E=0$

$$\nabla\times\nabla\times E=-\nabla^2 E \quad \text{A.10}$$

c is the speed of light and $c=\frac{1}{\sqrt{\mu_0\varepsilon_0}}$

$$\nabla^2 E-\mu_0\sigma\frac{\partial E}{\partial t}-\mu_0\varepsilon_0\frac{\partial^2 E}{\partial t^2}=\nabla^2 E-\frac{\sigma}{\varepsilon_0 c^2}\frac{\partial E}{\partial t}-\frac{1}{c^2}\frac{\partial^2 E}{\partial t^2}=\frac{1}{\varepsilon_0 c^2}\frac{\partial^2 P}{\partial t^2}$$

A.11

Assuming the field is time harmonic,

$$E(x,y,z,t)=\mathrm{Re}\{\tilde{E}(x,y,z)e^{-i\omega t}\} \quad \text{A.12}$$

$$P(x,y,z,t)=\mathrm{Re}\{\tilde{P}(x,y,z)e^{-i\omega t}\} \quad \text{A.13}$$

Hence, equation A.11 can be written as

$$\nabla^2\tilde{E}+k_0^2\left(1+\frac{i\sigma}{\varepsilon_0\omega}\right)\tilde{E}=-\frac{k_0^2}{\varepsilon_0}\tilde{P} \quad \text{A.14}$$

$k_0$ is the wave number and is equal to $\omega/c$

The relationship between P and E is

$$\tilde{P} = \varepsilon_0 \chi(\omega) \tilde{E} \qquad \text{A.15}$$

Where $\chi$ is the material susceptibility and can be written as follows:

$$\chi = \chi_0 + \chi_p \qquad \text{A.16}$$

In which,

$\chi_0$ : medium susceptibility in the absence of external pumping

$\chi_p$ : further additive susceptibility relevant to the pumping strength

The current injection is the pumping source for RSOAs and $\chi_p$ depends on the carrier charge concentration.

Using the equations A.14 and A.15,

$$\nabla^2 \tilde{E} + k_0^2 (1 + \frac{i\sigma}{\varepsilon_0 \omega}) \tilde{E} + k_0^2 \chi \tilde{E} = \nabla^2 \tilde{E} + \varepsilon k_0^2 \tilde{E} = 0 \qquad \text{A.17}$$

in which, $\varepsilon$ can be expressed as

$$\varepsilon = 1 + \chi + \frac{i\sigma}{\varepsilon_0 \omega} = 1 + \chi_0 + \chi_p + \frac{i\sigma}{\varepsilon_0 \omega} = n_b^2 + \varepsilon' \qquad \text{A.18}$$

Where, $n_b = \sqrt{1 + \mathrm{Re}\{\chi_0\}}$ is the unpumped material's background refractive index, and $\varepsilon'$ is the remain part of $\varepsilon$.

In conclusion, the wave equation (Agrawal and Dutta, 2013) can be written as in A.19 by transforming the equation A.17 to its time-domain.

$$\nabla^2 E - \frac{\varepsilon}{c^2} \frac{\partial^2 E}{\partial t^2} = 0 \qquad \text{A.19}$$

**A.2 Wave Propagation**

The slowly varying envelope approximation is needed to be used to solve the wave equations. Assuming that the electric field is linearly polarized, the propagation can be written as in equation A.20.

$$E(x,y,z,t) = F(x,y)A(z,t)e^{i(kz-\omega t)} \quad \text{A.20}$$

In which,

A(z,t): envelope,

F(x,y): waveguide mode distribution

k: material waveguide and can be expressed as: $k = k_0 n_{eff}$

Substituting equation A.20 into A.19,

$$\left(\frac{\partial^2}{\partial x^2}+\frac{\partial^2}{\partial y^2}\right)F.Ae^{i(kz-\omega t)}+F.\left(-k^2A+ik\frac{\partial}{\partial z}A+\frac{\partial^2}{\partial z^2}A\right).e^{i(kz-\omega t)}=\frac{\varepsilon}{c^2}F.\left(-\omega^2A-i\omega\frac{\partial}{\partial t}A+\frac{\partial^2}{\partial t^2}A\right)e^{i(kz-\omega t)} \quad \text{A.21}$$

The equation A.22 should be verified by waveguide mode distribution.

$$\frac{\partial^2 F}{\partial x^2}+\frac{\partial^2 F}{\partial y^2}+(n_b^2-n_{eff}^2)\frac{\omega^2}{c^2}F=0 \quad \text{A.22}$$

The envelope change is slow under slowly varying envelope approximation. Thus, the second derivative of A(z,t) in equation A.21 can be neglected. Using the equation A.22, we get

$$k\frac{\partial}{\partial z}A.F+\frac{\varepsilon\omega}{c^2}\frac{\partial}{\partial t}A.F=ik_0^2\varepsilon^{'}A.F \quad \text{A.23}$$

We obtain the equation A.24 by multiplying both sides of equation A.23 with $F^*$ and integrating over y and x-axes.

$$\frac{1}{v_g}\frac{\partial A}{\partial t}+\frac{\partial A}{\partial z}=GA \quad \text{A.24}$$

In which,

G: integration constant

$v_g$ : group velocity

Wave envelope propagation is presented in A.24. G can be expressed as in A.25 in an active semiconductor medium.

$$G = g - a \tag{A.25}$$

Here, G is the net gain, g is the medium gain and a is the material loss.

In the case of the electric field propagate in the forward direction, we obtain,

$$\frac{1}{v_g}\frac{\partial A^+}{\partial t} + \frac{\partial A^+}{\partial z} = (g - a)A^+ \tag{A.26}$$

In the case of the electric field propagate in the backward direction, we obtain,

$$\frac{1}{v_g}\frac{\partial A^-}{\partial t} - \frac{\partial A^-}{\partial z} = (g - a)A^- \tag{A.27}$$

### A.3.Carrier Rate

The holes and electrons are carriers in semiconductors. Hence, usually, two equations are required to define the carrier rate equation. However, the densities of holes and electrons are dependent and, only electrons are taken into account to simplify the equation.

The carrier density change is:

$$\frac{\partial n}{\partial t} = Injection + diffusion - recombination \quad \text{A.28}$$

Diffusion equation is given in A.29.

$$Diffusion = D\nabla^2 n \quad \text{A.29}$$

In which,

D: diffusion coefficient

The diffusion term is assumed to be nearly constant due to the carrier density cannot change notably over the active medium's length. Thus, this term can be neglected from equation A.28.

The injection equation is given in A.30.

$$Injection = \frac{J}{qd} \quad \text{A.30}$$

Where, q is electrons charge and equal to $1.602 \times 10^{-19}$ C.

$$J = \frac{I}{\omega L} \quad \text{A.31}$$

Where J is current density and L is active region length and I is the injection current.

The recombination can be studied in two parts as stimulated emission and the other mechanisms. The RSOA uses the stimulated emission for light amplification process. The ‘g’ term in equation A.26 represents the real gain part of the active medium.

$$R_{sim} = v_g g n_{ph} \quad \text{A.32}$$

In which $R_{sim}$ is the stimulated emission recombination rate and $n_{ph}$ is the photon density.

In the case of electric field envelope normalization:

$$|A|^2 = n_{ph}.\hbar\omega.\omega dv_g \quad \text{A.33}$$

Where $|A|^2$ light power, $\hbar$ is the plank constant and equal to 1.0546 J s.

The other recombination mechanisms are nonradiative recombination, auger recombination, and bimolecular recombination. The relationship with carrier density:

$$R(n) = A_{nr}n + Bn^2 + Cn^3 \quad \text{A.34}$$

Where,

$A_{nr}$ : nonradiative recombination rate

B: bimolecular recombination coefficient

C: Auger recombination coefficient

Finally, carrier rate equation can be written using the equations A.28, A.32, and A.34.

$$\frac{\partial n}{\partial t} = \frac{J}{qd} - v_g g(n_{ph}^{+} + n_{ph}^{-}) - R(n) \quad \text{A.35}$$

This equation includes backward and forward waves.

**A.4. The Gain Model**

The approach in equation A.36 is used to analyze semiconductor amplifiers. In this equation, the gain relationship with carrier density is given as in follows.

$$g = \Gamma\alpha(n - n_0) \quad \text{A.36}$$

Where,

$\alpha$ : gain constant

$\Gamma$ : confinement factor

$n_0$ : transparency carrier density,

g: gain that is equal to zero when $n = n_0$

The equation A.36 is good enough to explain the characteristics of the single pass optical amplifiers and semiconductor lasers. However, it is not adequate to describe RSOAs due to its high gain saturation characteristic (Duill et al., 2012).

The major difference between RSOA and SOA is the waves in the cavity. While wave only travels in the forward direction in SOA, it travels in both directions as backward and forward in RSOA. Thus, a mutual effect occurs. The gain equation of an RSOA can be defined as in equation A.37 by modifying the A.36.

$$g^{+} = \frac{\Gamma \alpha (n - n_0)}{1 + \varepsilon_{11} n_{ph}^{+} + \varepsilon_{12} n_{ph}^{-}} \quad \text{A.37}$$

$$g^{-} = \frac{\Gamma \alpha (n - n_0)}{1 + \varepsilon_{22} n_{ph}^{-} + \varepsilon_{21} n_{ph}^{+}} \quad \text{A.38}$$

In which,

$g^{+}$ : the gain of the forward propagating electric field,

$g^{-}$ : the gain of the backward propagating electric field

$\varepsilon_{11}$ and $\varepsilon_{22}$ :self-gain saturation factors

$\varepsilon_{12}$ and $\varepsilon_{21}$ :cross-gain saturation factors

Assuming $\varepsilon_{12} = 2\varepsilon_{11}$ because of cross-gain is stronger than self-gain saturation (Zaitsu et al., 2010).

**B. Figure of Merits**

The specific components of an optical communication system are used to measure and characterize the performance of the system. The main figure-of-merits of a WDM-PON system are bit error rate, quality factor, extinction ratio, and eye diagram (Lam, 2011).

**B.1.Eye Diagram**

The eye diagram method is helpful for evaluating the data-handling capability of an optical system. It is used to monitor the transmitted or received signal quality. The output of the random bit generator is applied to the input of the test system (optical

receiver, transmitter, fiber cable). Then, the system's output is applied to the input of the oscilloscope. The random bit pattern sweep leads to an eye pattern shape in the oscilloscope screen (Singal, 2016).

The time-domain signal and overlapping symbols create an eye diagram. Hence, an oscilloscope is usually used to display the eye diagrams. The random pulse is given to the oscilloscope's vertical input. A saw-tooth model generator, which is time-dependent, is put to an oscilloscope's horizontal input. The time period of the generator is equal to incoming data. That provides equal symbol and sweep rates. The clock of the symbol is operated as external triggering. The signal is wrapped around to the beginning of the time axis at the end of the constant time interval. In this way, an eye diagram forms overlapping lines (Singal, 2016).

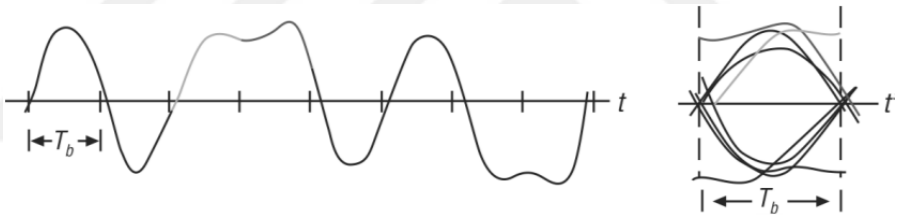



Figure Appendix B1. The eye diagram concept (T is the pulse width) (Singal, 2016)

The eye-opening determines the quality of the communication link. The figure below demonstrates the width and height of the eye.

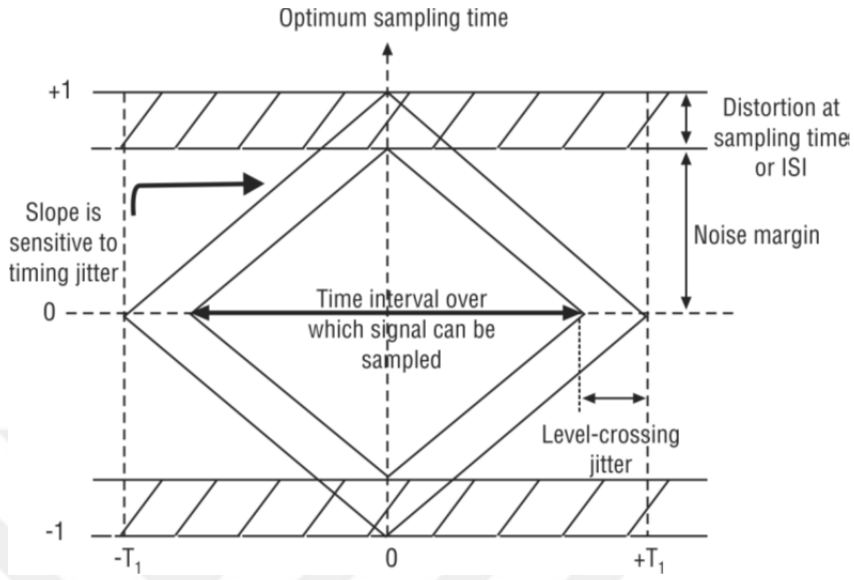



Figure Appendix B2. Eye pattern parameters (Singal, 2016)

The wide eye-opening indicates transmission without noise. The eye diagram defines signal quality by measuring parameters such as noise margin, amplitude distortion, and, timing jitter (Singal, 2016).

**B.2. Bit Error Rate**

BER is the parameter that quantitatively evaluates the transmitted signal. It can be defined as the probability of an incorrect identification of a bit by the receiver's decision circuit and written as in (Ramaswami et al., 2009):

$$BER = Pb(1)\,Pb(0/1) + Pb(0)\,Pb(1/0) \quad \text{B.1}$$

Pb (1) and Pb (0) are the probabilities of receiving bits "1" and "0", respectively; Pb (0/1) is the probability of deciding by "0" when "1" is received, and Pb (1/0) is the probability of deciding by "1" when "0" is received. Considering that bits "1" and "0" have the same probability of occurring, that is, Pb (1) = Pb (0), then BER becomes as in equation B2 (Ramaswami et al., 2009):

$$BER = \frac{1}{2}[Pb(0/1) + Pb(1/0)] \quad \text{B.2}$$

In a simplified way, BER can be understood as the number of bit errors divided by the total number of bits sent in a time interval (Lam, 2011):

$$BER = \frac{Number\ of\ bit\ errors}{Total\ number\ of\ bits\ sent} \quad \text{B.3}$$

Conventionally, a digital transmission system is free of errors when the BER is less than or equal to $10^{-12}$ (Ramaswami et al., 2009), this means that it is guaranteed that the receiver will be able to correctly recover the signal transmitted by the transmitter. Moreover, commercial systems with a BER less than or equal to $10^{-9}$ are considered reliable, and the signal sent by the transmitter will be correctly recovered (Lam, 2011).

### B.3 Extinction Ratio (ER)

The ER is interpreted as the ratio between the optical power of the logic levels "1" and "0".

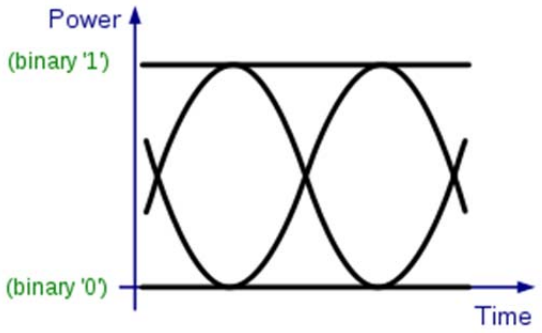



Figure Appendix B3. Eye pattern of power levels in an on-off-keying modulation

The formula of the ER can be defined in equations B4 and B5.

$$ER = \frac{P_1}{P_0} \quad \text{B.4}$$

$$ER(dB) = 10\log\frac{P_1}{P_0} \quad \text{B.5}$$

In a WDM-PON network that uses the carrier reuse technique, it is desired that the signal at the RSOA output it has an ER close to 0 dB since this means that the optical characteristics of the downstream seed have been erased (Takesue and Sugie, 2002).

***List of Author's Published Articles***

***<u>List of Published Articles in International Journals</u>***

- ***N. NACAR ÇIKAN**, M. AKSOY, "Data erasure in Fabry Perot Diode Lasers:effects of facet reflectivity," Journal of Modern Optics, vol. 67, no. 6, pp. 515–522, May 2020. doi: 10.1080/09500340.2019.1699182*
- ***N. NACAR ÇIKAN**, M. AKSOY, "Data erasure analysis of FPLD based on remodulation bidirectional PON system," Journal of Modern Optics, vol. 67, no. 2, pp. 139–145, Jan. 2020. doi: 10.1080/09500340.2020.1759716*
- ***N. NACAR ÇIKAN**, M. Aksoy, ''A Review of Self-Seeded RSOA Based on WDM PON,'' Can J Electrical Computer Engineering 2019, 42 (1), 2–9. doi:10.1109/CJECE.2018.2872433.*
- ***N. NACAR ÇIKAN**, M. AKSOY, "Q Factor and BER Analysis of a PON System at Different Distances in Bidirectional Optical Fiber Communication," Advanced Research in Electrical Electronics Systems (AREES), vol. 2, no. 2, pp. 44–50, Dec. 2017.*
- ***N. NACAR ÇIKAN**, M. AKSOY, "A 10 GS s 3-bit Flash ADC in 180 nm CMOS," Advanced Research in Electrical Electronics Systems (AREES), vol. 2, no. 1, pp. 1–6, Jun. 2017.*
- ***N. NACAR ÇIKAN**, M. AKSOY, "Analog Dijital Çeviricilerin İncelenmesi," Kahramanmaras Sutcu Imam University Journal of Engineering Sciences, vol.19, no.3, pp.189-194, Dec 2016*

***<u>List of Published Articles in International Conferences</u>***

- ***N. NACAR ÇIKAN**, M. AKSOY, "Comparison of NRZ and RZ in Bidirectional Fiber Communication," International Mediterranean Science and Engineering Congress (IMSEC), Adana, 2017.*

- ***N. NACAR ÇIKAN**, M. AKSOY, "Low Cost and Colorless Solution for WDM PON Systems," International Mediterranean Science and Engineering Congress (IMSEC), Adana, 2017.*
- ***N. NACAR ÇIKAN**, M. AKSOY, "A Review of Emerging Optical Access Solutions for Broadband Access," 3rd International Conference on Engineering and Natural Sciences (ICENS), Budapest, 2017.*
- ***N. NACAR ÇIKAN**, M. AKSOY, "Q Factor and BER Analysis of A PON System at Different Distances in Bidirectional Optical Fiber Communication," International Engineering Conference (IEC), Antalya, 2017(Selected-paper).*
- ***N. NACAR ÇIKAN**, M. AKSOY, "Analog to Digital Converters Performance Evaluation Using Figure of Merits FOM In Industrial Applications," IEEE-EMS2016, Pisa, 2016.*
- ***N. NACAR ÇIKAN**, M. AKSOY, "4-bit Flash Analog to Digital Converter," 3rd International Conference on Engineering and Natural Sciences, Budapest, 2017.*
- ***N. NACAR ÇIKAN**, M. AKSOY, "Static and Dynamic Characteristics of Flash Analog to Digital Converter," International Engineering Conference (IEC), Antalya, 2017.*
- ***N. NACAR ÇIKAN**, M. AKSOY, "Hybrid Type of Photonic Analog to Digital Converters," ICAT, Roma, 2016.*
- ***N. NACAR ÇIKAN**, M. AKSOY, "Analog Dijital Çeviricilerin Performans Belirleyici Parametreleri," INESEG, 2016.*
- ***N. NACAR ÇIKAN** and M. AKSOY, "A 10 GS s 3-bit Flash ADC in 180 nm CMOS," INESEG, 2016 (Selected-paper).*